The AEROMMA 2023 experiment (Atmospheric Emissions and Reactions Observed from Megacities to Marine Areas)

Carsten Warneke[1], Rebecca Schwantes[1], Patrick R. Veres[1], Andrew Rollins[1], Sunil Baidar[1,2], Wm Alan Brewer[1], Christoph Senff[1,2], Andrew Langford[1], Kenneth Aikin[1,2], Gregory Frost[1], David Fahey[1], Laura Judd[3], Barry Lefer[4], R. Bradley Pierce[5], Shobha Kondragunta[6], Chelsea Stockwell[1,2], Drew Gentner[8], Andrew T. Lambe[9], Dylan B. Millet[10], Delphine Farmer[11], Nga Lee Ng[12], Jennifer Kaiser[12], Cora Young[13], John E. Mak[14], Glenn M. Wolfe[15], John Sullivan[15], Kimberly Mueller[16], Anna Karion[16], Lukas Valin[17], Mikael Witte[18], Lynn M. Russell[19], Xinrong Ren[20], Russell Dickerson[21], Peter Decarlo[22], Brian McDonald[1], Steven S. Brown[1]

[1] NOAA Chemical Sciences Laboratory, Boulder, Colorado, United States
[2] CIRES, CU Boulder, Boulder, Colorado, United States
[3] NASA LARC, Langley, Virginia, United States
[4] NASA Headquarters, Washington, DC, United States
[5] University of Wisconsin-Madison, Madison, WI
[6] NOAA NESDIS Center for Satellite Applications and Research, Silver Springs, Maryland, United States
[8] Yale University, New Haven, Connecticut, United States
[9] Aerodyne Research, Inc., Billerica, Massachusetts, United States
[10] University of Minnesota, St. Paul, Minnesota, United States
[11] Colorado State University, Ft. Collins, Colorado, United States
[12] Georgia Institute of Technology, Atlanta, Georgia, United States
[13] York University, Toronto, Ontario, Canada
[14] Stony Brook University, Stony Brook, New York, United States
[15] NASA Goddard Space Flight Center, Greenbelt, Maryland, United States
[16] NIST Greenhouse Gas Measurement Program, Gaithersburg, Maryland, United States
[17] EPA Office of Research and Development, Research Triangle Park, North Carolina, United States
[18] Naval Postgraduate School, Monterey, California, United States
[19] University of California, San Diego, Scripps Institution of Oceanography, La Jolla, California, United States
[20] NOAA Air Resources Laboratory, College Park, Maryland, United States
[21] University of Maryland, College Park, Maryland, United States
[22] Johns Hopkins University, Baltimore, Maryland, United States

Abstract

This paper is an introduction to the planned National Oceanic and Atmospheric Administration (NOAA) Chemical Sciences Laboratory (CSL) Atmospheric Emissions and Reactions Observed from Megacities to Marine Areas (AEROMMA 2023) mission. AEROMMA will collaborate with several other missions planned by partners for summer 2023 under the name of AGES+ (AEROMMA+CUPiDS, GOTHAAM, EPCAPE, STAQS, and others). Recent NOAA CSL science foci are current topics that have also generated broad interest in the atmospheric science, air quality, and climate communities: changing emissions in urban areas, advances in marine and remote atmosphere chemistry, and satellite data assessment. NOAA CSL, its collaborators and stakeholders have an unparalleled opportunity to lead and participate in efforts to (1) understand the changing paradigms in emissions and their implications for future U.S. urban air quality, (2) refine our understanding of the marine atmosphere, and (3) validate remote sensing capabilities from satellites in urban and remote atmospheres.

To achieve these goals, NOAA CSL will conduct the AEROMMA 2023 mission, a multi-agency, multi-platform experiment planned for summer 2023 to provide new observations from megacities to marine environments. AEROMMA will bring together airborne, surface, and satellite observing systems, and state-of-the-art air quality and climate models. Major objectives of the AEROMMA 2023 project include:

- Timely information to environmental managers and stakeholder groups on emissions that impact climate and air quality;
- Improvement in the representation of emissions and chemical and physical processes in the next generation weather-chemistry models;
- Reductions in global climate model uncertainties through provisions of improved observational constraints;
- Quantification of the emissions of Volatile Chemical Products (VCPs), cooking, mobile and other trace gas sources in urban areas;
- Accurate representation of chemistry and aerosol microphysics in the marine atmosphere;
- Comprehensive aircraft observations of atmospheric composition under TEMPO (Tropospheric Emissions: Monitoring Pollution) during its initial measurements;
- Value assessment and risk reduction for future satellite missions such as NOAA GEO-XO (NOAA's Geostationary Extended Observations).

1. Emerging research needs in our understanding of urban and marine emissions, chemistry, and remote sensing capabilities

1.1. Current and future urban air quality research needs

Over half of the world's population lives in cities, and that number is anticipated to grow in all regions (UN, 2018). Air pollution is the fifth largest human health risk factor globally (Cohen et al., 2017; Gakidou et al., 2017; Murray et al., 2020) and a public health concern in megacities around the world. In addition to the emissions of short-lived air pollutants, cities are also estimated to account for ~70% of the global fossil carbon dioxide (CO_2) emissions (Duren and Miller, 2012), and CO_2 is the largest positive forcing on global climate (IPCC, 2018).

After decades of decline in ground-level ozone and fine particulate matter ($PM_{2.5}$) in the U.S., the downward trends are slowing in the most recent years (https://www.epa.gov/air-trends). This could be a result of unanticipated trends in emissions (Jiang et al., 2018; McDonald et al., 2018a), increasing influence of regional background sources (Silvern et al., 2019), long-range transport (Cooper et al., 2015), changes in atmospheric chemistry (Laughner and Cohen, 2019), and/or a consequence of a changing climate with heat waves in the US becoming more frequent, longer in duration, and more intense (Habeeb et al., 2015). Many US metropolitan areas violate the 8-hour ozone standard as regulated under the Clean Air Act, which is of concern to environmental managers. In addition to air quality, many cities and states are developing plans to reduce their carbon footprint, including for CO_2 and methane (CH_4). Such efforts will impact future emissions of VOCs and NO_x with potential co-benefits on air quality.

In most urban areas in the U.S. and Europe, long-term reductions in emissions of volatile organic compounds (VOCs) from sources such as motor vehicles (Warneke et al., 2012) have made volatile chemical products (VCPs = personal care products, cleaning agents, coatings, adhesives, inks, etc.) the major VOC source in densely populated areas (Coggon et al., 2021; Gkatzelis et al., 2021b; McDonald et al., 2018a). The emissions and impacts of VCPs on atmospheric chemistry are not well understood. In the presence of nitrogen oxides (NO_x = NO + NO_2), VOCs undergo chemistry that leads to the formation of ground-level ozone and aerosols. In a pilot study performed in conjunction with the Long Island Sound Tropospheric Ozone Study (LISTOS 2018), NOAA CSL field measurements in New York City revealed that VCPs account for over half of the anthropogenic VOC emissions, and enhance formation of ground-level ozone during a heatwave event (Coggon et al., 2021). While VCPs emissions are included in the US National Emissions Inventory (NEI) and have been regulated for their impacts on ozone formation and air toxics [*EPA*, 1995], their emissions may be underestimated by a factor of 2-3 (McDonald et al., 2018a; Qin et al., 2021). Over time the composition of VCPs has changed, shifting away from aromatics and chlorinated solvents towards oxygenated VOCs with the inclusion of fragranced components such as d-limonene (Weschler, 2009).

1.2. Improved understanding of chemistry in the marine atmosphere

Oceans cover ~70% of the surface area of the globe. Marine biogeochemical cycles, notably the emission and subsequent oxidation of dimethyl sulfide (DMS, CH_3SCH_3) from phytoplankton, strongly influence the natural climate system. DMS oxidation produces sulfate aerosol, which can serve as cloud

condensation nuclei (CCN) (Andreae, 1990). Anthropogenic emissions strongly perturb the sulfur oxidation cycle, leading to large but unexplored differences in sulfur cycling between remote and urban-influenced environments. Many of the U.S.'s largest cities are located on or near coastlines, providing an opportunity to assess interactions of anthropogenic and marine emissions, and atmospheric chemistry affecting both climate and air quality.

Biogenic sulfur oxidation products, mainly from oceanic DMS emissions, are the primary driver of particulate sulfur formation in the remote atmosphere. The DMS oxidation mechanism is not fully characterized and many of the key intermediates affecting aerosol, sulfur dioxide (SO_2), and carbonyl sulfide (OCS) yields have only been theorized. Accurate representation of both the DMS oxidation product branching fractions and timescales in chemical transport models are critical to establish a quantitative relationship between oceanic DMS emissions, atmospheric particle number and CCN concentrations in the marine boundary layer (MBL). The recent development in the understanding of this system by the discovery of hydroperoxymethyl thioformate (HPMTF) (Veres et al., 2020) highlights the degree to which global models inaccurately parameterize this chemistry. These recent advances motivate a reexamination of several decades of research assessing the role of DMS derived CCN relative to other sources of marine CCN, such as sea-spray aerosol, long-range transport of terrestrial particles, and secondary marine aerosol produced from non-DMS precursors (O'Dowd and De Leeuw, 2007; Prather et al., 2013; Quinn and Bates, 2011) in both pre-industrial and present-day atmospheres (Carslaw et al., 2013).

AEROMMA will result in a significant step forward in our ability to explain the fate of marine sourced species and their impacts on aerosols and CCN, by bringing a comprehensive modern analytical suite to the NASA DC-8 and positioning it in representative locations in the marine atmosphere to observe the relevant chemistry and aerosol formation.

1.3. New capabilities for remote sensing of atmospheric composition

The NASA / SAO (Smithsonian Astrophysical Observatory) TEMPO (Tropospheric Emissions: Monitoring Pollution) instrument (Zoogman et al., 2017) is a UV-visible spectrometer, and will be the first ever space-based instrument to monitor air pollutants at hourly time resolution across the North American continent during daytime. Current space-based observations of these products over greater North America are limited to low-earth orbiting satellites that provide only one or two overpasses per day. Launching in early 2023, its data products include high spatial resolution measurements of nitrogen dioxide, formaldehyde, ozone, and other pollutants. Field studies occurring in summer 2023, including AEROMMA, will be some of the first observations to provide context on how TEMPO measurements can integrate into air pollution monitoring over its field of regard.

NOAA's Geostationary Extended Observations (GEO-XO) satellite system is the ground-breaking mission that will advance Earth observations from geostationary orbit. GEO-XO will supply vital information to address major environmental challenges of the future in support of US weather, ocean, and climate operations. The GEO-XO mission will continue and expand observations provided by the GOES-R Series as NOAA's next generation of geostationary satellites as well as bring new capabilities to address emerging environmental issues and challenges to foster the security and well-being of the Nation. NOAA is working to ensure these critical observations are in place by the early 2030s as the GOES-R Series nears the end of its operational lifetime.

In this new era of atmospheric composition measurements from space over the US, large-scale airborne missions are needed to conduct related science and satellite validation for TEMPO and other similar missions, which deliver value assessments and risk reduction for the future with GEO-XO.

2. Recent urban and marine research and future directions

2.1. The dominance of mobile sources in urban is decreasing

2.1.1. North American megacity VOC emissions, chemistry, and trends

VOCs emitted into the urban atmosphere are one of the needed ingredients for ozone and aerosol formation and therefore significantly impact air quality. For decades, fossil fuel usage has been considered to be the primary source of urban VOCs in megacities around the world, such as Los Angeles (Parrish et al., 2009). As tighter emission regulations in the US and Europe have led to sharp reductions in transportation VOCs (Figure 1, Past Trend) (Bahreini et al., 2012; Warneke et al., 2012), new sources of pollution have emerged as potentially important precursors to ozone and aerosol formation. McDonald et al. (2018a) have shown that VCPs are a major under-studied source of urban VOCs that potentially play a significant role in urban air quality and human health. In industrialized cities, VCPs may make up as much as 50% of the total petrochemical VOC emissions and, consequently, could be responsible for as much as 50% of the mass associated with fossil-derived secondary organic aerosol (SOA) formation (Figure 1, Current Inventory) (McDonald et al., 2018a).

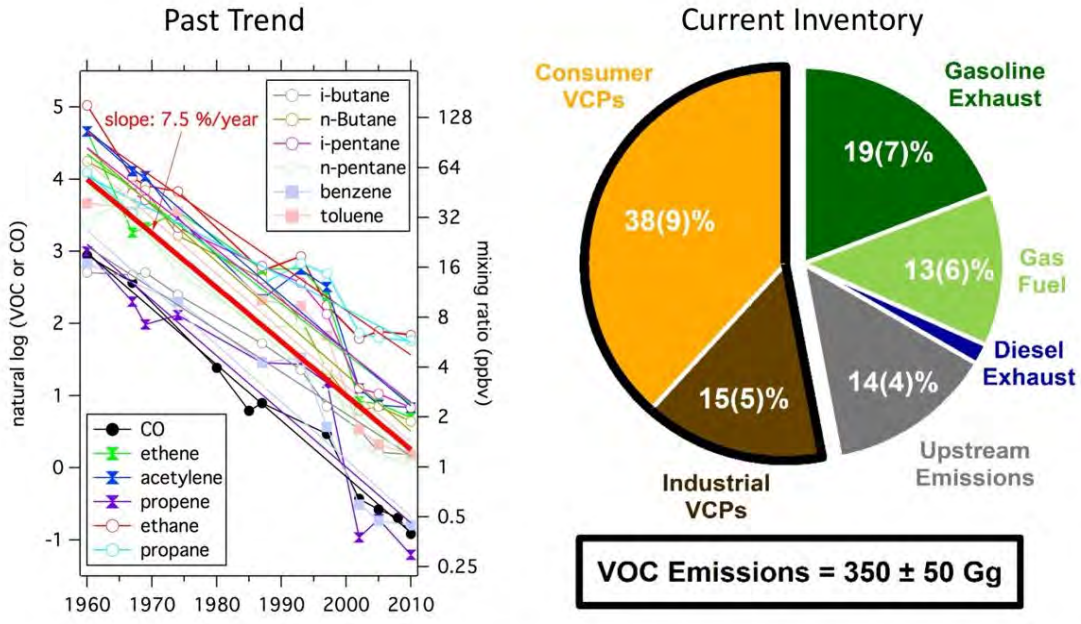

Figure 1: (Past Trend) Trends in Los Angeles anthropogenic VOC emissions show sharp decreases in fossil-VOCs observed from 1960 to 2010 (Warneke et al., 2012). (Current Inventory) Future decreases in

fossil-derived VOCs expected to be slower due to growing influence of VCP emissions (McDonald et al., 2018a).

Unlike emissions from vehicles and energy production, VCPs are emitted from a wide range of human activities over a dispersed area. Quantifying the chemical fingerprint and emission strength is challenging. For instance, a significant fraction of VCPs likely originates from use in residential or commercial buildings, and are emitted via building exhaust. Though it is not well understood what fraction of VCP emissions could also occur outside or at waste facilities (e.g., landfills and wastewater treatment plants). These "indoor" VCPs, which include cleaning and personal care products, constitute approximately 50% of VCP emissions and are composed of oxygenated molecules that can form SOA efficiently (McDonald et al., 2018a). In addition to VCPs, there could be other indoor sources of VOCs from cooking (Klein et al., 2016) and building materials (Singer et al., 2016) that can contribute primary emissions of reactive aldehydes to the atmosphere.

A recent pilot study in New York City and other major urban areas has shown that there is a clear signature of VCP emissions, such as D5-siloxanes from personal care products and anthropogenic monoterpenes from fragrances in personal care and cleaning products. VOCs such as monoterpenes from VCPs are efficient at producing ozone and SOA in an urban environment (Coggon et al., 2021). D5 siloxanes and monoterpenes show the largest enhancements in the most densely populated areas around Manhattan and are well correlated with population density (Figure 2). Speciation measurements by GC-MS found that limonene, the most commonly used monoterpene in fragrances, was the dominant monoterpene isomer in downtown NYC during both winter and summer campaigns, compared to α- and β-pinene from biogenic emissions in New Jersey and Long Island. The monoterpene speciation, the high wintertime mixing ratios, and the correlation with population density clearly prove anthropogenic emissions of monoterpenes, particularly limonene.

Using New York City data, together with a bottom-up fuel-based inventory of vehicle emissions and volatile chemical products (FIVE-VCP) inventory, *Gkatzelis et al.,* (2021a) identified tracer compounds for different VCP categories: decamethylcyclopentasiloxane (D5-siloxane) for personal care products, monoterpenes for fragrances, p-dichlorobenzene for insecticides, D4-siloxane for adhesives, para-chlorobenzotrifluoride (PCBTF) for solvent-based coatings, and Texanol for water-based coatings. Furthermore *Gkatzelis et al.,* (2021b) did a source apportionment using NYC and Boulder, CO data and showed that VCP-dominated emissions contributed to 42% and 78% of anthropogenic VOC emissions for Boulder and NYC, respectively, while mobile source emissions contributed 58% and 22%.

Elevated monoterpene emissions were also measured in other major U.S. cities (Chicago, Denver, and Pittsburgh). Figure 2 shows the ratios of D5 siloxane and monoterpenes to benzene (a marker for vehicle emissions) versus the population density for those cities, where NYC is separated into different areas of the NYC metro area. Emissions from VCPs (D5 siloxane and monoterpenes) are enhanced compared to traffic (benzene) with higher population density, as might be expected, because fewer miles are driven per person at higher population densities (Gately et al., 2015).

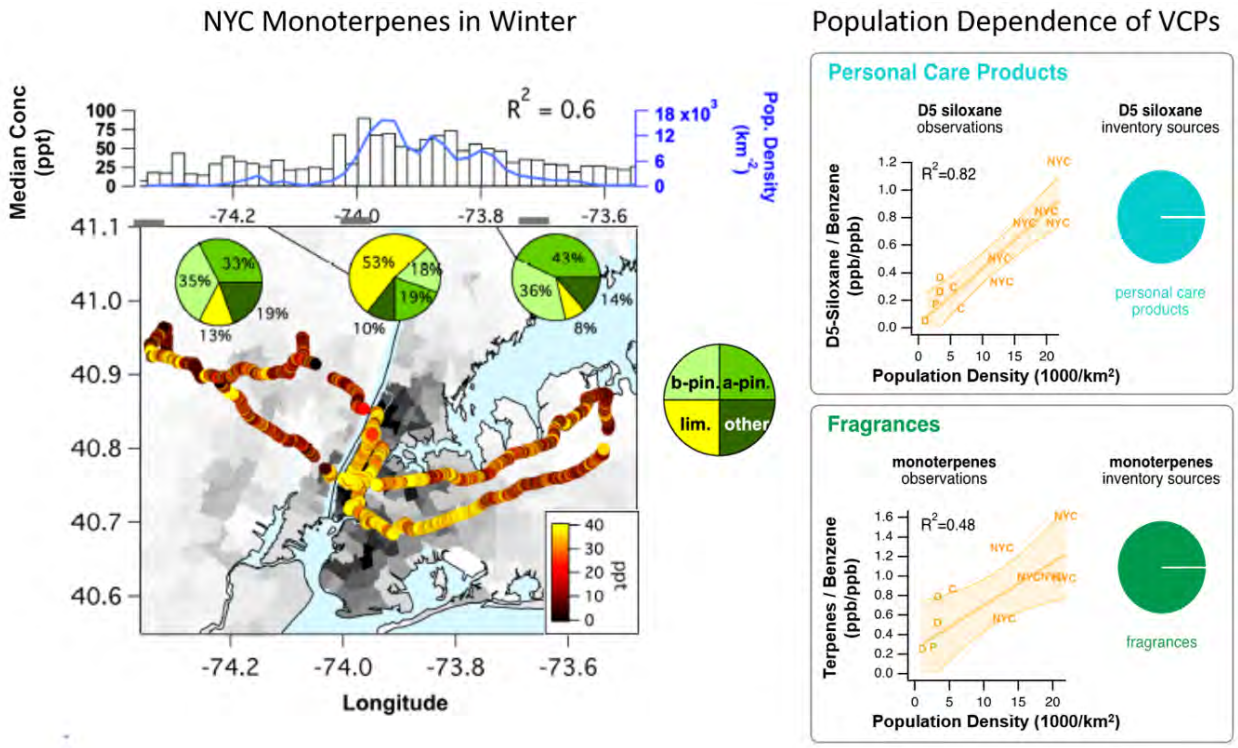

Figure 2: (NYC Monoterpenes in Winter) The drive track of the NOAA mobile laboratory color-coded with the sum of the monoterpenes measured with PTR-ToF-MS on top of the population density map of the New York City metropolitan area. The pie charts indicate the monoterpene composition determined by GC-MS. (Population Density Dependence of VCPs) The enhancements of D5-siloxane and monoterpenes relative to the traffic marker benzene for U.S. cities with different population densities. (Reproduced from Coggon et al., (2021))

The VOCs emitted from VCPs play an important role in the production of ozone and SOA as demonstrated by VOC data from a study in NYC during LISTOS 2018 (https://www-air.larc.nasa.gov/missions/listos). On July 2, 2018 an ozone exceedance event occurred in and downwind of NYC, arising from a major heatwave. Figure 3 shows results from the Weather Research Forecasting with Chemistry (WRF-Chem) model, simulating this ozone exceedance (Coggon et al., 2021). The model shows that background ozone plus NO_x and biogenic VOCs contribute ~80 ppb of 8-hour ozone to the urban corridor (panel A), which is enhanced by up to 30 ppb from the addition of anthropogenic VOCs, including from fossil fuel VOCs (panel B) and VCPs (panel C). Ozone levels reached as high as ~120 ppb, which is well in exceedance of the 70 ppb 8-hour ozone standard, and ~25 million people were exposed to unhealthy air according to the US air quality index (AQI). The same ozone episode was used to initialize a box model simulation, which was used for a VOC sensitivity study. The box modeling found that fossil fuel VOC emissions are responsible for about 60% and VCPs for almost 40% of the anthropogenic ozone formation related to VOC emissions. The VCP fraction was about evenly split into coatings, cleaning products and personal care products. Ethanol and fragrances were two of the most important VOCs for ozone production during this exceedance event (Coggon et al., 2021).

As fossil fuel VOC emissions decline and the relative importance of VCP emissions increase, anthropogenic-influenced VOC mixtures in urban regions are changing. Emissions from fossil fuels are largely hydrocarbons, which are well represented in traditional reduced chemical mechanisms, but VCPs

include many oxygenated VOCs (oVCPs), which are not as well represented. Fig. 3D shows ozone simulations when oVCP chemistry is included in the WRF-Chem model. This change in chemistry results in a small increase in ozone (1 ppb). Despite the marginal impact on the magnitude of ozone, the OH chemistry of oxygenates markedly impacts model simulations of other secondary products that have implications on downwind air quality. Oxidation of NO_x occurs simultaneously with ozone production and leads to different compound classes that serve as either permanent sinks or temporary reservoirs of NO_x. Two important NO_x reservoir compounds are organic nitrates and peroxyacetyl nitrates (PAN), which have different atmospheric fates and therefore potentially different impacts on ozone formation downwind. The inclusion of oVCP chemistry increases PAN (Fig. 3H) by 15 to 20% at the expense of organic nitrates.

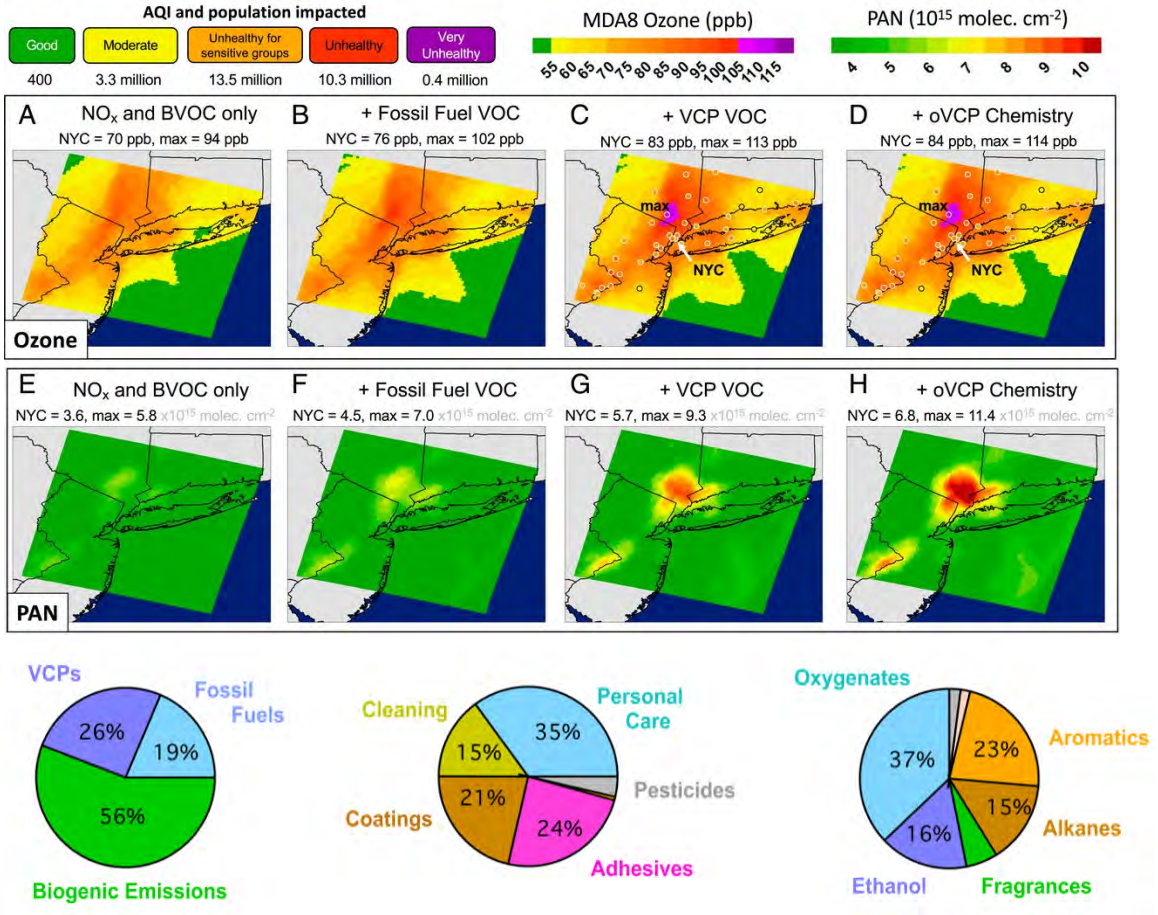

Figure 3: WRF-Chem simulations of MDA8 ozone (parts per billion) and midday (2:00 PM local time) column integrated PAN (molecules cm^{-2}) during the July 2, 2018, pollution episode. Shown are the simulations for global background ozone + NO_x and BVOCs (A and E), results from A and E with fossil fuel VOCs added (B and F), and results from B and F with VOCs from VCPs added (C and G). A–C and E–G show ozone and PAN produced without oVCP chemistry. D and H shows the simulation using full emissions but under the assumption of oVCP chemistry. Circles show the ozone mixing ratios measured at monitoring stations in the NYC area; those bolded in white exceeded US NAAQS. The numbers above each panel show the surface ozone or column PAN simulated in NYC and at the location of the MDA8 ozone maximum downwind of NYC (max). The pie charts show the ozone attribution by source, source category, and chemical class. (Reproduced from Coggon et al., (2021))

In addition to their contributions to ozone, McDonald et al. (2018a) suggested that VCPs can also contribute to SOA. A recent oxidation flow reactor (OFR) and high-resolution aerosol mass spectrometer (HR-AMS) experiment in New York City and Pittsburgh suggested VCPs have significant SOA formation potential (Shah et al., 2020). The study compared the measured SOA from the OFR with predicted SOA formed from mobile sources and biogenics (Figure 4). The measured SOA concentrations were under-predicted by a factor of ~2 when compared with the predicted SOA concentrations. The study further investigated what the missing source of urban SOA could be, and performed oxidation experiments on VCP emissions, which revealed that VCPs can efficiently form SOA. More recently, updates to emissions and SOA formation processes for VCPs in 3D atmospheric chemistry models reduced model biases for $PM_{2.5}$ and SOA compared to observations from the CalNex 2010 field campaign and suggested that VCPs contributed approximately 41% of the SOA during the 2010 summer in Los Angeles (Pennington et al., 2021; Qin et al., 2021).

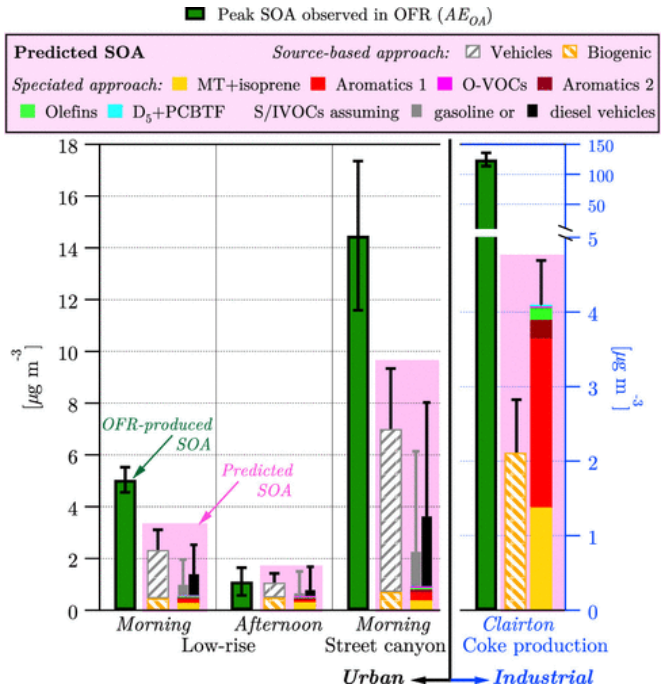

Figure 4: Measured and predicted SOA in urban and industrial environments at 2 equivalent days of OH exposure. SOA measured in the OFR is shown by the green bar and predicted SOA based on speciated VOC data by the pink tints. The predicted SOA only accounts for traditional gasoline, diesel and biogenic sources of precursors and under-predicts the observed values by a factor of ~2 in the morning time street canyon and suggests the influence of VCPs on SOA (Shah et al., 2020).

Additionally, during the COVID-19 pandemic, government and societal interventions led to large changes in atmospheric emissions including reductions of transportation emissions of NO_x and VOCs. Similar reductions in emissions are expected to occur in the future as electrification of motor vehicles increases. While the impact of these COVID-19 interventions on NO_x is clear, the impact on VOCs remains understudied (Gkatzelis et al., 2021c). Given the large impact of VOCs on urban air quality through ozone and SOA production, more current measurements with state-of-the-art VOC speciation capabilities are

needed to understand how VOC concentration and composition has changed over the last decade in order to improve predictions of air quality now and in the future.

These measurement and modeling studies indicate the importance of VCPs, in addition to traditional fossil fuel sources, for ozone and SOA and clearly demonstrate the need for understanding their chemistry in the urban environment and for taking VCPs into account in air quality management.

2.1.2. North American megacity NO_x emissions, chemistry, and trends

Nitrogen oxides NO_x are the other major emissions that contribute to ozone and secondary aerosol formation. US NO_x emissions have been decreasing: for example, in Los Angeles where emissions decreased at a rate of 2.6% per year between 1960 - 2010 (Pollack et al., 2013). Similar rates of decrease in NO_2 mixing ratios are observed nationwide (https://www.epa.gov/air-trends/nitrogen-dioxide-trends), but satellite retrievals of NO_2 columns from the Ozone Monitoring Instrument (OMI) indicate a markedly slower rate of decrease since 2011 (Figure 5, left panel) (Jiang et al., 2018). A variety of hypotheses have been suggested on why this trend is slowing, including: (i) a decrease in the rate of decline in anthropogenic NO_x emissions (Jiang et al., 2018), (ii) the growing influence of background and free tropospheric NO_2 (Silvern et al., 2019), and (iii) changes in NO_x lifetime (Laughner and Cohen, 2019).

Heavy-duty diesel trucks have become the leading source of NO_x in the Los Angeles basin (Kim et al., 2016), and in cities over the eastern U.S. (McDonald et al., 2018b). Starting in 2010, new heavy-duty diesel trucks are required to install selective catalytic reduction (SCR) systems. Under highway driving conditions, the SCR systems are effective at reducing NO_x emissions. However, under urban driving, the SCR systems are ineffective and result in significantly elevated emissions of NO_x (Dixit et al., 2017; Thiruvengadam et al., 2015). The reagent used to reduce NO_x within the SCR is urea, and if slippage occurs, could also result in a local urban source of ammonia (NH_3).

A recent study suggested that agricultural soils are a dominant source of NO_x pollution in California, with especially high soil NO_x emissions from the state's Central Valley region (Figure 5, right panel). This large NO_x source from cropland soil could increase the NO_x budget by 20 to 51% (Almaraz et al., 2018). Fertilizer application also results in nitrous oxide (N_2O) emissions, a potent greenhouse gas, and emissions are strongest in the Midwestern corn/soy belt and in spring/early summer (Eckl et al., 2021). These results are consistent with NOAA CSL modeling of ozone over the Eastern US also suggested an under-accounted soil NO_x source in the Upper Midwest (McDonald et al., 2018b). It is possible that the increasing importance of soil NO_x emissions could be contributing to the reduced rate of change observed in satellite NO_2 columns shown in Figure 5.

In addition to uncertain NO_x trends, recent studies have also suggested significant uncertainties in current vehicle emission models of mobile source NO_x based on a variety of field campaigns (McDonald et al., 2018a; Travis et al., 2016). It is critical to improve inventories of NO_x for accurate model predictions of ozone and aerosol chemistry. With the launch of the Sentinel-5P Tropospheric Ozone Monitoring Instrument (TROPOMI) (Veefkind et al., 2012) and enhanced spatial resolution of its satellite products (3.5 km x 7 km), satellite NO_2 and formaldehyde data are becoming an increasingly useful tool for evaluating and constraining emission inventories (Beirle et al., 2019; Goldberg et al., 2019) and VOCs (Kim et al., 2018). Remote sensing capabilities to discern diurnal profiles are expected to become available with the launch of the geostationary TEMPO satellite in 2023 (Chance et al., 2013; Zoogman et al., 2017).

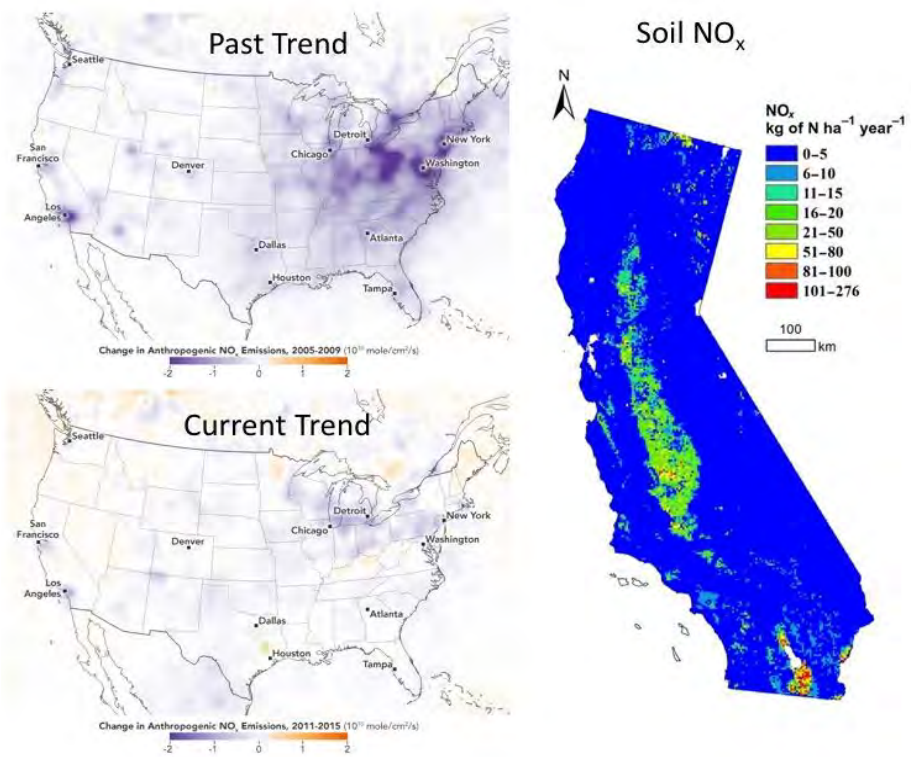

Figure 5: Trends in US NO_x emissions derived from OMI satellite products using an inverse modeling framework (Jiang et al., 2018). NO_x emissions decreased from 2005-2009 (Past Trend) but the rate of decrease slowed during 2011-2015 (Current Trend). (Soil NO_x) NO_x emissions from California soils (natural and cropland) generated using stable isotopic modeling and the IMAGE model (Almaraz et al., 2018).

2.1.3. North American tropospheric ozone formation and trends

The ozone trends since 1980 in the potential target cities for AEROMMA are shown in Figure 6 (https://www.epa.gov/outdoor-air-quality-data/air-data-concentration-plot). Plotted are the 4th highest annual maximum of the MDA8 ozone values of the Core Based Statistical Areas (CBSAs) in Los Angeles, NYC, and Chicago together with their respective downwind CBSAs and trends in other U.S cities that might be AEROMMA targets. In the most recent years, the downward trend has slowed significantly, especially in Los Angeles, NYC, and Chicago. The trends in NO_x and VOCs emissions from the FIVE emission inventory in Los Angeles are shown in the bottom panel of Figure 6 (Kim et al., 2022). NO_x emissions have been decreasing linearly over the past thirty years, while VOCs showed a slower decrease over the past twenty years mainly because of the VCP sector. These trends caused the VOC/NO_x ratio to increase over the past decade. Kim et al., (2022) concluded that the Los Angeles basin is undergoing a significant transition in photochemistry toward lower ozone concentrations, but the lack of recent progress in O_3 design value is a subject of intense current research.

Overall, summertime levels of surface ozone have been trending downward from 2000-2014 (Gaudel et al., 2018) together with its precursors as described above. In the southeast U.S., it was shown recently that ozone maxima decreased in proportion with NO_x emissions (Blanchard et al., 2014). Prior to

the 2008 recession, large emission reductions have been observed from space due to U.S. regulatory efforts to control NO_x from power plants and transportation (Tong et al., 2015).

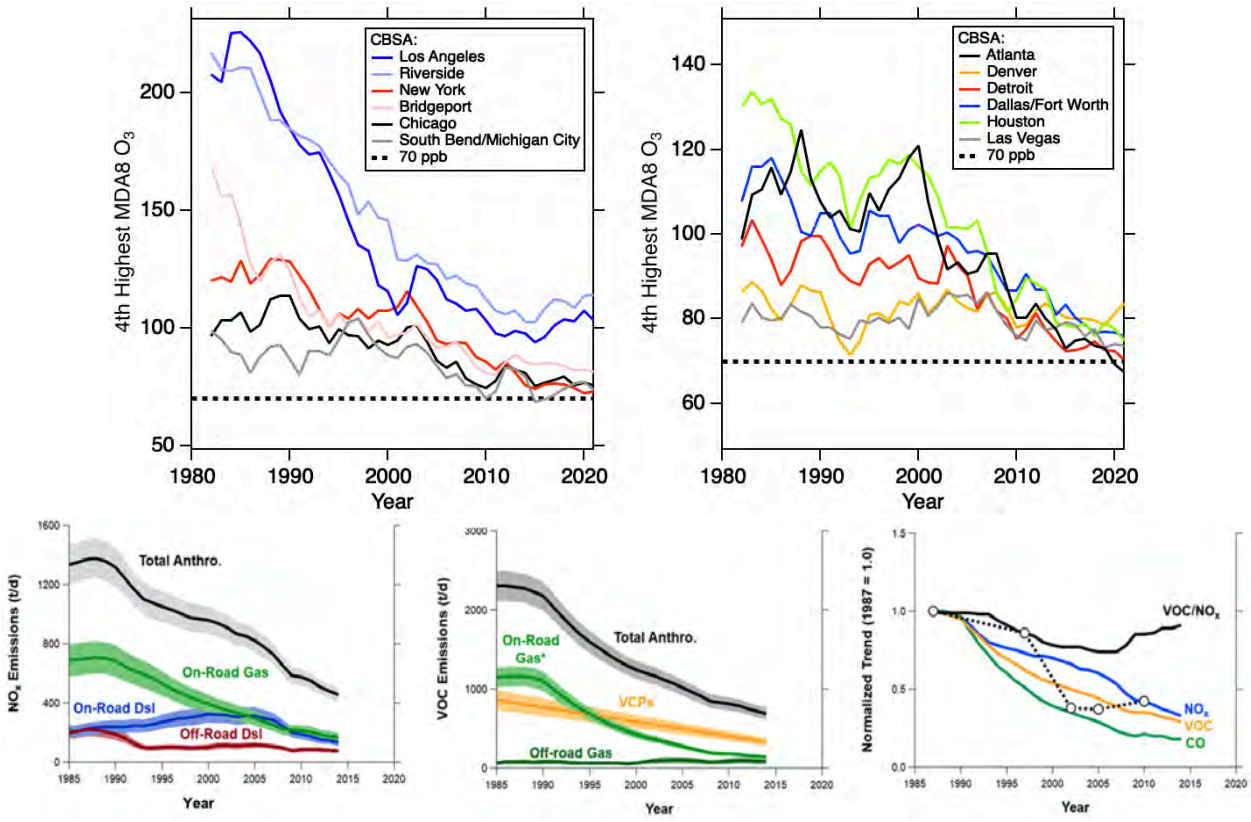

Figure 6: (top) Trends in the 4th highest annual maximum of the MDA8 ozone in the AEROMMA target cities and their downwind areas since 1980. (bottom) Trends in the FIVE-VCP NO_x and VOC total and sectoral emissions (ton day^{-1}, t/d) in the Los Angeles Basin from 1987 to 2014. Trends in the FIVE-VCP emissions normalized to the values in 1987 for NO_x, VOC, CO and VOC/NO_x. The top-down model adjusted VOC/NO_x emissions trend is shown by the dashed black line and open markers denote model years simulated in WRF-Chem (Kim et al., 2022).

2.1.4. Aerosol formation and trends

Nationally, organic aerosol (OA) comprises around half of ambient fine particulate matter ($PM_{2.5}$) mass, and U.S. $PM_{2.5}$ concentrations have been decreasing since 1990. Ridley et al. (2018) attribute the decreases in atmospheric concentrations of OA to reductions in transportation and residential fuel burning emissions, including directly emitted particles and VOC precursors (Figure 7). Similarly, McDonald et al. (2015) found that OA concentrations were decreasing in Los Angeles due to reductions in tailpipe emissions of primary and secondary OA (Figure 7), although the decreases were not as large as expected from the observed reductions in mobile source emissions. The study suggested that other VOC sources could be contributing to the slower-than-expected decreases in OA concentrations. McDonald et al. (2018a) later found that the slow OA decrease is likely due to a shift away from the dominance of mobile sources.

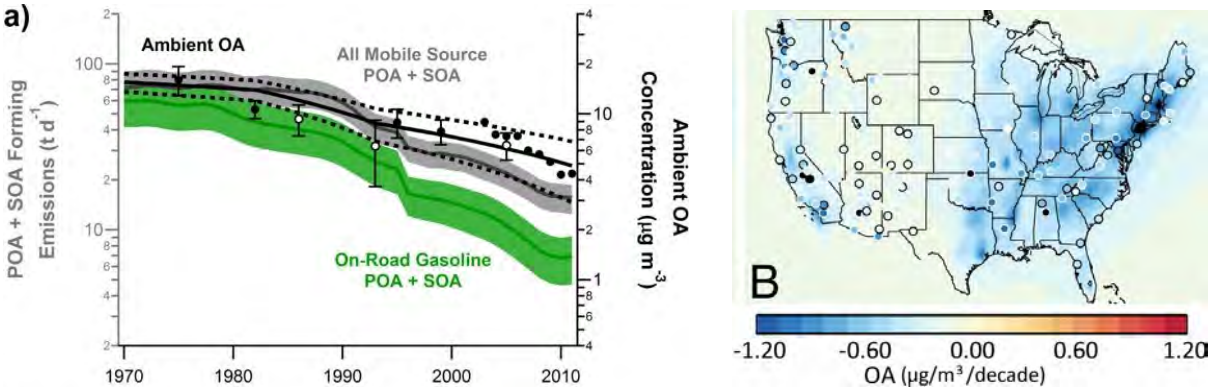

Figure 7: Trends in organic aerosol concentrations in the Los Angeles basin (McDonald et al., 2015) and in the U.S. from GEOS-Chem and IMPROVE sites (Ridley et al., 2018). Decreases are attributed to reductions in motor vehicle emissions and other sources of SOA.

2.1.5. Greenhouse gases and air quality co-benefits

Globally, cities account for ~50% of the world population and at least 70% of the CO_2 emissions (Duren and Miller, 2012). A robust urban carbon monitoring system for CO_2 and CH_4 has not yet been established to track trends in greenhouse gas emissions, though urban testbeds have been established in Indianapolis (INFLUX), Los Angeles (Megacities Carbon Project), and Baltimore/Washington, DC (Northeast Corridor Urban Test Bed) with support from NIST (https://www.nist.gov/topics/greenhouse-gas-measurements/urban-test-beds).

In most U.S. cities, buildings and transportation comprise the two largest sources of CO_2 emissions (Gately and Hutyra, 2017; McDonald et al., 2014). These sources also are the two main NO_x sources in cities (McDonald et al., 2018b) and sources for VOCs to the urban atmosphere (McDonald et al., 2018a) contributing to ozone and $PM_{2.5}$. Fugitive leaks of methane have been shown to occur from the oil and natural gas production and supply infrastructure and landfills (Alvarez et al., 2018; Kuwayama et al., 2019; Plant et al., 2019). Refineries remain an important source of reactive VOCs (Johansson et al., 2014) and oil and natural gas infrastructure are a source of light alkanes (Peischl et al., 2013). Relatively little attention has been paid to VOC emissions from landfills, though they could be a potential emission pathway by which VCPs are emitted into the atmosphere. Given the overlap in emission sources that contribute to both air pollutants and greenhouse gases, there are potential synergies for cities to optimize management of air quality and the carbon cycle.

2.1.6. The role of heatwaves, meteorology, and long-range transport in urban air quality

Over the last 50-60 years, U.S. heatwaves have become more frequent, longer lasting, and higher intensity (Habeeb et al., 2015). Heatwaves have been associated with enhanced levels of ozone (Meehl et al., 2018), as well as human mortality (Mora et al., 2017). As Figure 3 illustrates for New York City, heatwaves can significantly enhance ozone well in exceedance of national ambient air quality standards (Coggon et al., 2021). However, the impacts of meteorology on ozone and aerosol formation are complex through dependencies on temperature, sunlight, precipitation, and effects on dynamical and physical processes (Doherty et al., 2017). For example, warmer temperatures are expected to result in a higher

planetary boundary layer which enhances dilution and lowers air pollutant concentrations. This can be offset if a heatwave results in stagnant wind conditions and/or recirculation of air masses that allow for build-up of air pollution.

It is well established from prior field campaigns that coastal dynamics affect the transport of ozone and other air pollutants, including during NEAQS2002, ICARTT2004, TEXAQS2000, TEXAQS2006, and CALNEX2010 (Angevine et al., 2013; Angevine et al., 1996; Angevine et al., 2012; Banta et al., 2011; Banta et al., 2005; Darby et al., 2007; White et al., 2007). As Figure 8 illustrates, chemical transport modeling from ICARTT2004 shows that ozone can be transported from Washington, DC through New York City up to the Gulf of Maine, driven by mesoscale meteorology along the coast (Lee et al., 2011). There is a lack of high-quality wind profiler and thermodynamic measurements over water surfaces, which inhibits evaluation of numerical weather prediction models (Banta et al., 2018). Ship or airborne lidars fill a critical measurement gap in providing data that can improve models of the marine boundary layer, land-sea breeze recirculation, vertical mixing, as well as characterizing offshore wind energy resources (Pichugina et al., 2017; Tunved et al., 2006).

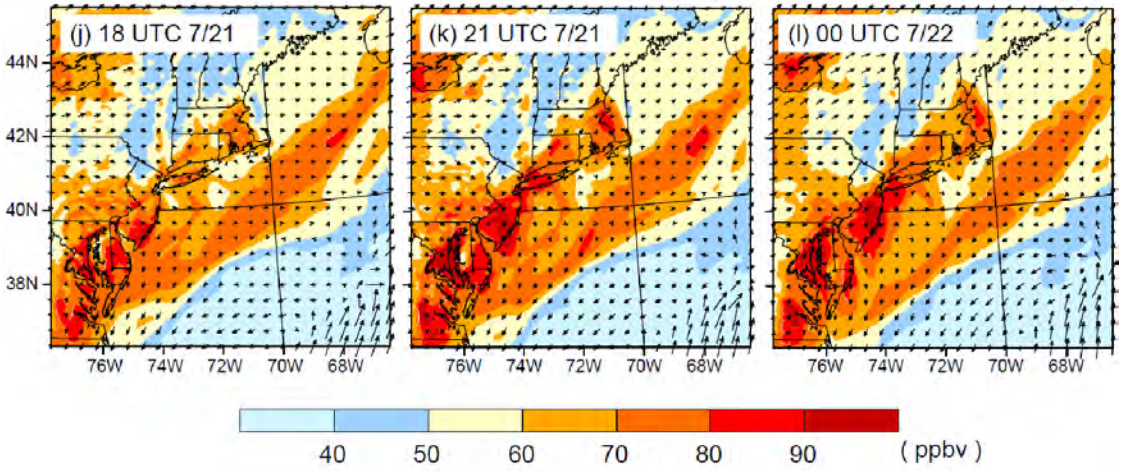

Figure 8. Transport of ozone (in ppb) as modeled in WRF-Chem along the US East Coast, from the Mid-Atlantic through the Gulf of Maine, during the ICARTT 2004 field campaign (Lee et al., 2011).

In addition to coastal dynamics, urbanization results in the modification of land surfaces that alter the surface energy balance. Urban heat islands (UHI) result when asphalt or concrete with low albedo replaces soils and vegetation and inhibit evapotranspiration. The magnitude of UHI can be modeled as a function of population and precipitation, with the effect stronger in the most populated cities (Manoli et al., 2019). Accounting for the urban canopy in chemical transport models was shown to improve model predictions of ozone in New York City during the ICARTT 2004 field campaign (Lee et al., 2011). Using high-resolution vegetation maps and albedo maps was shown to improve the WRF model performance of urban meteorology in Los Angeles (Vahmani and Ban-Weiss, 2016). The effects of urbanization are additional factors to consider for the meteorology of coastal cities. A key question is to what extent does the urban canopy need to be parameterized and represented in chemical transport models? Often the urban canopy is overlooked in operational weather forecasts due to computational cost.

Ozone and aerosols can be transported on regional to continental scales. Global contributions to background ozone are estimated to be ~30 ppb over the Eastern U.S., with a higher contribution in the Western U.S. of ~40 ppb at high-altitude sites (Zhang et al., 2011). With the lowering of the 8-hour U.S.

ozone standard to 70 ppb, and generally increasing trends in global background ozone (Cooper et al., 2010; Gaudel et al., 2018), it is becoming more challenging for cities to meet national ambient air quality standards (Cooper et al., 2015). Ozone can also be transported from the stratosphere to the troposphere, especially in the intermountain west (Langford et al., 2017; Langford et al., 2015; Sullivan et al., 2015). Terrain can result in lofting of air pollution from Los Angeles, which lowers concentrations in Los Angeles and elevates pollutants transported over long distance to other states (Langford et al., 2010). Ozone and aerosol lidars that report vertically-resolved concentrations can be helpful in discerning local versus long-range transport of air pollution, as well as whether there is mixing from the free troposphere to the surface. Figure 9 shows an example of ozone lidar measurements made by the NASA TOLNet (https://www-air.larc.nasa.gov/missions/TOLNet/) mobile ozone lidar from the Langley Mobile Ozone Lidar (LMOL) (Gronoff et al., 2019) downwind of New York City at Westport, CT during LISTOS 2018 (Coggon et al., 2021; Torres-Vazquez et al., 2022; Zhang et al., 2020b). In addition to other TOLNet lidars, specific efforts have been established to support ozone profiles at the Westport, CT site for the 2023 measurement period. While high ozone levels at the surface are generally decoupled from the free troposphere, there are instances where downward transport of ozone to the surface via local meteorology is evident (Sullivan et al., 2017). Similarly, for aerosols, wildfire smoke from Northwest U.S./Canada has been shown to be transported over North America and contribute to a 5-30 $\mu g/m^3$ $PM_{2.5}$ increase in New York City (Wu et al., 2018; Wu et al., 2021). The vertical mixing and transport between the stratosphere, free troposphere, and planetary boundary layer is an additional consideration for coastal meteorology that can affect urban air quality.

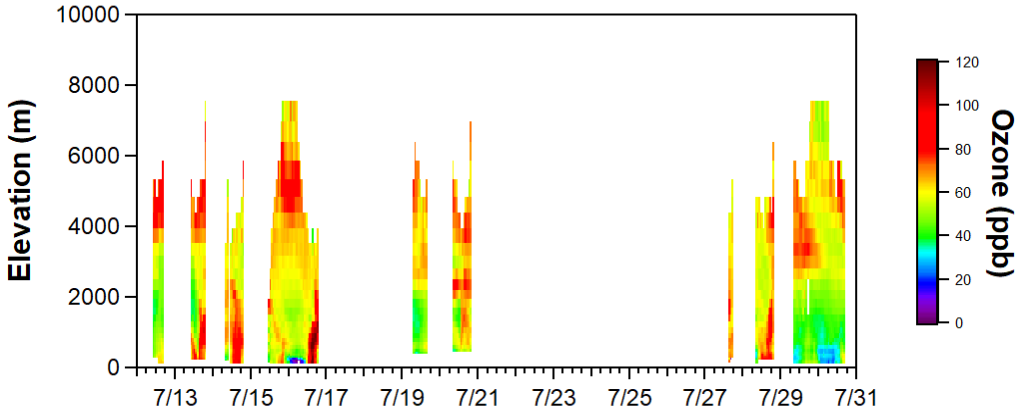

Figure 9: Example of ozone lidar measurements by NASA Langley during LISTOS 2018 at Westport, CT.

2.1.7. Role of observations for evaluating and improving research, regulatory, and operational 3D atmospheric chemistry models

Past ground site, mobile, and aircraft campaigns with comprehensive measurements of gases and aerosols have been critical for evaluating and improving model processes and prediction of air pollutants in 3D atmospheric chemistry models. For example, observations from CalNex 2010 and LISTOS 2018 have motivated an update of emissions and chemistry from VCPs leading to improved predictions of ozone and SOA (Coggon et al., 2021; Pennington et al., 2021; Qin et al., 2021). Aircraft and ground site campaigns are particularly important for evaluating model processes because unlike routine monitoring, which only measure a small number of gases and aerosols like ozone and $PM_{2.5}$, aircraft campaigns provide co-located detailed high-quality chemical measurements including ozone precursors (e.g., VOCs and NO_x) and

speciated aerosols. Additionally, aircraft campaigns provide broader spatial and vertical coverage than routine ground site monitors. This greater chemical, spatial, and vertical detail in aircraft observations is important for accurately identifying the cause of model biases and for evaluating potential model improvements.

New measurements of the atmospheric composition with broad spatial and vertical coverage over urban regions are needed to compare to past measurements in order to understand how air quality has changed over the last decades and evaluate if research, regulatory, and operational models are accurately reflecting these changes. Studies suggest that anthropogenic emissions are changing more rapidly than can be reflected in traditional inventories such as the US EPA National Emissions Inventory (Ahmadov et al., 2015; Jiang et al., 2018; Li et al., 2021; Ma et al., 2021; McDonald et al., 2018a; Negron et al., 2018), especially for exceptional events such as the 2008 Global Economic Recession (Tong et al., 2015) and the COVID-19 pandemic (Campbell et al., 2021; Gkatzelis et al., 2021c). Up-to-date detailed chemical measurements in urban regions are needed for creating and evaluating new approaches that allow for emission inventories to be updated in near real time, which is particularly important for improving air quality predictions in NOAA and other operational models (Tong et al., 2012). Additionally, more measurements of VOCs with a wider range of volatilities are needed in urban regions for developing and evaluating new chemical mechanisms such as CRACMM - Community Regional Atmospheric Chemistry Multiphase Mechanism (Pye et al., 2022). CRACMM will reflect the changing VOC distribution in urban regions (e.g., reduced contribution of hydrocarbons from fossil fuels and increased contribution of oxygenated VOCs from VCPs), include scientific advances such as improved representation of heterogeneous processes, and be reduced enough to be considered for regulatory and operational applications. In addition, a new model diagnostic tool called MELODIES MONET is under development (https://melodies-monet.readthedocs.io/) to encourage more complete evaluation of research, regulatory, and operational models against a variety of surface, aircraft, and satellite observations all within the same framework. A more rigorous and accurate understanding of model biases covering chemical, spatial, vertical, and temporal scales can be achieved by evaluating models against a combination of different types of observations, of which aircraft campaign measurements are an important component for providing detailed chemical, spatial, and vertical resolution.

2.2. Recent advances in understanding of the remote marine atmosphere

2.2.1. Biogenic sulfur oxidation

Biogenic emissions of sulfur from Earth's oceans are well known to influence global climate, but potential feedbacks affecting radiative budgets have been an ongoing topic of debate (Carslaw et al., 2013; Charlson et al., 1987; Quinn and Bates, 2011). DMS is one of the most abundant biological sources of sulfur to the marine atmosphere and is central to this research (Andreae, 1990; Andreae et al., 1985; Bates et al., 1992). DMS oxidation is the source of up to 18% of the global sulfate burden in the present-day atmosphere, with an approximate contribution in the preindustrial background of over 48% (Gondwe et al., 2003; Tilmes et al., 2019; Yang et al., 2017). Understanding the importance of DMS derived sulfate relative to other marine aerosol sources such as sea-spray aerosol, long-range transport of terrestrial particles, and secondary marine aerosol produced from non-DMS precursors (O'Dowd and De Leeuw, 2007; Prather et al., 2013;

Quinn and Bates, 2011), in both pre-industrial and present-day atmospheres, requires a complete understanding of the chemical and physical processes affecting DMS oxidation products.

Once in the atmosphere, DMS undergoes radical-initiated oxidation by hydroxyl (OH), halogen radicals (e.g. chlorine, Cl, and bromine oxide, BrO), and the nitrate radical (NO_3) to form a suite of oxidation products (Andreae, 1990; Andreae et al., 1985; Chen et al., 2018; Hoffmann et al., 2016). Gas phase sulfur dioxide (SO_2), one of these oxidation products, can react further with OH to form sulfuric acid (H_2SO_4), a key precursor to new particles formed via homogeneous nucleation in air masses where the existing condensation sink is small (Kulmala, 2003). These newly formed particles may grow by further condensation and coagulation to sizes large enough to serve as cloud condensation nuclei (CCN), thus affecting cloud optical properties and climate (Merikanto et al., 2009). In addition, SO_2 and methane sulfonic acid (MSA, CH_3SO_3H) can partition to aerosol liquid water to form additional non-sea salt sulfate (nss-SO_4^{2-}) (Boniface et al., 2000; Hodshire et al., 2019; Saltzman et al., 1983).

Despite the crucial role DMS plays as a natural source of aerosol sulfate, parameterizations of its complex oxidation pathways remain insufficient. Previous work has focused almost exclusively on the yields and fate of the terminal products SO_2 and MSA and their impact on the concentration of CCN (Merikanto et al., 2009). These observational limitations as well as computational restrictions on global and regional chemical transport models have led to an oversimplification of DMS formation and loss processes, where DMS reactions are typically represented as a binary oxidation reaction to produce SO_2 and MSA (Chin et al., 1996).

Recent research has confronted this oversimplification through the identification of a previously unobserved DMS oxidation product, hydroperoxymethyl thioformate (HPMTF) highlighted in Figure 10 (Veres et al., 2020), and quantification of a new, potentially significant source of biogenic marine sulfur, methanethiol (Lawson et al., 2020; Novak et al., 2022). Cloud uptake of HPMTF alone, a previously unidentified loss process for marine sulfur, accounts for a global reduction of approximately 35% in net SO_2 production and results in significant changes to the spatial distribution of sulfate in marine environments (Novak et al., 2021; Veres et al., 2020; Vermeuel et al., 2019). Additionally, carbonyl sulfide (OCS), a key climate gas through its role as the source of stratospheric aerosol mass (Bruhl et al., 2012), has been recently identified as a product of HPMTF oxidation (Jernigan et al., 2022).

Collectively, these recent discoveries highlight the role of DMS in regulating the temporal and spatial distributions of SO_2, H_2SO_4, and non-sea salt sulfate. The sensitivity of global aerosol radiative forcing simulations to new descriptions of the formation and loss process of marine sulfur motivates further research into the fate of sulfur species in the remote atmosphere (Fung et al., 2022). AEROMMA will deploy a comprehensive measurement suite capable of detecting both gas and particle phase sulfur species including gas phase observations of HPMTF (Iodide time of flight mass spectrometer, I CIMS), DMS and methanethiol (Vocus-PTR), SO_2, OCS, and particle phase sulfate and MSA tracers (particle-into-liquid sampler with online ion chromatography, PILS-IC, and a high-resolution time of flight aerosol mass spectrometer, HR-AMS). Flight plans will be designed to span a range of meteorological conditions and geographical conditions to provide ample statistics on the impacts of aerosols and clouds on the marine sulfur system.

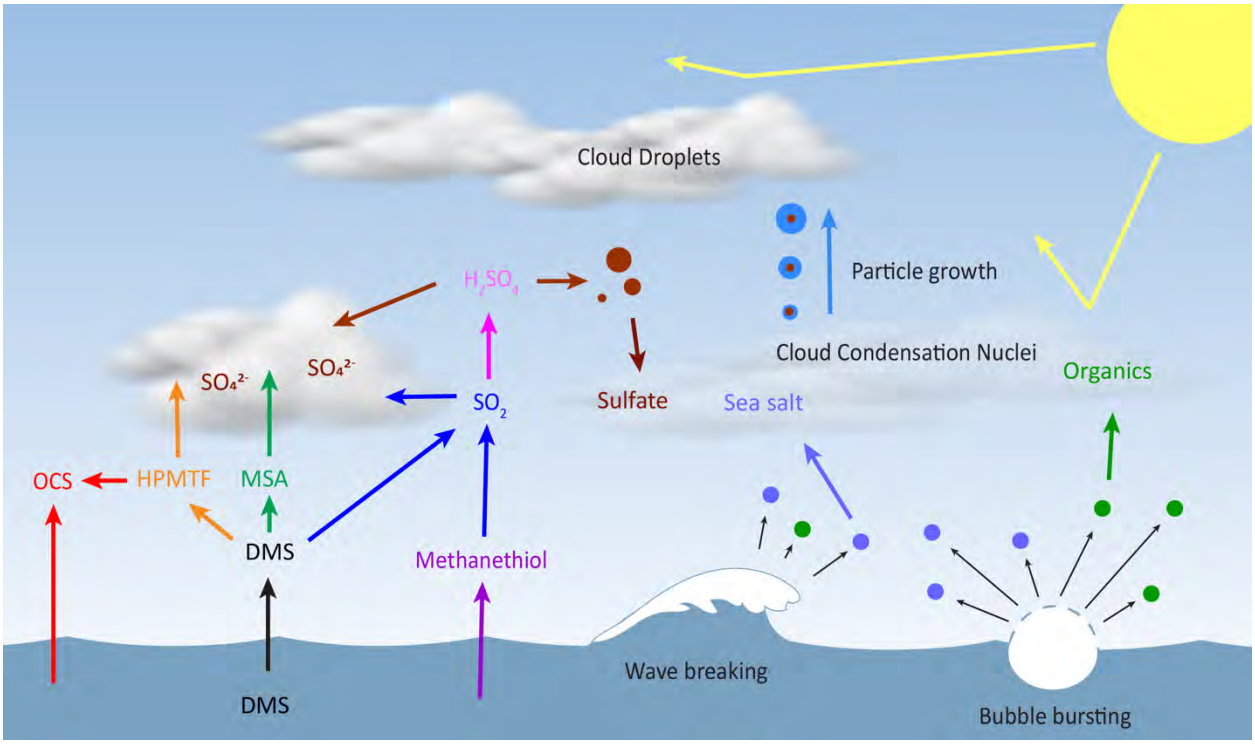

Figure 10: A simplified overview of the linkages between oceanic emissions and processes that contribute to the formation and growth of clouds and aerosol. The AEROMMA marine flights will be designed to provide addition insight into these gas and aerosol processes.

2.2.2. Marine halogens

Globally, the marine atmosphere is the main source of natural halogen-containing (e.g Br, Cl, I) gases. Halogen species originate from a variety of natural processes including reactions on sea salt aerosol (SSA), stratospheric transport, and rapid cycling with inorganic reservoirs (Platt and Honninger, 2003; Wang et al., 2019). Halogens can impact the oxidative capacity of the atmosphere by altering VOC, NO_x and HO_x budgets in both coastal urban and pristine marine environments (Saiz-Lopez and von Glasow, 2012; Simpson et al., 2015).

Halogen oxides (BrO, ClO, IO) play an important role in the ozone depletion cycle. Halogens have been shown to reduce O_3 concentrations in marine environments by up to 20% (Saiz-Lopez and von Glasow, 2012; Sherwen et al., 2016). Similarly, in coastal urban regions, a recent modeling study approximates a 10% increase in secondary organic aerosol and reductions in O_3 and NO_x in the city of Los Angeles due to these species (Muñiz-Unamunzaga et al., 2018; Raff et al., 2009). Conversely, increases in tropospheric ozone and secondary organic aerosol production have occurred following the reaction of $ClNO_2$ on marine aerosols in coastal urban areas (Hossaini et al., 2016; Osthoff et al., 2008). Additional, improved measurements of these key halogen species are required to further quantify their impact on baseline continental O_3.

BrO in particular reacts with key atmospheric species such as DMS, HO_2, and NO_x to activate halogens radicals, form reactive halogen species or yield key reservoir species. Reactions of DMS with BrO have been of recent interest, however, there remains disagreement over the relative impact of this

reaction on DMS oxidation. In one recent modeling study, BrO oxidation accounted for up to 46% of the DMS oxidation (Hoffmann et al., 2016), however others have suggested significantly lower net impacts, less than 5% (Veres et al., 2020). Recent studies have further highlighted the discrepancies between measurements and modeled Cl and BrO abundances, which impacts our ability to accurately describe their impact on DMS chemistry (Wang et al., 2021).

Large uncertainties remain in the sources, abundance, and chemical mechanisms of marine sourced halogens. These uncertainties limit our ability to accurately describe the role of halogens on the tropospheric ozone and global NO_x and HO_x budgets. The AEROMMA study will provide additional field observations of marine halogen species, BrO, $ClNO_2$, Cl_2 (I-CIMS), VOCs (Vocus-PTR), NO_x (Laser Induced Fluorescence (LIF)), and particulate chloride (HR-AMS). These observations will be used to test model descriptions to further constrain the impact of marine halogens on the oxidative budget of urban regions, and to assess the role of these emissions for urban air quality in a changing atmosphere.

2.2.3. Marine sources of VOC, NO_x, and aerosols, Ozone transport and deposition

The global background concentrations of ozone and the oxidation capacity in remote regions are impacted significantly by air-sea exchange of reactive species such as O_3, nitrogen oxides, and trace organics. One key need is to understand the production and chemical or physical loss of O_3 over the oceans which control the present-day baseline continental O_3 due to onshore flow, as well as to estimate preindustrial O_3. In addition, moderately long-lived climate and ozone active gases such as methane and methyl chloroform are controlled by the hydroxyl radical, which is quite sensitive to the low mixing ratios of nitric oxide over the Earth's marine environments (Montzka et al., 2011; Travis et al., 2020). Trace organic species such as acetaldehyde and isoprene are important reactive carbon reservoirs and indicators of biological processes in the air/sea interface. These organics may act as precursors for organic aerosol formation in pristine areas where models frequently underestimate their abundance (Wang et al., 2019).

Measurements of the fluxes of key species including O_3, NO_x, and marine sourced organics are needed to advance the understanding of air-sea exchange and its impact on the atmosphere. Ozone deposition velocities have been measured in a limited number of locations and can vary widely (Hannun et al., 2020; Helmig et al., 2012; Novak et al., 2020), but remain an important uncertainty in the marine O_3 budget. Additional high-quality measurements of this deposition rate are urgently needed. Nitrogen oxides in pristine marine environments have almost always been measured in higher abundance than can be explained by known sources, which are mostly limited to transport of continental or lightning NO_x into the MBL. Numerous mechanisms have been proposed that might act as sources of NO_x over the ocean. These include the direct photolytic production of NO_x (Carpenter and Nightingale, 2015; Reed et al., 2017) or HONO (Crilley et al., 2021) from photolysis of nitrate in the surface sea waters or in aerosols in the MBL, as well as biotic mechanisms which may be more prevalent in oxygen depletion zones. While differences between modeled and measured NO_x have implied a missing marine source, direct flux measurements that could confirm a marine source of NO_x have not been reported.

While the NASA Atmospheric Tomography (ATom) mission provided global scale measurements of O_3, NO_x and some organic compounds, only O_3 was measured with sufficient precision to perform eddy-covariance flux calculations. Fast measurements of non-oxygenated organics such as DMS and isoprene were not available on that mission. In addition, dwell time in the MBL, which allowed for some EC-Flux

measurements of O_3 deposition velocity, was only a minor part of the flight time. AEROMMA data will be used to expand our knowledge of air/sea exchange of these species by focusing flight hours on lower altitudes (~500 feet) and stacked flight legs allowing for measurement of the flux divergence near the sea surface. Also available on AEROMMA will be higher precision measurements of NO (LIF) (Rollins et al., 2020) and many organics (Vocus-PTR) which should allow for concurrent flux measurements of the light organics.

2.2.4. Marine aerosols and radiative impacts

Marine aerosols are produced primarily through three processes: sea-spray, secondary production of sulfate, and secondary production of organics. Marine aerosols can affect the amount of solar radiation reaching the Earth's surface through the production of CCN (Figure 11). The remote marine atmosphere is particularly sensitive to the production of additional CCN due to the low concentrations of CCN in this environment. Production of CCN can dramatically change the number and size of cloud droplets (Andreae and Rosenfeld, 2008; Moore et al., 2013). One study in particular observed a doubling in the cloud droplet number concentration as a result of a marine aerosol production associated with a phytoplankton bloom in the Southern Ocean, resulting in a calculated change in the local radiative flux of -15 W m^{-2} (Meskhidze and Nenes, 2006). These indirect effects of marine aerosols on clouds remain the largest uncertainty in current IPCC radiative forcing estimates. Therefore, parameterization of the sources of aerosols is important to understanding changes in Earth's radiation balance in response to changes in the burden and properties of these aerosols due to changing climate. In-situ atmospheric measurements with high spatial resolution of MBL aerosol loading and microphysical properties, effects of cloud processing and entrainment of aerosols from the free troposphere and non-sea salt sulfate are required to improve parameterization of ocean ecosystem-CCN-clouds for Earth system models.

Although direct anthropogenic emissions of SO_2 currently dominate indirect biogenic sources on a global scale, natural DMS emissions may have a more important impact on global climate. Anthropogenic SO_2 emissions originate primarily from northern midlatitude continental point sources, and the SO_2 atmospheric lifetime of approximately a few days limits the resulting global impact. DMS, on the other hand, is emitted over vast regions of Earth's oceans, and is the main source of particulate sulfate over the majority of the tropical marine boundary layer. These particles in turn play an important role in controlling the albedo of tropical marine cumulus clouds. Global anthropogenic SO_2 is expected to continue to decrease as a result of emissions regulation (Klimont et al., 2013; Krotkov et al., 2016), while emissions of DMS continue to increase in a warming climate (Galí et al., 2019; Grandey and Wang, 2015), further increasing the relative impact of the DMS fraction of global reactive sulfur in the future.

Globally, the most important source region for new particles is thought to be the tropical free and upper troposphere (UT) (Williamson et al., 2019). Trace gases in this region are primarily transported there via intense tropical deep convection, bringing air from the marine boundary layer into the UT. The small amount of SO_2 in this region (which is a key ingredient for new particle formation) is therefore most likely sourced from oxidation of DMS. Understanding the SO_2 yield from DMS oxidation is therefore key to understanding the availability of SO_2 for UT aerosol nucleation and growth.

Nucleation and growth of aerosol particles to reach CCN active sizes is a global phenomenon which has control over CCN concentrations in clean environments (Dunne et al., 2016; Williamson et al., 2019). Limitations in the understanding of the chemistry controlling aerosol nucleation and growth rates in the

cleanest marine environments leads to a major uncertainty in the abundance of CCN in preindustrial times and is one of the primary reasons for the current magnitude of uncertainty in aerosol indirect effect on global climate (Carslaw et al., 2013; Gordon et al., 2016). Observations in regions with limited influence from anthropogenic emissions have demonstrated that new particle formation (NPF) can occur in pristine regions near Earth's surface. Many studies conducted in forested regions (*e.g.*, (Andreae et al., 2022)) have demonstrated frequent observations of NPF that are likely due to condensation of species other than H_2SO_4. Current understanding centers around the idea that low volatility organic compounds may be formed by oxidation of biogenic VOCs, either by organic peroxide formation from $RO_2 + RO_2$ chemistry, or from autoxidation processes, both of which can only occur in environments with very low NO concentrations and long peroxy radical lifetimes (Bianchi et al., 2019). A number of studies have demonstrated that NPF at some coastal sites is associated with iodine chemistry (McFiggans et al., 2010; Sipila et al., 2016) occurring during exposure of algal species at low tide. However, characterization of NPF over the open ocean which might be of clear global importance is lacking.

Veres et al. (2020) presented anecdotal evidence from observations during ATom that biogenic sulfur chemistry very likely results in new particle formation in outflow regions of marine cloud decks. However, a comprehensive suite of measurements and significant dwell time observing aerosol nucleation and growth was not possible during ATom. An understanding of MBL NPF sufficient for implementation into global climate models would require detailed in-situ observations that could fully track NPF events in time and characterize their chemistry well enough to confidently constrain a useful parameterization.

The chemical and microphysical payload that will be deployed for AEROMMA will provide a much more detailed characterization of the chemical mechanisms of NPF in the marine atmosphere. AEROMMA will target the sampling of regions over the open ocean likely to experience NPF, such as open cell cloud structures, and dwell sufficiently long in those regions to derive aerosol nucleation and growth rates. Such a sampling strategy is challenging because NPF events are inherently fleeting and will require real-time guidance based on satellite imagery of locations that appear likely to provide the conditions for those events. The gas-phase chemical observations available will allow for identification of the role specific species, such as DMS oxidation products, play in the nucleation or growth periods of NPF.

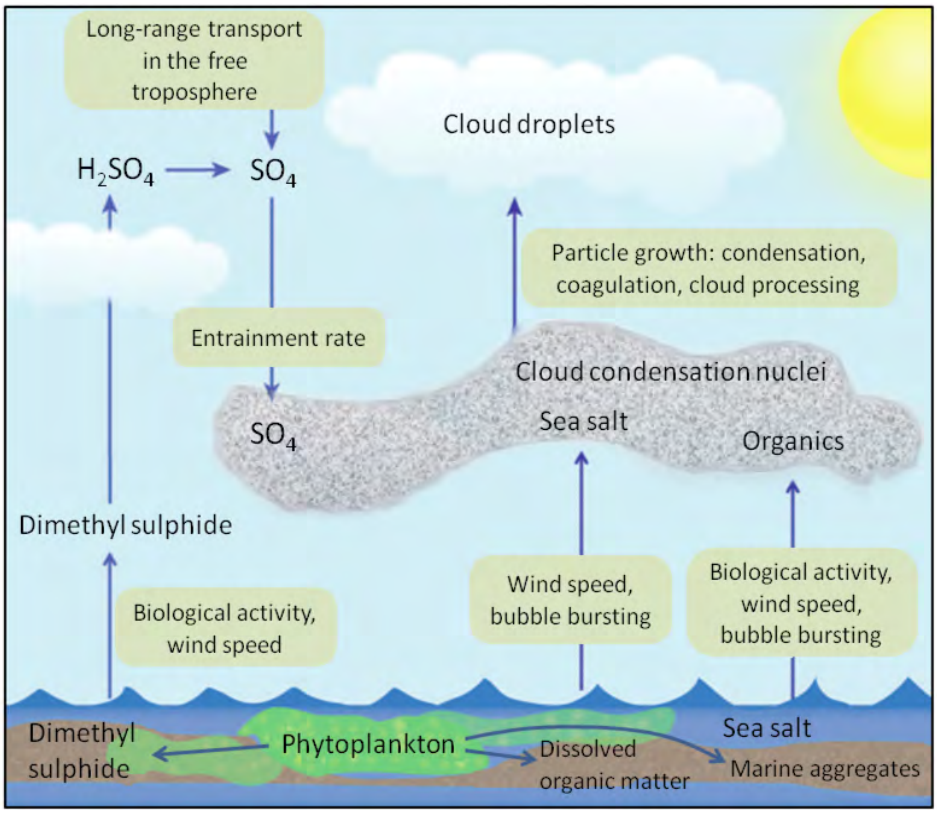

Figure 11: Linkages between air-sea exchange and the production of CCN in the remote marine atmosphere [*Quinn and Bates*, 2011]**.**

2.3. Spaceborne atmospheric composition capabilities during AEROMMA

2.3.1. Current and planned geostationary satellite observations

NOAA's Geostationary Operational Environmental Satellite (GOES) - R Series (https://www.goes-r.gov/) weather satellites are currently in geostationary orbit over North America. The first two of the four satellites have been launched; GOES-16 (East), GOES-17 (West), and GOES-18 have been operational since 2017, 2019, and 2022, respectively. The onboard Advanced Baseline Imager (ABI) consists of 16 spectral bands in the visible, near-infrared and infrared, and "tracks and monitors cloud formation, atmospheric motion, convection, land surface temperature, ocean dynamics, flow of water, fire, smoke, volcanic ash plumes, aerosols and air quality, and vegetative health" (https://www.goes-r.gov/spacesegment/abi.html). The GOES-16/GOES-17 satellite imagery from ABI is able to scan the Continental US and Pacific U.S. (including Hawaii) at 0.5 - 2 km spatial resolution every five minutes and can be used to identify areas of cloudy and cloud-free scenes over continental, coastal, and remote marine atmospheres.

GOES-16 and 17 satellite imagery were used extensively during past aircraft missions such as NOAA/NASA Fire Influence on Regional to Global Environments and Air Quality (FIREX-AQ 2019) and the Atlantic Tradewind Ocean-Atmosphere Mesoscale Interaction Campaign (ATOMIC 2020) for flight planning. Smoke plume images were used to direct the NASA DC-8, the NOAA Twin Otter, and the NASA ER-2 to the fires in the western US wildfires and detections of small fires were used to find agricultural burns with the NASA DC-8 in the southeastern U.S.. In addition, Narenpitak et al. (2021) used GOES-16 satellite imagery for coordinated airborne and shipborne measurements during ATOMIC 2020. The measurements and satellite imagery were used to improve the model representation of clouds from small shallow "sugar" to wide deep "flower" clouds (Narenpitak et al., 2021). In addition to detecting clouds and smoke, efforts have been made to retrieve atmospheric composition data, including diurnally-varying aerosol optical depth (AOD) from GOES-16 (Zhang et al., 2020).

TEMPO is a NASA Earth Venture Instrument with an anticipated launch in Q1 2023 (http://tempo.si.edu/overview.html) with data collection expected during the AEROMMA and other summer 2023 field studies. TEMPO will be located in geostationary orbit over North America providing data from one of three regions within a geostationary constellation of air pollution monitoring satellites. The other two instruments will be located over Europe (Sentinel 4 likely launching in 2024) and Asia (GEMS launched in 2020). By being in geostationary orbit, TEMPO will provide hourly observations over North America during the daytime at approximately 4.4 km x 2.1 km at the center of the field of regard (see Figure 12 for domain coverage and representation of expected NO_2 hotspots). The TEMPO instrument measures in the ultraviolet and visible (290-490 nm, 540-740 nm) spectrum (Zoogman et al., 2017). Species and data products that TEMPO will be able to detect include many species relevant to urban air quality, including columns of near-surface (0-2 km), free tropospheric, and total O_3, tropospheric and total NO_2, formaldehyde, glyoxal, SO_2, and aerosol optical depth (AOD). TEMPO can also measure select reactive halogens, such as bromine oxide (BrO) present in the marine boundary layer. Existing algorithms used to derive aerosol layer height from space-borne observations will be extended to TEMPO.

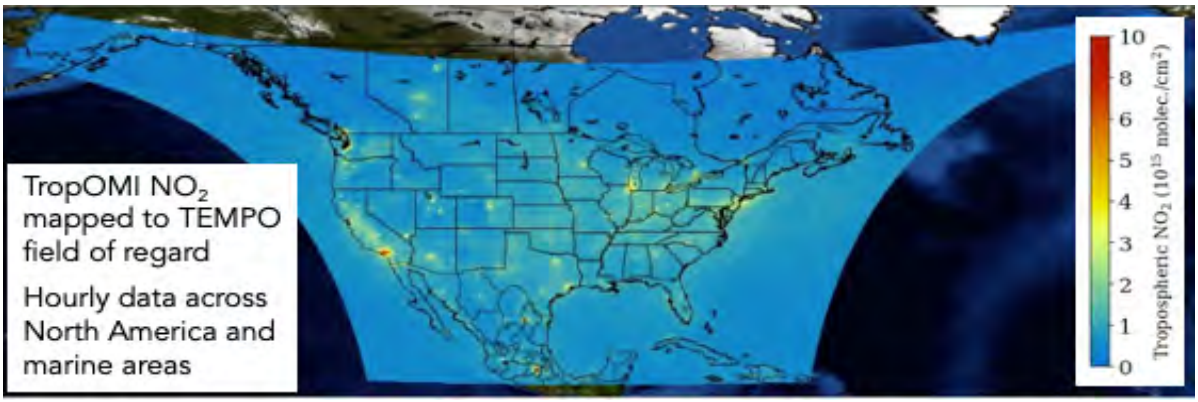

Figure 12: Tropospheric NO_2 from TropOMI on the TEMPO field of regard which includes most of the AEROMMA 2023 study region**.**

Currently, NOAA is planning the successor to the GOES-R series of satellites with the Geostationary Extended Observations (GEO-XO) satellite system to be launched in the 2030s (https://www.nesdis.noaa.gov/next-generation-satellites/geostationary-extended-observations-geoxo). The GEO-XO constellation will continue existing capabilities of GOES-R and also proposes new recommended capabilities addressing environmental challenges associated with weather, oceans, and climate. Core

capabilities that will continue include the visible/infrared imager. New recommended capabilities relevant to AEROMMA include Atmospheric Composition (a follow-on to NASA TEMPO), Hyperspectral Infrared Sounder, and Ocean Color Imager (see Figure 13).

Figure 13: The GeoXO constellation planned for 2030 and beyond**.**

The recommended configuration of the Atmospheric Composition instrument is a UV-VIS spectrometer similar in specifications to TEMPO. It is important to note that capabilities for monitoring atmospheric composition are not limited to species in the UV-visible spectrum alone, but also in the shortwave-IR, midwave-IR, and thermal-IR. Many trace gases can be retrieved from the IASI/MetOp sounder (Clerbaux et al., 2009), which include greenhouse gases (e.g., CO_2, CH_4, N_2O), carbon monoxide (CO), and reactive gases (e.g., SO_2, NH_3, VOCs such as CFCs, OCS, ethene, methanol, formic acid, and PAN). Airborne data collected from AEROMMA will provide insights into what might be observed from a Hyperspectral Infrared Sounder and/or partner payload with short- to thermal-IR capabilities, in conjunction with trace gas and aerosol species remotely sensed by a UV-VIS Atmospheric Composition instrument. This will also provide insights into extending capabilities to compounds such as isoprene of the Joint Polar Satellite System (JPSS) Cross-track Infrared Sounder (CrIS) (Wells et al., 2020; Wells et al., 2022).

2.3.2. Polar-Orbiting satellite science

Polar-orbiting satellites can provide global coverage of trace gases and aerosols at midday, which complement observations from geostationary satellites over targeted domains. To date, polar-orbiting satellites have helped improve understanding of emission sources and trends, and nonlinear chemical processes. NOAA CSL scientists have contributed to studies using TROPOMI NO_2 to constrain urban and background sources of US NO_x emissions (Li et al., 2021), evaluate changes in NO_x due to COVID-19 (Kondragunta et al., 2021), and assess inequality in NO_2 exposures (Demetillo et al., 2021; Demetillo et al., 2020). Kim et al. (2018) illustrated the importance of high-resolution a-priori profiles of formaldehyde for spaceborne observations over the Los Angeles basin. Modeling of the New York City region suggested the potential of peroxyacetyl nitrate (PAN) along with formaldehyde, both can be remotely sensed, to constrain

anthropogenic VOC emissions (Coggon et al., 2021). NOAA CSL field campaign data have been used to advance new retrievals of reactive VOCs from CrIS, including isoprene (Wells et al., 2020). CrIS retrievals have helped reveal the importance of vehicular sources of ammonia in Los Angeles (Cao et al., 2020). Lastly, TROPOMI NO_2 and CH_4 retrievals illustrate the intersection of co-emitted air pollutants and greenhouse gases, including over oil and gas fields (Francoeur et al., 2021). Spaceborne atmospheric composition capabilities have advanced greatly, and the AEROMMA campaign will help ensure continued advancement of satellite algorithms of trace gases and aerosols, and improved model representations of emissions and chemistry over the North American continent.

2.3.3. Satellite retrievals evaluations from ground-based networks and previous field experiments

Ground-based networks of remote sensors, including Pandora spectrometers within the Pandonia Global Network (PGN) (https://www.pandonia-global-network.org/) and AERONET (https://aeronet.gsfc.nasa.gov/) provide a reference dataset that can be used to characterize uncertainties in satellite retrievals of trace gases and aerosols. Figure 14 shows Pandora and AERONET sites, located in urban regions that will be targeted by AEROMMA and are within the TEMPO field of regard. All Pandora sites retrieve columns of NO_2 and O_3, and some also SO_2 and formaldehyde. The AERONET sites retrieve aerosol optical depth (AOD).

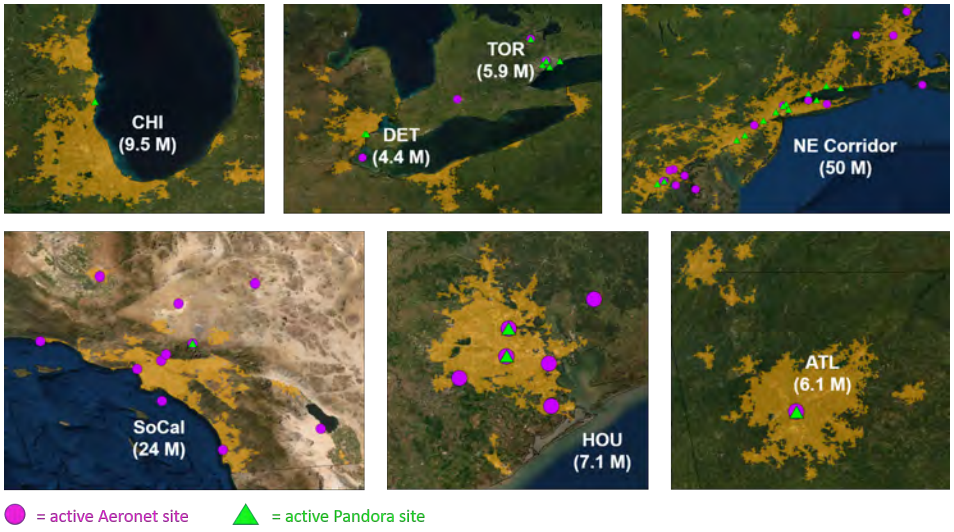

Figure 14. Sites that are currently active from AERONET (purple) and Pandora (green) located in the AEROMMA target city regions.

Zhang et al. (2020a) demonstrated the importance of bias-correcting GOES-16 AOD retrievals using empirical observations from AERONET (Figure 15). This example highlights the critical importance of field-intensive data, along with ground-based remote sensing networks, to evaluate and improve satellite retrievals of atmospheric composition.

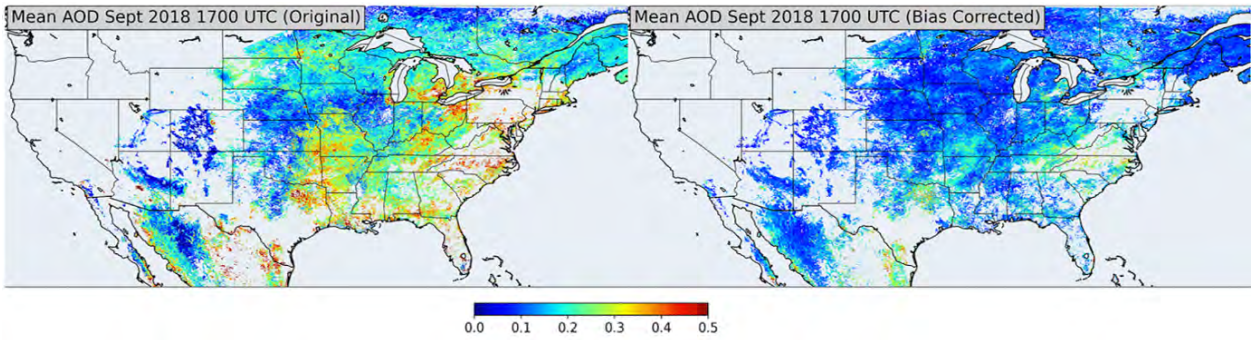

Figure 15. GOES-16 ABI AOD without and with empirical bias correction (Zhang et al., 2020a).

Over the remote ocean, airborne measurements from the Atmospheric Tomography Missions (ATom) have been used to evaluate satellite retrievals of AOD. Brock et al. (2021) derived aerosol extinction profiles and AOD by combining in-situ aerosol measurements of dry size distribution, ambient size distribution, single particle composition, bulk composition, black carbon, and water-soluble brown carbon, along with meteorological parameters (H_2O, temperature, pressure) and compositional, hygroscopic growth, and optical models (see Figure 16). From the in-situ derived aerosol extinction profiles, the sources of aerosols can also be distinguished, including biomass burning, sulfate/organic aerosol, sea salt, and dust. This helps to improve evaluation of satellite AOD products, such as from the Suomi-NPP Visible Infrared Imaging Radiometer Suite (VIIRS). Improving satellite AOD products and understanding sources of aerosols over open and coastal ocean helps increase confidence in ingesting satellite AOD for NOAA global forecast models.

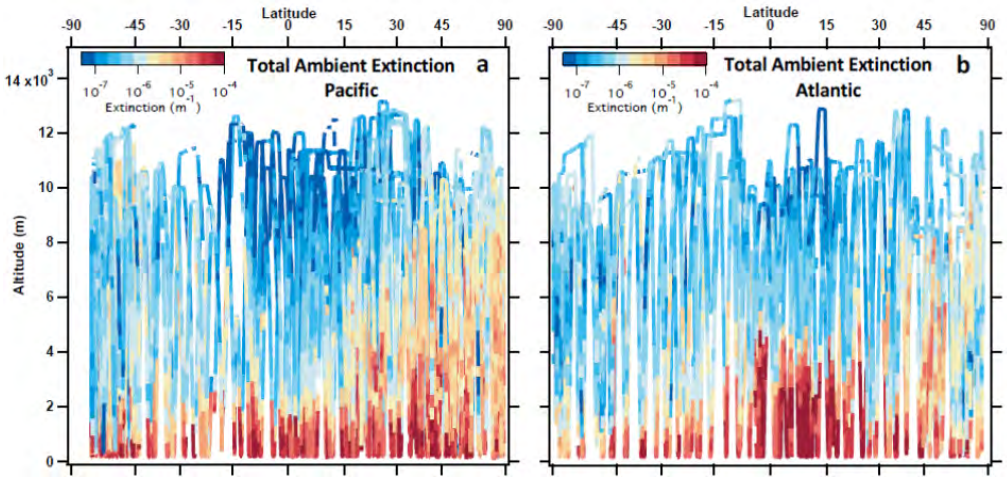

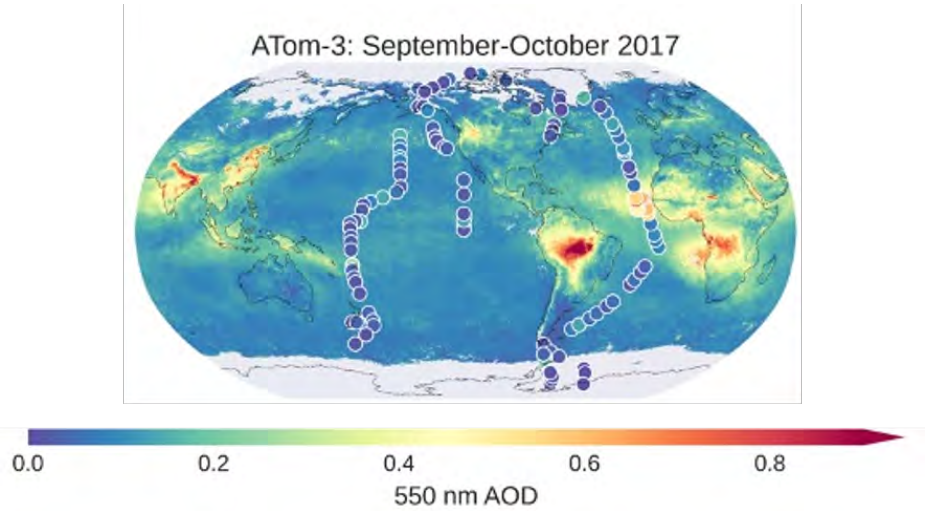

Figure 16: (top from Brock et al. (2021)) Aerosol extinction profiles derived from in-situ airborne instrumentation on-board the NASA DC-8 during the ATom field campaign. (bottom) Evaluation of AOD derived from airborne data with Suomi-NPP/VIIRS AOD products.

2.3.4. NOAA User Readiness Plan

In its value assessment of atmospheric composition capabilities (Frost et al., 2020), NOAA outlined 7 application areas on: (1) Air Quality Forecasting, (2) Weather and Climate Forecasting, (3) Fire Weather Forecasting, (4) Hazards Forecasting, (5) Stratospheric Ozone Monitoring, (6) Greenhouse Gas Monitoring, and (7) Air Quality Monitoring. The data collected from AEROMMA across both megacity and marine environments will provide data that will inform GEO-XO and demonstrate its potential to contribute to several of these application areas, including on air quality forecasting, weather and climate forecasting, greenhouse gas monitoring, and air quality monitoring. AEROMMA provides the opportunity to assess the enhanced capabilities of TEMPO during its first summer of measurements to monitor air pollution over the continental U.S. and explore whether data delivered can be utilized in operational air quality forecasting. In partnership with the U.S. Environmental Protection Agency, NOAA issues forecast guidance and warns the public of poor air quality episodes through its National Air Quality Forecast Capability (NAQFC), which is part of the Unified Forecast System (UFS). Figure 17 highlights the importance of advancing the NAQFC. In the U.S., annually over 100,000 premature deaths are associated with enhanced ozone and $PM_{2.5}$, greatly exceeding the number of deaths associated with other weather-related fatalities, which amount to 500 per year combined (Fann et al., 2012).

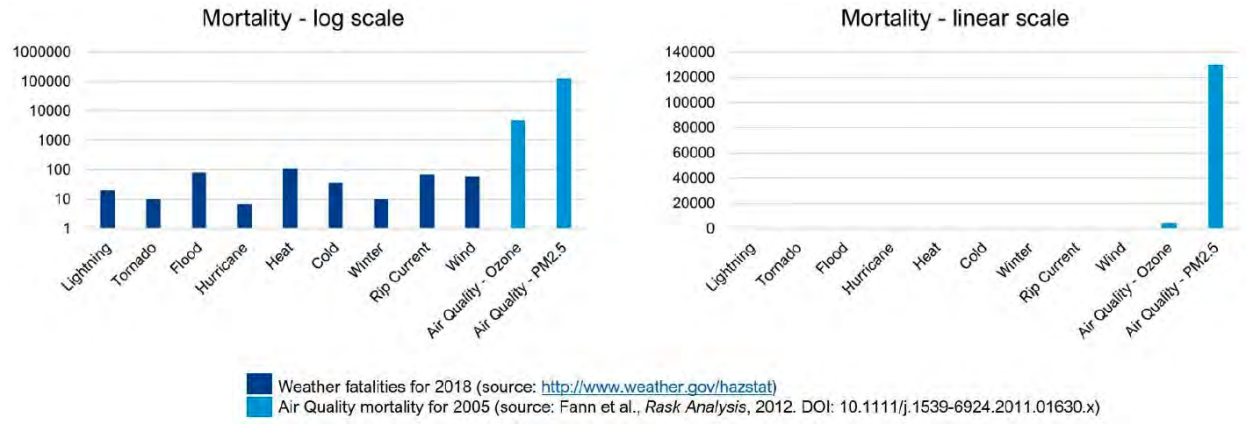

Figure 17: The U.S. weather mortality rates (figure from GeoXO Value Assessment, 2020)**.**

Field data collected over the marine atmosphere will also aid Earth System Models (https://www.gfdl.noaa.gov/earth-system-models/) developed by the NOAA Geophysical Fluid Dynamics Laboratory, by improving oceanic emissions and chemical processes that affect chemistry-climate interactions. Measurements over the North American continent will help improve anthropogenic and biogenic emissions that affect climate, and provide observations that leverage global-to-regional refinement capabilities of the Finite Volume Cubed-Sphere (FV3) dynamical core (https://www.gfdl.noaa.gov/fv3/).

Because TEMPO is a new satellite instrument providing the first hourly observation capabilities of air pollution over greater North America, it is important to evaluate the advanced capabilities of TEMPO and reduce risk of utilizing satellite data for forecasting and regulatory applications by characterizing uncertainties. Specifically, it is important to characterize uncertainty in relating satellite columns to surface concentrations.

3. Platforms in summer 2023

AEROMMA 2023 will be part of a large multi-platform experiment that integrates the NOAA CSL activities with simultaneous related efforts from several other agencies and partners using airborne and surface platforms. The coordinated effort in 2023 is named AGES+ (**A**EROMMA+CUPiDS, **G**OTHAAM, **E**PCAPE, **S**TAQS, and others).

Research platforms for the AGES 2023 coordinated field activities as well as routine air quality monitoring are listed in Table 1 and details for each effort will be discussed below. An overview of the various deployment areas is pictured in Figure 18.

Platform	Experiment name	AEROMMA contact PIs	Affiliation	Sponsor	Web resource
Aircraft					
NASA DC-8	AEROMMA (Atmospheric Emissions and Reactions Observed from Megacities to Marine Areas)	Urban: Carsten Warneke, Rebecca Schwantes Marine: Patrick	NOAA CSL	NOAA, NOAA NESDIS, NOAA	https://csl.noaa.gov/projects/aeromma/

		Veres, Drew Rollins		GeoXO	
NOAA Twin Otter	CUPiDS (Coastal Urban Plume Dynamics Study)	Sunil Baidar, Alan Brewer	NOAA CSL	NOAA	https://csl.noaa.gov/projects/aeromma/cupids/
NASA GV and GIII	STAQS (Synergistic TEMPO Air Quality Science)	Laura Judd John Sullivan	NASA LaRC NASA GSFC	NASA	https://www-air.larc.nasa.gov/missions/staqs
NCAR/NSF C-130	GOTHAAM (Greater NY Oxidant, Trace gas, Halogen, and Aerosol Airborne Mission)	John Mak	Stony Brook	NSF	https://www.nsf.gov/awardsearch/showAward?AWD_ID=2023574&HistoricalAwards=false
NPS Twin Otter	SCILLA (Southern California Interactions of Low cloud and Land Aerosol)	Mikael Witte	Naval Postgraduate School	ONR, DOE	
ARL/UMD Cessna	NEC-AQ-GHG (NEC Air Quality and Greenhouse Gas Study)	Xinrong Ren Russ Dickerson	NOAA ARL U. Maryland	NOAA ARL	
Ground sites					
NYC CUNY	NYC-METS (New York City metropolitan Measurements of Emissions and TransformationS)	Drew Gentner, Andrew Lambe	Yale, Aerodyne	NOAA AC4	https://csl.noaa.gov/projects/aeromma/partners/NYC-METS_ProjectSummary&MeasurementLocations.pdf
NYC Yale Coastal Site	NYC-METS	Drew Gentner, Andrew Lambe	Yale, Aerodyne	NOAA AC4	https://csl.noaa.gov/projects/aeromma/partners/NYC-METS_ProjectSummary&MeasurementLocations.pdf
NYC Minneola	FROG-NY (Fluxes of Reactive Organic Gases in New York)	Delphine Farmer, Dylan Millet	CSU, U. Minnesota	NOAA AC4	
Atlanta		Nga Lee Ng, Jennifer Kaiser	Georgia Tech.	NSF, NOAA AC4	
Toronto	THE CIX (Toronto Halogens, Emissions, Contaminants, and Inorganics eXperiment)	Cora Young	York U.	Various	www.cjygroup.com/the-cix
Scripps Pier and Mt. Soledad, La Jolla	EPCAPE (Eastern Pacific Cloud Aerosol Precipitation Experiment)	Lynn Russell	Scripps	DOE, NSF	https://www.arm.gov/research/campaigns/amf2023epcape
Long term monitoring					
7 cities and	TOLNet (Tropospheric	John Sullivan	NASA	NASA	https://www-

mobile units (part of STAQS)	Ozone Lidar Network)		Goddard		air.larc.nasa.gov/missions/TOLNet/
Globally distributed	AERONET (Aerosol Robotic Network)	David Giles	NASA GSFC	NASA	https://aeronet.gsfc.nasa.gov/
multiple locations	Pandonia Global Network	Thomas Hanisco	NASA GSFC	NASA	https://pandora.gsfc.nasa.gov/
43 cities	PAMS (Photochemical Assessment Monitoring Stations)	Luke Valin	EPA	EPA	https://www.epa.gov/amtic/photochemical-assessment-monitoring-stations-pams
Indianapolis, Los Angeles, North East Corridor	Urban Test Bed Measurements: greenhouse gas fluxes	Kimberly Mueller, Anna Karion	NIST	NIST	https://www.nist.gov/topics/greenhouse-gas-measurements/urban-test-beds
12 sites	ASCENT (Atmospheric Science and mEasurement NeTwork)	Nga Lee Ng	Georgia Tech.	NSF	https://ascent.research.gatech.edu

Table 1: Research platforms for AEROMMA 2023 and coordinated activities.

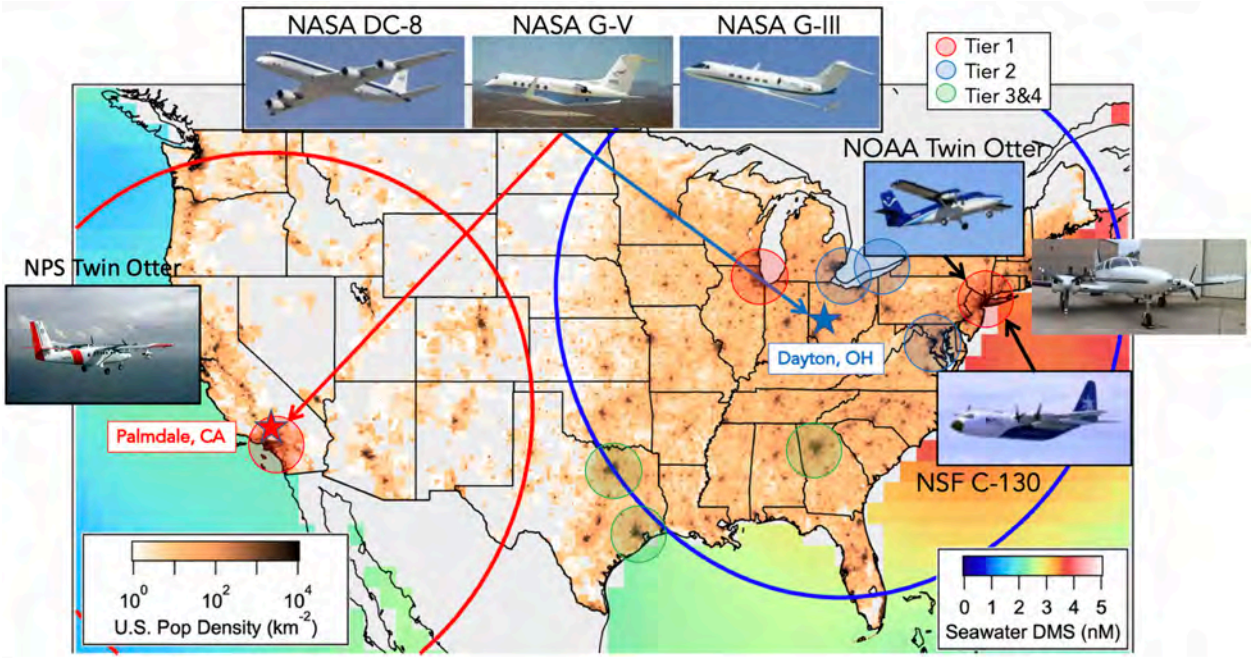

Figure 18: The deployment areas for AEROMMA and related activities in 2023.

4. Proposed experimental plan for AEROMMA 2023 (NASA DC-8)

4.1. AEROMMA 2023 science objectives and questions

4.1.1. Urban

AEROMMA 2023 will determine organics emissions and chemistry, including for understudied VCPs and cooking, in the most populated urban areas in the United States. The objective is to better understand the impact on ozone and aerosol formation and to study their relative importance on urban air quality compared to other sources of VOCs including energy-related and biogenic sources.

1. How well do **current emission inventories** quantify the flux of anthropogenic VOC emissions over North American cities, including VCPs, mobile sources, cooking, and industrial facilities?
2. How does the relative **distribution of VOC emissions** vary by city and population density, influencing the ratio of VCP to mobile source emissions?
3. What **chemical tracers** can be used to source apportion VOCs amongst VCPs, energy-related, cooking, and biogenic sources?
4. How have **emissions changed** between AEROMMA2023 and previous urban measurements (NEAQS2002, ICARTT2004, TEXAQS2006, CalNex2010, SENEX2013, WINTER2015, UWFPS2017, NY-ICE/LISTOS2018, FIREX-AQ2019, SUNVEx2021)?
5. What is the **composition of gas- and aerosol phase organics in the urban atmosphere**, including aromatics, alkanes, terpenes, cycloalkanes, oxygenated VOCs (including water-soluble organics such as alcohols, esters, glycols, and glycol ethers), and organic aerosol?
6. How well do reduced chemical mechanisms used in models represent the current composition of gas- and aerosol phase organics in the urban atmosphere including **oxygenated VOCs from VCPs**?
7. What is the relative role of **anthropogenic (including VCPs and cooking) versus biogenic VOCs** on ozone and SOA formation, and how does this vary between vegetated and non-vegetated regions?
8. How do **organics affect the evolution of particle** size, number distribution, and aerosol optical properties (e.g., brown carbon) in urban outflow, and to what extent does urban outflow contribute to cloud condensation nuclei (CCN) formation?
9. How well do models represent the oxidation chemistry of **understudied oxygenated VOCs from VCPs** and how does this impact simulated ozone and SOA formation in and downwind of urban regions?

AEROMMA 2023 will determine reactive nitrogen emissions and chemistry in major urban corridors (i.e., urban core to suburban and outlying rural areas) to understand the current importance of combustion and non-combustion sources, constrain trend analyses, and determine changes in the reactive nitrogen cycle chemistry and its influence on ozone and aerosol formation.

1. How well do **current emission inventories** quantify the flux of anthropogenic nitrogen oxides ($NO_x = NO + NO_2$) over North American cities, including from mobile sources, buildings, industrial facilities, and outlying agricultural regions and power generation?

2. How have **NO_x emissions changed** between AEROMMA2023 and previous NOAA-led measurements (e.g., NEAQS2002, ICARTT2004, TEXAQS2006, CalNex2010, SENEX2013, WINTER2015, UWFPS2017, NY-ICE/LISTOS2018, FIREX-AQ2019, SUNVEx2021)?
3. What is the **relative role of combustion** (e.g., mobile sources) versus non-combustion sources (e.g., agricultural soils) of NO_x, nitrous acid (HONO), ammonia (NH_3), and VOCs on ozone and particulate formation?
4. How do the formation rates of ozone and particulate matter in urban outflow evolve from **high to low NO_x regions**? What is the **spatial distribution** of high or low NO_x regimes?
5. What is the **speciation of oxidized reactive nitrogen** in the continental background and in urban outflow in 2023 and how well is it represented in models?
6. What is the **lifetime of NO_x**, and what are its major loss processes in 2023? How does this relate to and inform **diurnally resolved remote sensing** measurements?
7. How have changes in particulate matter composition, mass and surface area altered **heterogeneous processes**, particularly with respect to nitrogen oxides?
8. What is the distribution of nitrogen oxides, VOCs and other short-lived primary pollutants in urban areas, and how does this relate to **economic and racial disparities** at urban scale?

AEROMMA 2023 will: i) investigate the co-benefits between managing air quality and the carbon cycle; ii) investigate urban and coastal meteorology to better understand extreme heat effects on urban air quality; and iii) assess how the emissions in U.S. urban areas recover after the COVID-19 outbreak.

1. How well do **current emission inventories** quantify the flux of anthropogenic CO_2 and CH_4 emissions over North American cities, including from mobile sources, buildings, industrial facilities, natural gas infrastructure, and landfills?
2. How does the flux of **CO_2 and CH_4 emissions vary between North American cities**, including as a function of population density and age of energy infrastructure?
3. How does **extreme heat** affect urban and coastal meteorology, photochemistry, and ozone and aerosol formation?
4. How does the **urban canopy affect** urban heat islands, land-sea breezes, and planetary boundary layer (PBL) dynamics?
5. How have **emissions recovered** after the decrease in economic activities during COVID-19?
6. Have the distribution and magnitude of VCP, mobile source, and industrial emissions changed; **is there a new normal after COVID-19**?

4.1.2. Urban marine interface

AEROMMA 2023 will provide observations at the interface of the marine atmosphere and the urban airshed to quantify what impact marine emissions have on urban air quality and composition, and the impact of urban outflow on marine chemistry. Observations of SO_2 and aerosol abundance will resolve the relative contributions to SO_2, sulfate aerosols, and CCN from biogenic and anthropogenic sources.

1. How does anthropogenic **NO_x impact oxidation of biogenic sulfur** and the product distributions of secondary species in the marine atmosphere?

2. What impacts do **marine halogens** have on the atmospheric oxidant budget in coastal urban areas through the key marine reactive halogen species, e.g., $ClNO_2$, Cl_2, and BrO?
3. Are marine gases important factors for **ozone formation in coastal urban regions**?
4. How is the baseline continental O_3 controlled by O_3 imported from onshore flow?

4.1.3. Marine

AEROMMA 2023 will exploit the range and capabilities of the NASA DC-8 to sample the pristine marine atmosphere in regions with (1) limited to moderate impacts from anthropogenic sources, (2) high atmospheric burden from biogenic sulfur emissions, (3) stable meteorology, (4) a well-defined marine boundary layer, and (5) varying cloud fields. AEROMMA marine science foci will include two primary themes.

Investigation of the emissions and chemistry in the remote marine atmosphere that drive the formation of secondary products and marine aerosols. Flux observations will be used to better quantify the air-sea exchange of VOCs, NO_x, O_3, and halogen species to better understand the atmospheric budget of gas-phase precursor species in the remote atmosphere.

1. What are the sources of VOCs and **volatile sulfur in the remote marine** atmosphere?
2. How well do we understand the **net oceanic flux** of biogenic sulfur?
3. How do primary oceanic emissions of sea spray impact the **marine aerosol burden**, spatial distribution and properties?
4. At what rates are atmospheric gases and aerosol **deposited to the ocean's surface**?
5. How important is **NO_x that is emitted from the sea surface** or generated in the marine boundary layer compared to transported NO_x?
6. What are the emissions, fluxes, chemistry and transport of organic and inorganic **marine halogen species**?

Observations to better characterize the marine sulfur oxidation cycle and secondary aerosol formation and dependencies on key parameters such as temperature, NO_x, and background aerosol.

1. Do we sufficiently understand **oxidation of biogenic sulfur** and VOCs in the remote marine atmosphere?
2. What are the key details linking the oxidation of biogenic marine emissions to **aerosol production and growth**? Do biogenic species other than sulfuric acid generate new particles in the MBL or free troposphere?
3. What are the processes that drive the **removal of gases and aerosols** throughout the marine boundary layer?
4. What fraction of the organic aerosol is **primary versus secondary** at various time scales?
5. How well do **current models** represent primary and secondary marine aerosols and their radiative properties, and what are the largest associated uncertainties?
6. How do **aerosol optical properties** evolve due to secondary production and particle phase transitions?

7. What are the sources of **new particles in the remote troposphere**, how rapidly do they grow to CCN-active sizes, and how well are these processes represented in chemistry-climate models?

4.1.4. Satellite

AEROMMA 2023 will provide observations for proving and reducing risk of GEO-XO, JPSS, and GOES-R science and near real-time trace gas and aerosol products.

1. How well does the diurnal cycle of geostationary trace gas (**NO_2, HCHO, O_3**) and aerosol (**AOD and ALH**) products correspond to observations from heavy-lift in-situ aircraft, airborne remote sensing, and ground-based observing networks (e.g., Pandora and AERONET)?
2. How does the NO_x lifetime affect the interpretation of satellite retrievals of nitrogen dioxide (NO_2) as a **constraint on urban to rural NO_x** emission inventories?
3. How well do **TEMPO science and near real-time** data products correspond to existing polar-orbiting and geostationary satellites, including Sentinel-5P/TROPOMI, NOAA-20/OMPS, NOAA-20/VIIRS and GOES-16/17 ABI over urban and marine areas?
4. How well can **TEMPO tropospheric ozone and aerosol layer height** be derived over urban, coastal, and marine areas to improve vertical information of atmospheric composition?
5. What is the value of extending **NOAA JPSS and GeoXO** spaceborne infrared and UV-VIS remote sensing capabilities to include additional greenhouse gases and other reactive gas and aerosol precursors for monitoring emissions, air quality, and climate?

AEROMMA 2023 will provide field observations for evaluating NOAA's next generation weather-chemistry models and chemical data assimilation of atmospheric composition satellite data.

1. Does **chemical data assimilation** of TEMPO and GOES-R trace gas and aerosol products help improve near real-time emissions updating and air quality forecasting capabilities?
2. How well do next generation NOAA weather-chemistry models using the **FV3 dynamical core** (e.g., RRFS-CMAQ) perform when evaluated with aircraft and geostationary/polar-orbiting satellite observations?
3. How can NOAA field campaigns lead to more direct improvements of NOAA operational air quality models using tools such as MELODIES MONET?

4.2. Deployment location and calendar

To meet the overall AEROMMA 2023 science objectives, the NASA DC-8 aircraft will be deployed out of Palmdale, CA and Dayton, OH. The combination of these locations provides the ideal access to both remote marine regions as well as populated urban centers, by minimizing the required aircraft transit times to regions of interest. With the long range of the DC-8, from Palmdale all major urban areas in the western half of the US and marine flights spanning a large portion of the Pacific Ocean can be reached and from Dayton, OH all major urban areas in the eastern half of the U.S..

The DC-8 deployment window runs from approximately June to mid-August, 2023. AEROMMA marine science goals are best accomplished in late spring and early summer, while urban science goals are better accomplished later in summer during ozone season. Therefore, flights will initially prioritize the marine science objectives and commence based out of Palmdale, CA in June. The AEROMMA project will afterwards have a one-week period of urban focused science flights and then participate in the NASA Student Airborne Research Program (SARP) in June based out of Palmdale, CA. AEROMMA will have a break in operations from late- June to late- July. Flight operations will transition to Dayton, OH from late-July to mid-August to conduct the remainder of the urban and satellite science focused research flights.

Palmdale, CA has been selected as the initial base of operations due to its proximity to marine environments with limited anthropogenic influence off the western coast of the US. In the near field, elevated marine sulfur chemistry in coastal regions is expected, which is a common feature globally, and was validated for coastal CA during an AEROMMA 2023 concept flight performed out of Palmdale, CA during the NASA SARP project in September 2019. Palmdale, CA will also provide the DC-8 access to the urban areas of Los Angeles and flight opportunities in the California Central Valley to investigate agricultural influences. The Salton Sea, where high DMS and halogen emissions have been previously observed, provides an additional region of interest to investigate sulfur oxidation in a region impacted by urban and agricultural emissions.

From Dayton, OH, the DC-8 can survey all the major urban areas on the east coast such as New York, Chicago, and Toronto, together with agriculture in Wisconsin, Iowa, and Illinois and other cities such as Atlanta, Houston, and Dallas. Anthropogenic outflow on the Eastern coast of the US provides ideal conditions to study the composition and aging of urban emission. The TROPOMI monthly average NO_2 map in Figure 18 clearly shows the large urban areas that will be investigated during AEROMMA 2023.

4.3. Potential DC-8 payload

The proposed DC-8 payload, shown in Figure 19 and listed in Table 2, is designed to characterize the atmospheric composition in urban and marine environments with detailed in-situ and remote sensing instruments that include a complete set of gas phase, aerosol composition and optical properties, and radiation measurements. Most instruments will have a high enough sampling frequency to enable wavelet eddy covariance flux measurements to determine emissions and deposition of VOCs, NO_x, CO, CO_2, and CH_4.

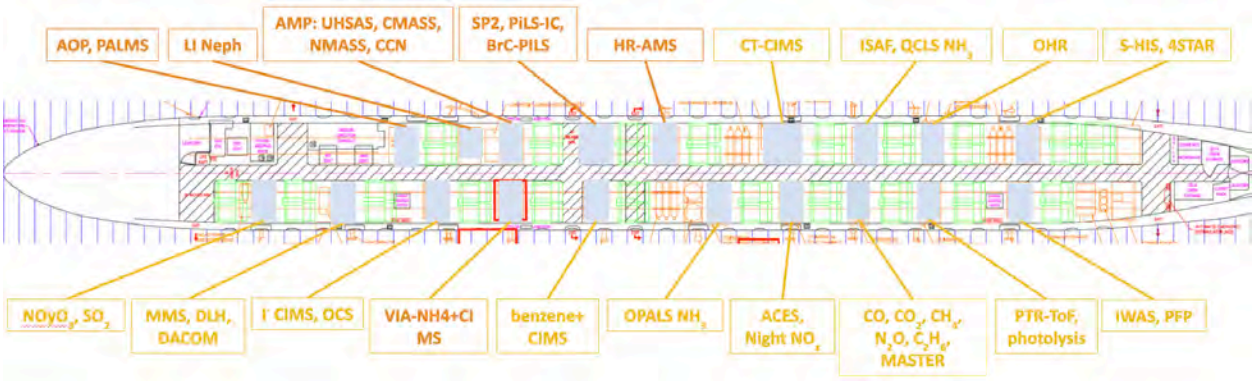

Figure 19: Suggested payload for the NASA DC-8 aircraft for AEROMMA. Diagram is current as of December 2022.

Species Measured	Technique	PI-name	Institution
Gas phase measurements			
O_3, NO, NO_2, NOy	$NOyO_3$	Andrew Rollins, Steven Brown, Jeff Peischl	NOAA CSL
HPMTF, PANs, HONO, OVOCs, $ClNO_2$, organic nitrogen	Iodide ToF-CIMS (I^- CIMS)	Patrick Veres, Chris Jernigan	NOAA CSL
CO, CO_2, CH_4, H_2O	Cavity Enhanced Absorption (LGR+Picarro)	Jeff Peischl	NOAA CSL
CO, CO_2, CH_4, N_2O, H_2O	DACOM, DLH	Glenn Diskin	NASA LaRC
SO_2	Laser Induced Fluorescence	Andrew Rollins	NOAA CSL
OCS	Cavity Enhanced Absorption	Andrew Rollins, Colin Gurganus	NOAA CSL
NH_3	QC-TILDAS (QCLS NH_3)	Ilana Pollack	CSU
NH_3	Open-Path Ammonia Laser Spectrometer (OPALS)	Mark Zondlo	Princeton
CH_3COCHO, CHOCHO, NO_2, UV aerosol extinction	Cavity Enhanced Spectrometer (ACES)	Carrie Womack	NOAA CSL
NO_2, O_3, NO_3, N_2O_5	NightNOx (NNOx)	Steven Brown	NOAA CSL
Speciated hydrocarbons and OVOCs	H_3O^+ Vocus ToF-CIMS (PTR-ToF)	Carsten Warneke	NOAA CSL
C_2-C_{10} Alkanes, C_2-C_4 Alkenes, C_6-C_9 Aromatics, C_1-C_5 Alkylnitrates, etc.	Whole Air Sampling (iWAS)	Jessica Gilman	NOAA CSL
Hydro- and halocarbons	Portable Flask Package (PFP)	John Miller	NOAA GML
Formaldehyde (HCHO)	Laser Induced Fluorescence (ISAF)	Jennifer Kaiser	Georgia Tech
Highly Oxygenated VOCs	Benzene+ Vocus ToF-CIMS (benzene+CIMS)	John Liggio	ECCC Canada
OH reactivity	Direct OH loss rate by LP–LIF (OHR)	Hendrik Fuchs	FZ Juelich
H_2O_2, organic peroxides, organic acids, isoprene oxidation products, etc.	CalTech-CIMS (CT-CIMS)	Paul Wennberg	CalTech
Aerosol measurements (physical/optical/chemical)			
Bulk aerosol composition, HNO_3	Filter sampling and mist chamber (PiLS-IC)	Amy Sullivan	CSU
BrC	Spectro-photometer (BrC PiLS)	Amy Sullivan	CSU
Aerosol absorption and extinction at multiple wavelengths and RH	Cavity ringdown extinction and photoacoustic absorption spectrometers (AOP)	Charles Brock	NOAA CSL

Aerosol scattering phase function at UV and visible (blue) wavelengths	Laser Imaging Nephelometer (Li-Neph)	Dan Murphy	NOAA CSL
Aerosol number density, size dist., and physical properties, CCN	Particle counters, nephelometers, etc. (UHSAS, CMASS, NMASS, CCN) (AMP)	Charles Brock, Rich Moore	NOAA CSL, NASA LaRC
BC concentration, size, mixing state	Humidified-Dual SP2	Joshua Schwarz	NOAA CSL
Submicron aerosol composition	Aerosol mass spectrometer (HR-AMS)	Ann Middlebrook	NOAA CSL
Submicron aerosol composition	Vocus Inlet for Aerosols with $NH4^+$ CIMS detection (VIA-NH4+CIMS)	Carsten Warneke	NOAA CSL
Single particle composition	PALMS	Daniel Cziczo	Purdue
Cloud probes	CARE	Bernadett Weinzierl	U. Vienna
Radiation/Remote sensing			
Zenith/nadir solar actinic flux and photolysis frequencies	4π-sr spectroradiometry (CCD)	Birger Bohn	FZ Juelich
Scanning High-resolution Interferometer Sounder (S-HIS)	thermal radiation at high spectral resolution)	Joseph Taylor	SSEC, U. Wisconsin
MODIS/ASTER Airborne Simulator (MASTER)	Multispectral Imager, VNIR/SWIR/MWIR/LWIR Imagery	Jeffrey Duvall, Jorge Gonzalez-cruz	NASA JPL, CCNY
4STAR (AOD profiles, NO2 columns above aircraft)	Spectrometer for Sky-Scanning, Sun-Tracking Atmospheric Research	Samuel Leblanc	BAER

Table 2: Proposed payload of the NASA DC-8 for AEROMMA 2023.

4.4. AEROMMA DC-8 flight plans

AEROMMA 2023 will require 150 NASA DC-8 flight hours, which includes test and transit flights and approximately 18 science flights. In addition, three flight days will be coordinated with NASA SARP.

4.4.1. Urban Flight Objectives

Up to 13 science flights are anticipated with two transit flights for urban areas as listed in Table 3. Flights will cover weekday/weekend, urban/rural gradients, and diurnal cycles with up to 100 hours. For science flights and 10 hours for transit. Depending on meteorological conditions each flight to a megacity can cover other smaller cities or more than one megacity. The priorities of the cities for AEROMMA are indicated by Tier 1-4 in Table 3. Two additional flights in Los Angeles and the Central Valley were already conducted during FIREX-AQ in 2019. Potential AEROMMA flight tracks are shown in Figure 20.

City	# of flights / city	# of 10 km profiles / flight	# of 4 km profiles / flight	Repeat Patterns / flight
Los Angeles (Tier 1)	3	0	9	3
New York (Tier 1)	4	2	4	2

Chicago (Tier 1)	4	2	4	2
Toronto (Tier 2)	2	2	4	2
Houston (Tier 3)	Back-up	2	1	1
Atlanta (Tier 3)	Back-up	2	4	2
Transit	2	2		

Table 3: Priority cities and number of flights and profiles for AEROMMA urban flights.

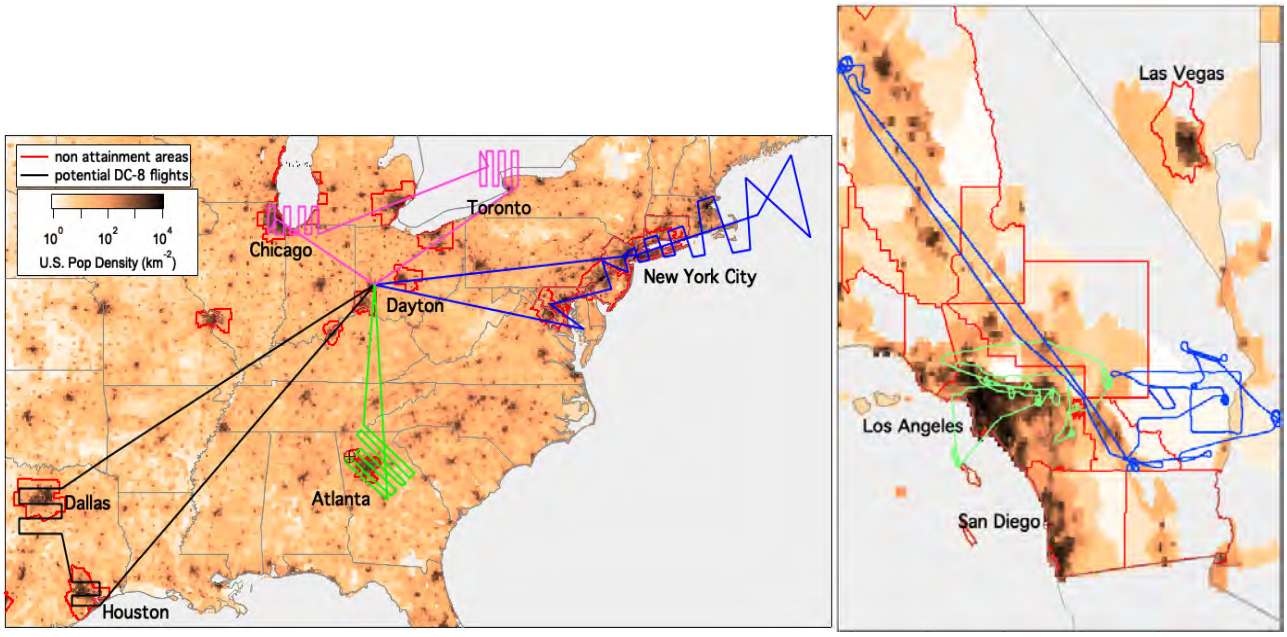

Figure 20: Examples of potential flight plans for the NASA DC-8 aircraft for urban focused flights over Los Angeles, New York City, Toronto, Chicago, Houston, Dallas, and Atlanta.

4.4.2. Satellite Flight Objectives

For every flight in urban areas, vertical profiles of in-situ measurements of NO_2, HCHO, glyoxal, aerosol extinction, and other atmospheric components for satellite science will be flown. As shown in Table 3, we plan to do 2-3 repeat patterns over each city to acquire diurnal information. During these repeat patterns, we plan to mostly fly in the PBL with up to 3 vertical profiles, which will generally be located upwind, near to, and downwind of each city and flown up to ~ 6 km in altitude. For most cities, we also plan to extend the ~6 km vertical profiles up to ~10 km in altitude as we arrive to and depart from a city target to acquire additional vertical information without much added flight time since we plan to transit to/from a city at ~10 km in altitude. Flights will be coordinated with the coincident NASA GV and GIII remote sensing aircraft during STAQS, as described below.

4.4.3. Marine Flight Objectives

During the marine focused component of the AEROMMA study, the NASA DC-8 aircraft will be deployed from Palmdale, CA. Palmdale, CA, which offers access to the marine/urban interface, low NO_x marine environments, high DMS emission fields, and the tropical Eastern Pacific. The marine deployment will consist of 4 research flights (up to 40 flight hours).

Flight plan designs will directly address the science questions presented in sections 4.2 and 4.3, and will largely focus on 3 regions of interest throughout the project, as shown in Figure 21: 1) southern, low altitude surveys of the tropics/subtropics with a focus on air/sea exchange, 2) observations in the North Pacific surveying sulfur chemistry and NPF, and 3) coastal Pacific (indicated by the grey circle in Figure 22) where a confluence of NO_x gradients from urban influence and high DMS emission fields are expected.

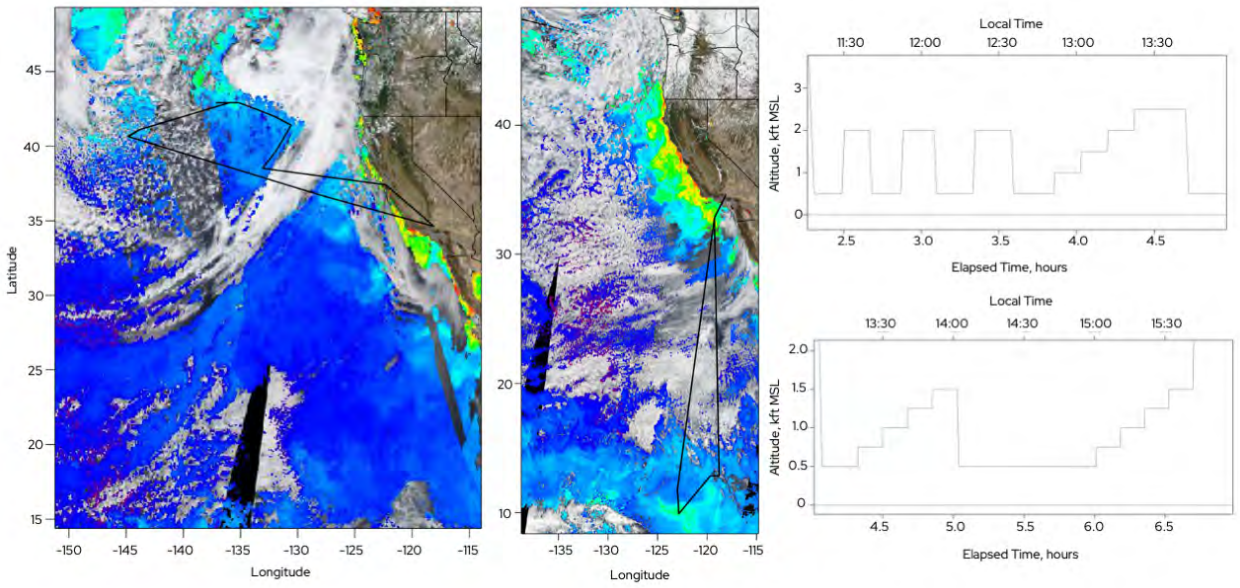

Figure 21: Examples of potential plans for the NASA DC-8 aircraft for marine focused research flights over the Pacific Ocean. Altitude profiles shown on the right are examples of the types of flight modules that will be used to perform vertical profile and airborne flux observations throughout the marine boundary layer.

5. Coordinated activities in summer 2023

5.1. Proposed experimental plan for CUPiDS 2023 (NOAA Twin Otter)

5.1.1. Science objectives

In order to better understand coastal meteorology and how it affects air quality in the New York City region, NOAA CSL will conduct the Coastal Urban Plume Dynamics Study (CUPiDS) in the summer

of 2023. CUPiDS will closely coordinate with the AEROMMA New York and support the AEROMMA science objectives related to urban emissions as affected by coastal meteorology.

An airborne scanning Doppler lidar operated from a NOAA Twin Otter aircraft will measure the vertical and horizontal structure of the evolving horizontal-wind field along its flight track over the U.S. East Coast to characterize the flows that carry plumes of air pollutants emitted from New York City (NYC) and other major areas along the urban corridor (Baltimore/Washington, Philadelphia, Boston). Data from the NOAA Twin Otter lidar will be used to study diurnal forcing of atmospheric dynamics on urban plume transport and mixing in coastal regions. Atmospheric effects such as the urban heat island and complex regional flows driven by sea/land breezes have a strong diurnal signature. They impact the depth to which urban emissions can mix in the boundary layer, and control the coherence and direction of low-level transport in coastal regions. If these processes are not properly represented in regional air quality models, the models will not accurately predict air quality in the region. In addition, the payload on the Twin Otter will include in-situ and column trace gas measurements to study reactive nitrogen emissions and their impact on ozone and aerosol formation, and evaluation of TEMPO products.

In addition to the AEROMMA science questions, important CUPiDS questions include:

- What flow regimes are conducive to high ozone in the NYC region?
- What is the role of sea-breeze circulations during daytime and land breezes at night on air quality in the NYC region?
- How does the atmospheric boundary layer evolve over land and water?
- What is the role of low-level jets in transporting pollutants into and out of the NYC region?
- How well do hi-res numerical models represent these features and how can we improve model performance?
- What are the spatial and vertical distributions of nitrogen oxides in the NYC region and how do they impact ozone and aerosol formation?
- How well can we quantify nitrogen oxides emissions by mass balance on the scale of megacities using airborne column, and in-situ NO_x measurements and wind profile measurements?

5.1.2. Deployment location and calendar

The NOAA Twin Otter aircraft will be deployed to the New York City region from approximately July 1 to August 8, 2023 for CUPiDS (Figure 22).

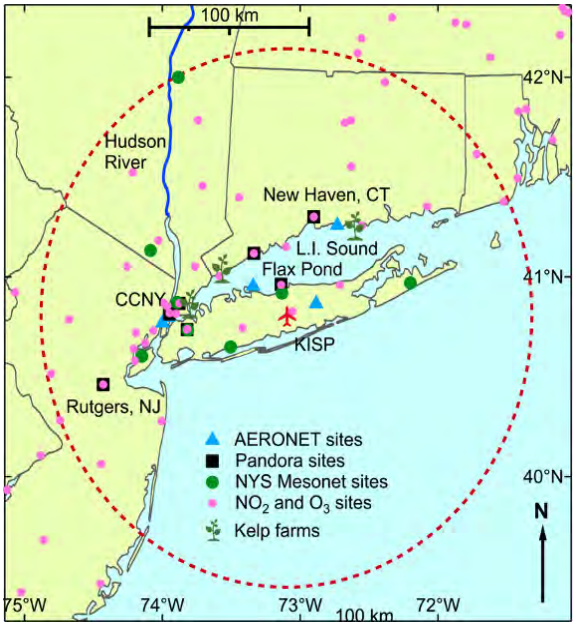

Figure 22: The study region for the NOAA Twin Otter for CUPiDS 2023.

5.1.3. Proposed payload

The proposed payload is pictured in Figure 23 and listed in detail in Table 4. The NOAA Twin Otter measurement systems will consist of a scanning Doppler lidar, developed by the NOAA CSL, which will measure profiles of horizontal winds, turbulence and aerosol backscatter intensity through the atmospheric boundary layer. Researchers from University of Colorado Boulder will deploy a MAX-DOAS on the Twin Otter to measure profiles/columns of HCHO, glyoxal, and NO_2. The payload will also include in-situ measurements of NO, NO_2, NO_y, O_3, CO, CO_2, H_2O, and CH_4. An upward/downward multi spectral radiometer will be used to identify land/ocean boundaries under the aircraft and will provide information on surface albedo, land usage, cloud cover and atmospheric haze conditions.

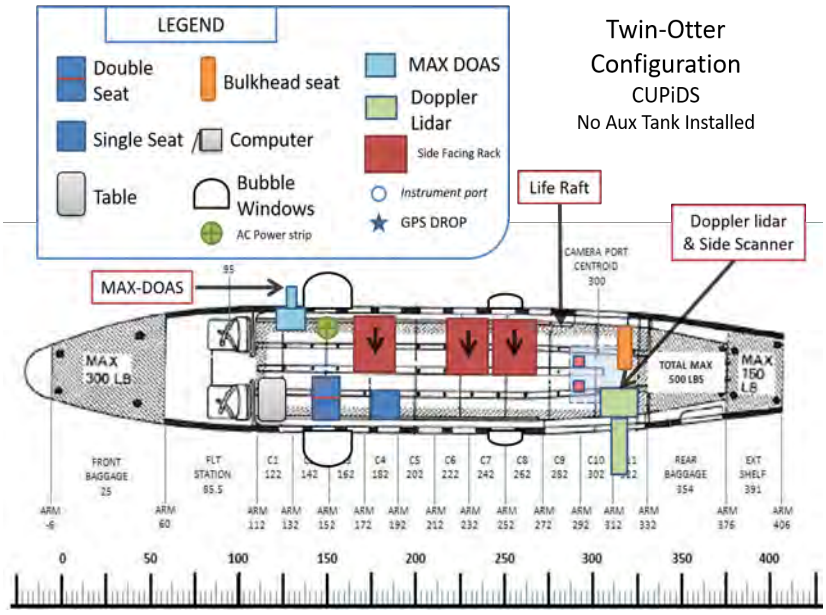

Figure 23: The proposed payload of the NOAA Twin Otter for CUPiDS 2023.

Species Measured	Technique	PI-name	Institution
Horizontal wind, turbulence and aerosol Backscatter intensity (ABI) profiles	Micro-pulse Scanning Doppler lidar	Alan Brewer	NOAA CSL
Multi spectral irradiance	Multi-channel radiometer	Alan Brewer	NOAA CSL
HCHO, glyoxal and NO_2 profiles/columns	Airborne MAX-DOAS	Rainer Volkamer	CU Boulder
NO, NO_2, NO_y, O_3	Cavity Ring Down	Steve Brown	NOAA CSL
CO, CO_2, CH_4, H_2O	Cavity Enhanced Absorption	Colm Sweeney	NOAA GML
Met package (P, T, RH)	AIMMS Probe	Alan Brewer	NOAA CSL

Table 4: Suggested payload of the NOAA Twin Otter for CUPiDS 2023.

5.1.4. CUPiDS flight plans

CUPiDS 2023 will include 175 NOAA Twin Otter flight hours and approximately 34 science flights. Two flights are anticipated every other day to target coastal dynamics over the Long Island Sound and New York Bight, and urban plumes along the Northeast Corridor, and to provide necessary statistics to improve NOAA weather-chemistry model predictions of coastal meteorology and urban plumes of gas-phase species. The Twin Otter will be based in the NYC area during the field campaign but may travel to other urban centers on the east coast.

The Twin Otter will perform cross plume transects advancing down wind of major urban centers to track the evolution of the urban plume. Transects oriented perpendicular to advancing onshore flow convergence fronts will be performed to determine the depth and lateral extent of the features and to determine their propagation speed and arrival time. To study the urban heat island effect, the Twin Otter will perform repeated transects across the urban center to investigate the development of the heat island throughout the day and into the evening both dynamically and in enhanced aerosol loading. Flight plans

will also include transects inside the boundary layer, and missed approaches at airports to characterize both spatial and vertical distribution of pollutants in the region.

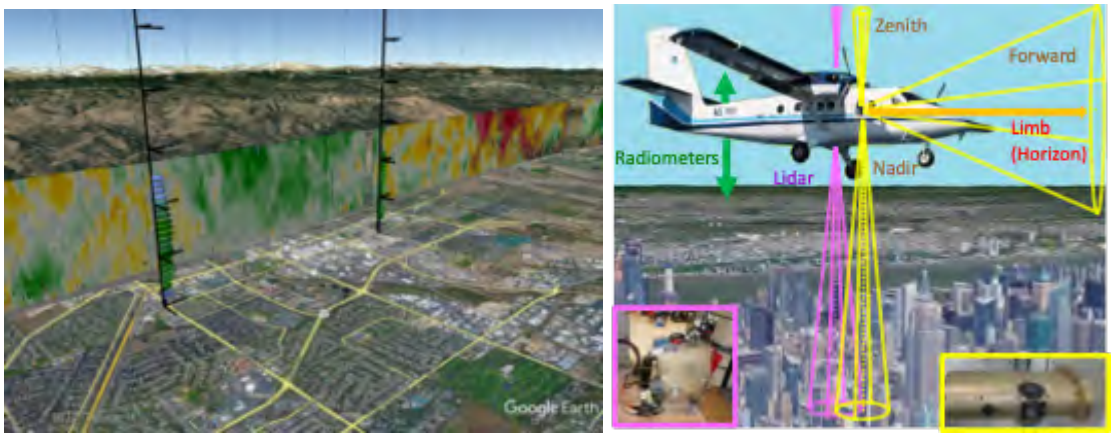

Figure 24: Example of airborne Doppler lidar vertical velocity data. (Left) and sensing volumes of remote measurements made from the NOAA Twin Otter during CUPiDS 2023 (Right).

5.2. Proposed experimental plan for STAQS 2023 (NASA GV and GIII)

5.2.1. Science Objectives

To accelerate TEMPO science soon after launch, the Synergistic TEMPO Air Quality Science (STAQS) mission seeks to integrate TEMPO satellite observations with traditional air quality monitoring to improve understanding of air quality science and increase societal benefit. STAQS will be conducted in summer 2023, targeting three primary domains in Los Angeles, Chicago, and New York City with ground and airborne based measurements. The framework for STAQS stems from measurements strategies and collaborations developed during airborne air quality studies from the last decade, most recently TRACER-AQ (Jensen et al., 2022). For STAQS, NASA is collaborating with the other scientific field studies listed within this section to build a synergistic observing system more robust than any singular entity could provide alone.

Objectives of STAQS include, but are not limited to:

- Evaluating TEMPO level 2 products geo-physically, spatially, and temporally
- Interpreting the temporal and spatial evolution of air quality events tracked by TEMPO
- Improving temporal estimates of anthropogenic, biogenic, and greenhouse gas emissions
- Assessing the benefit of assimilating TEMPO data into chemical transport models
- Linking air quality patterns to socio-demographic data

5.2.2. Deployment location, calendar, and payload

STAQS flights will coincide with AEROMMA flights by targeting New York, Chicago, and Los Angeles as the main targets as shown in Figure 25 and during the same time frame in July-August 2023 as shown in Figure 19. Over the course of summer 2023, up to 120 science flight hours on the NASA JSC G-V will be flown to collect data with the GeoCAPE Airborne Spectrometer (GCAS) and High Spectral Resolution Lidar (HSRL)-2 + Differential Optical Absorption Ozone. This payload was first demonstrated on this platform during the TRACER-AQ mission in September 2021 and provides repeated high-resolution mapping of NO_2, HCHO, ozone, and aerosols as an airborne proxy for TEMPO. Additionally, NASA will deploy the NASA LaRC G-3 with the High-Altitude Lidar Observatory (HALO) and Airborne Visible InfraRed Imaging Spectrometer - Next Generation (AVIRIS-NG) to provide a complementary view of methane and carbon dioxide. STAQS support also include the deployment of a suite of TOLNet lidars to multiple locations.

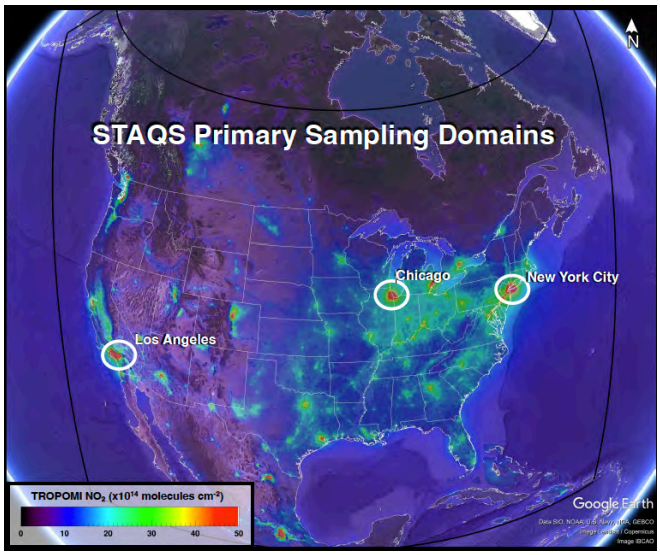

Figure 25: Map of the annual average TROPOMI NO_2 column density measurements for April 2018-March 2019 showing the currently planned primary (solid circles) sampling domains during STAQS within the TEMPO field of regard (black outline).

Species Measured on the Gulfstream aircraft	Technique	PI-name	Institution
NO_2, HCHO columns	GeoCAPE Airborne Spectrometer (GCAS)	Scott Janz	NASA GSFC
Aerosol and ozone profiles	High Spectral Resolution Lidar (HSRL)-2	John Hair	NASA LARC
Methane columns and aerosol profiles	High Altitude Lidar Observatory (HALO)	Amin Nehrir	NASA LARC
Methane and carbon dioxide emissions	Airborne Visible InfraRed Imaging Spectrometer - Next Generation (AVIRIS-NG)	Robert Green	JPL

Table 5: Confirmed instrument list of the NASA STAQS GV and G3 aircraft deployments.

5.3. Proposed experimental plan for GOTHAAM 2023 (NCAR C-130)

5.3.1. Science Objectives

The New York Metropolitan Area (NYMA) is home to more than 20 million people and experiences high levels of pollution. In the summer of 2021, 7 of 11 monitoring stations in the NYMA reported ozone levels in exceedance of the EPA National Ambient Air Quality Standard (https://www.dec.ny.gov/docs/air_pdf/2021o3.pdf, last accessed 2022 June 2). Total $PM_{2.5}$ loading has improved significantly in recent decades due to air quality regulations, but a growing contribution of organic matter to the total aerosol burden may have implications for particle toxicity and regulatory policy (Pitiranggon et al., 2021). Encompassing rural, urban, and marine environments (Figure 26), the NYMA is subject to a complex mixture of emissions, chemistry, and coastal meteorology that ultimately determine the production and fate of harmful pollutants.

The Greater New York Oxidant Trace Gas Halogen and Aerosol Airborne Mission (GOTHAAM) is an NSF-funded investigation of the detailed chemical processes controlling atmospheric composition in the NYMA. State-of-the-art in situ instrumentation will be deployed on the NSF C-130 aircraft in July and August 2023 to address four related objectives.

1. Quantify the relative contributions from various **volatile organic compound (VOC) sources** (biogenic, fossil fuel combustion, consumer products) and how they contribute to chemical reactivity.
2. Determine the relative potential contribution of each VOC class to **secondary organic aerosol (SOA)** as the anthropogenic plume evolves.
3. Quantify the relative importance of **oxidation pathways** for both gas phase and aerosol species and characterize how processes vary diurnally and between chemical systems (biogenic/urban/marine).
4. Investigate how **nighttime processes** influence next-day chemistry and composition.

GOTHAAM observations will improve understanding of formation of O_3 and $PM_{2.5}$ pollution in the NYMA. By sharing and disseminating results, GOTHAAM will help air quality agencies in the region and other similar mega cities take action to mitigate harmful pollution.

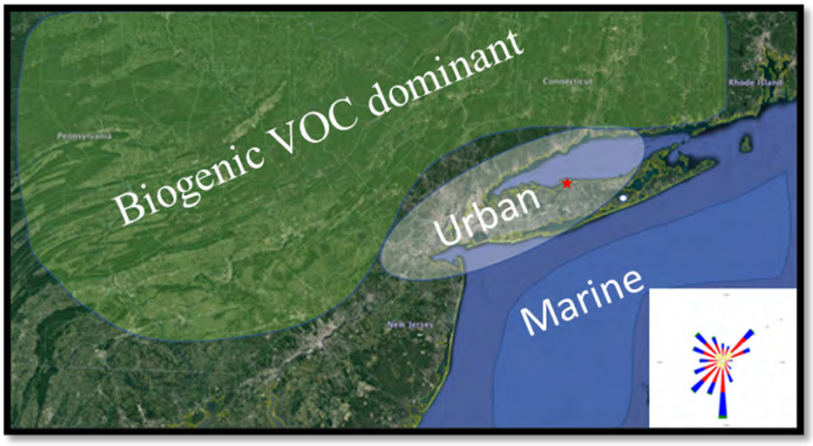

Figure 26. GOTHAAM will probe atmospheric chemistry in the diverse chemical environments (biogenic, urban, marine) found in the New York Metropolitan Area. The inset is a wind rose showing the origin of surface winds in the summertime. Southerly flow is most common, followed by southwesterly and northeasterly.

5.3.2. Proposed Payload

Table 6 lists core GOTHAAM instrumentation. All measurements are in situ. Gas-phase observations include speciated VOC, speciated and total reactive nitrogen, radicals (OH, HO_2, RO_2), greenhouse gases, sulfur and halogen-containing compounds, and more. Aerosol measurements include single-particle and bulk chemical composition, physical properties, and size distributions.

The C-130 payload is optimized to address GOTHAAM objectives. Multi-instrument VOC measurements will thoroughly characterize VOC sources and oxidation products in the high and intermediate volatility range (Objectives 1, 2, 3). Direct observations of key oxidants will constrain the lifetime of reactive carbon and nitrogen (Objective 3). Measurements of gas-phase aerosol precursors and aerosol composition will elucidate major pathways leading to secondary pollutants (Objectives 2, 3). Simultaneous observations of halogenated gases, sulfur-containing gases, and aerosol properties will illuminate how the marine atmosphere processes urban outflow (Objectives 3, 4). In combination, the GOTHAAM payload can yield a comprehensive picture of atmospheric chemistry in the NYMA.

Species Measured	**Technique**	**PI name**	**Institution**
OH, HO_2, RO_2, H_2SO_4	NO_3^- CIMS	Lee Mauldin	CU Boulder
oVOCs, halogens, $ClNO_2$, HONO, N_2O_5, etc	I^- CIMS	Joel Thornton	U. Washington
VOCs	PTR-TOF Vocus	Joel Thornton	U. Washington
VOCs	Mini WAAS	Eric Apel	NCAR
Organic gases	TOGA-TOF	Eric Apel	NCAR ACOM
HCHO	ISAF	Reem Hannun / Glenn Wolfe	UMD/NASA
NOx, ΣNOy, O_3	Chemiluminescence	Ale Franchin	NCAR ACOM
Speciated PANs	TD-CIMS	Frank Flocke	NCAR ACOM
GHG/CO/SO_2	Picarro	Teresa Campos	NCAR ACOM
Individual particle composition, including sea salt	ATOF-MS	Kerri Pratt	U. Michigan
SOA composition	AMS	Delphine Farmer	CSU
Aerosol impaction collector	TRAC	Daniel Knopf	Stony Brook
Aerosol size distributions	UHSAS, cloud probe	n/a	NCAR EOL
J-values	HARP actinic flux	Samuel Hall	NCAR ACOM

Table 6: Potential GOTHAAM C-130 payload.

5.3.3. Mission Execution

With 150 flight hours, GOTHAAM will generate a high-resolution 4-D portrait of atmospheric composition and processes in the NYMA during the peak ozone season. Flights will include a combination of Lagrangian and Eulerian strategies and focus on the domain shown in Figure 27. Missed approaches at designated airports will provide full vertical profiles of short-lived reactive species and improve connections to ground monitoring networks. Flights will also exploit natural variability in near-surface wind patterns to probe the various chemical regimes both independently and in combination (e.g., urban plume outflow over land vs. over water). Multi-scale models, including F0AM, CMAQ, and GEOS-Chem, will support forecasting and analysis

5.3.4. Anticipated Outcomes

The next-generation instrumentation on GOTHAAM will provide an unprecedented dataset detailing NYMA atmospheric composition. Analyses will reveal the controls on O_3 and PM formation, informing air quality stakeholders in both NY and other megacities. Regional and global models struggle in coastal regions, and GOTHAAM observations can serve as a benchmark constraint for pinpointing model shortfalls and testing new parameterizations. Finally, with potential concurrent sampling under TEMPO, GOTHAAM data will serve as a ground-truth resource for validation of satellite retrievals and applications of satellite data to studies of emissions and chemistry.

5.4. Proposed experimental plan for a**irborne NEC-AQ-GHG 2023 (NOAA/ARL-UMD-JHU Cessna Research Aircraft)**

5.4.1. **Science objectives**

To support the overall AEROMMA 2023 science objectives related to urban emissions that impact air quality and climate, the NOAA Air Resources Lab (ARL) and University of Maryland (UMD) will deploy a fully instrumented Cessna 402 research aircraft in the Northeast Corridor (NEC) region from Washington, DC to New York City (NYC) for the NEC Air Quality and Greenhouse Gas (NEC-AQ-GHG) study in the summer of 2023. An airborne measurement package operated from the Cessna research aircraft will measure short-lived air pollutants and greenhouse gases emitted from Baltimore/Washington, NYC as well as Philadelphia. Data from the Cessna research aircraft will be used to characterize the meteorology and chemistry leading to air pollution events and emissions of GHGs over this region. The research proposed here will provide the scientific basis for effective air quality and climate policies. In addition to the AEROMMA science questions, important NEC-AQ-GHG scientific objectives include:

- To characterize spatial and temporal patterns of O_3 and precursors during ozone exceedance events along with pre-exceedance conditions with a tie to key monitoring sites.
- To characterize spatial and temporal patterns of meteorological conditions (e.g., low-level jets, land-sea breeze, mixing heights, etc.) during ozone events.
- To investigate emission of NO_x, CO, CH_4, and VOCs from these urban areas and compare to emission inventories.

5.4.2. Deployment location and calendar

The Cessna research aircraft will be deployed to the NEC region from Washington, DC to NYC from approximately July 1 to August 15, 2023 for the NEC-AQ-GHG 2023 study (Figure 27).

Figure 27: The study region (shade red rectangle) for the Cessna research aircraft for NEC-AQ-GHG 2023.

5.4.3. Proposed payload

Figure 28 shows some pictures of the instrumentation on the Cessna research aircraft and Table 7 lists the measurements in detail. The measurement package on the Cessna research aircraft will consist of the following 1) a Picarro Model 2401-m analyzer to measure CO_2, CH_4, and CO; (2) a Teledyne Cavity Attenuation Phase Shift (CAPS) to measure NO_2; 3) a modified TECO 42C to measure NO and NO_y; (4) an AE43 Aethalometer to measure black carbon at 7 wavelengths; (5) a Tofwerk Elf proton-transfer-reaction Time-of-Flight mass spectrometry (PTR-ToF-MS) instrument to measure benzene, toluene, xylene, acetone, acetonitrile, acetaldehyde and potentially other VOCs, and (6) sensors to measure meteorological parameters of air temperature, pressure, relative humidity, wind speed and wind direction.

Figure 28: Pictures showing the instrument on the Cessna research aircraft.

This instrument payload will address the above objectives related to air quality and climate. These measurements of air pollutants and greenhouse gases (GHGs) will be used to detect spatial variations in biogenic and anthropogenic (including VCP) emissions across rural to urban gradients and to characterize spatial and temporal patterns of O_3 and its precursors together with GHGs. NIST-traceable standards will be used to calibrate analyzers used on the aircraft.

Species Measured	Technique	PI name	Institution
Position	GPS	Xinrong Ren	NOAA ARL
Meteorology (T, RH, P, 2-D Wind)	Thermistor Hygristor, Capacitance Manometer, Differential GPS	Russel Dickerson	Univ. of Maryland
Fast Greenhouse Gas Analyzer (CH_4/CO_2/CO/H_2O)	Cavity Ring Down Spectroscopy Picarro Model G2401-m	Russel Dickerson	Univ. of Maryland
Ozone (O_3)	UV Absorption	Xinrong Ren	NOAA ARL
Nitrogen Dioxide (NO_2), Nitric Oxide (NO) Nitrogen Oxides (NO_y)	CAPS, Teledyne Chemiluminescence, Thermal dissociation to NO	Xinrong Ren	NOAA ARL
VOCs	TofWerk PTR-ToF-MS	Peter Decarlo	Johns Hopkins Univ.
Black Carbon (370, 470, 520, 590, 660, 880, 950 nm)	Aethalometer, AE43	Xinrong Ren	NOAA ARL

Table 7. Potential Cessna Research Aircraft Instrumentation

5.3.4. NEC-AQ-GHG flight plans

NEC-AQ-GHG 2023 will include ~60 hours spanning approximately 15-20 science flights. Flight plans will be chosen in coordination with other airborne platforms and participating agencies. The measurements from these flights will augment data from other airborne platforms and ground monitoring sites along the NEC from Washington, DC to NYC area. Each flight will last 3 to 4 hours. The home base

of the aircraft is Fort Meade, MD. It is expected that about 6 missions (~3 flights each mission) will be flown out of MD with an overnight stay at Westchester Airport (White Plaines, NY).

Figure 29 shows flight tracks from the ARL/UMD Cessna on days that had high ozone concentrations forecasted in summer 2020. Such forecasts have proved consistently reliable for flights over Washington-Baltimore and NYC. O_3 mixing ratios above 120 ppb were observed on some flights in summer 2020, and surface monitors recorded violations of the NAAQS. Emissions of air pollutants and GHGs can be calculated based on the mass balance approach and enhancements ratios between the species.

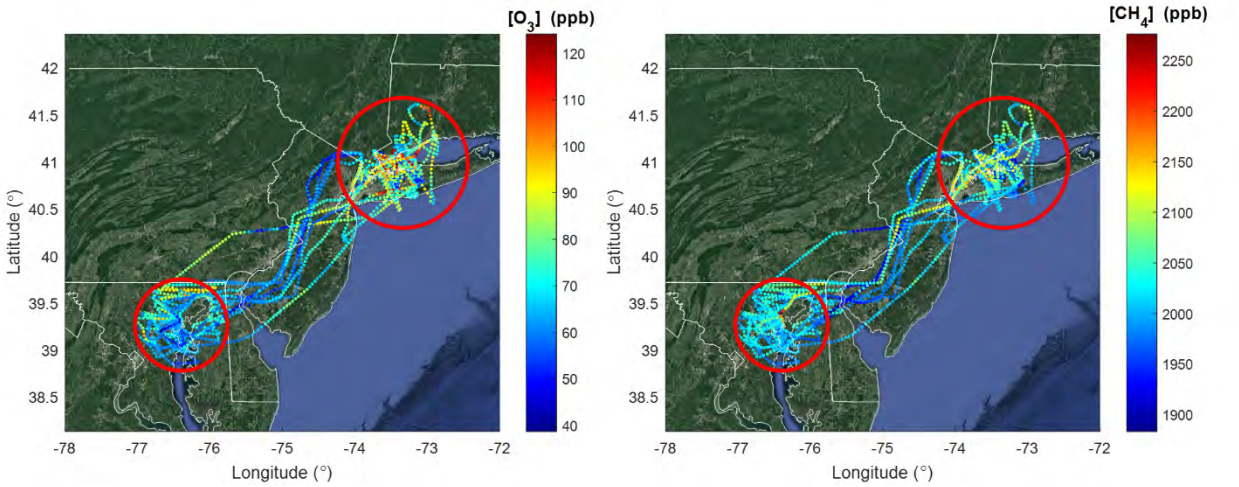

Figure 29: Example of airborne measurements of O_3 (left) and CH_4 (right) made from the Cessna research aircraft during summer 2020.

5.5. Proposed experimental plan for NYC-METS (NYC downtown and downwind)

While the AEROMMA and coordinated aircraft assets will investigate the regional and large-scale urban air quality implications, ground site measurements will investigate diurnal profiles, emission ratios, diurnal emission fluxes, and long-term records. Most AEROMMA cities (NYC, Atlanta, and Toronto) will have dedicated measurement sites during the study period. The NYC locations and the routine monitoring sites are shown in Figure 30.

Figure 30: Proposed locations for the NOAA AC4 (yellow stars) supported AEROMMA ground sites around NYC.

The instrumentation package at the NYC site in Manhattan seeks to examine the source contributions, emission rates, chemical composition, and oxidative aging of complex gas- and particle-phase mixtures, including top-down emissions studies with flux measurements and in situ oxidation experiments using an oxidation flow reactor. Concentrations, emissions, and oxidative aging of VOCs, OVOCs, I/SVOCs, and greenhouse gases will be investigated at the elevated site in Upper Manhattan, NY (CUNY ASRC in Figure 30 at 85 St Nicholas Terrace) and at a downwind site in Guilford, CT (Yale Coastal Field Station in Figure 31; 41.2583° N, 72.7312° W) that is influenced by atmospheric oxidative aging processes associated with emissions from NYC and elsewhere in the Northeast. Also relevant to AEROMMA marine science objectives, the site is situated on the Long Island Sound waterfront (including a small dock) with marine influences on emissions and chemical processing. Intensive measurements will be conducted during summer 2023 (e.g., July/August) at both sites, with a smaller campaign in summer 2022. Measurements are tentatively set to take place during a 4-week intensive to be scheduled in coordination with aircraft measurements. A combination of state-of-the-art online and offline spectroscopy-, chromatography-, and mass spectrometry-based techniques will be deployed as part of the NYC-METS project and other AC4-funded AEROMMA collaborators, and are summarized in Tables 8-9.

Species Measured	Technique	PI-name	Institution(s)
NYC-METS project			
VOCs-SVOCs, e.g., C_6-C_{12} aromatics, $(CH_3)_2CO$, CH_4S, $C_7H_4ClF_3$, D5-siloxane	Vocus PTR-ToF	Manjula Canagaratna	Aerodyne
Gas-phase compounds, e.g., HNO_3, HONO, HO_2NO_2, HNCO, N_2O_5, PANs, HCOOH, $CH_2(COOH)_2$, $C_5H_9O_4N$	Iodide HR-ToF-CIMS	Andrew Lambe	Aerodyne
CO, CO_2, CH_4, H_2O	Tunable Infrared Laser Direct Absorption Spectroscopy	Rob Roscioli	Aerodyne

Species Measured	Technique	PI-name	Institution(s)
Gas-phase VOCs-SVOCs (C_5-C_{25})	Offline GC-TOF/MS analysis of adsorbent tube samples	Drew Gentner	Yale
Particle-phase IVOCs-ELVOCs	Offline LC-TOF analysis of PM filter samples	Drew Gentner	Yale
Particle-phase organics, NO_3^-, SO_2^-, NH_4^+, Cl	Aerosol Chemical Speciation Monitor	Phil Croteau	Aerodyne
in situ OH/O_3/NO_3/Cl oxidation products of VOCs, I/SVOCs, OVOCs	Oxidation Flow Reactor	Andrew Lambe	Aerodyne
O_3, CO, CO_2, NO/NO_2, SO_2, $PM_{2.5}$, BC, Meteorology (e.g., wind, ceilometer)	Supporting baseline measurements	Misc.	CUNY, Yale, Aerodyne
NOAA AC4 AEROMMA funded collaborators			
Speciated hydrocarbons and OVOCs	Online GC-TOF-MS	Megan Claflin, Pawel Misztal	Aerodyne, U. Texas Austin
OH reactivity	Comparative reactivity method with PTR-TOF-MS detector	Saewung Kim	UC Irvine
Size resolved organic aerosol composition	MOUDI, offline AMS, UHR/MS, single particle microspectroscopy	Rachel O'Brian, Andy Ault	U. Michigan
Gas- and particle-phase organic compounds, HNO_3, $ClNO_2$, biogenic sulfur compounds	FIGAERO HR-ToF I-CIMS	Joel Thornton, Nga Lee Ng	U Washington Georgia Tech,
Peroxy and hydroperoxy radicals (RO_2 + HO_2)	ECHAMP peroxy radical monitor	Ezra Wood	Drexel U.

Table 8: Potential instrument list of the NYC-METS 2023 CUNY ASRC ground site deployment.

Species Measured	Technique	PI-name	Institution(s)
NYC-METS and AC4 AEROMMA collaborators			
O_3, CO, $PM_{2.5}$, NO/NO_2, CO_2, BC, SO_2, Meteorology	Supporting baseline measurements	Drew Gentner	Yale
VOCs-SVOCs, e.g., C_6-C_{12} aromatics, $(CH_3)_2CO$, CH_4S, $C_7H_4ClF_3$, D5-siloxane	Vocus PTR-ToF	Manjula Canagaratna	Aerodyne
Particle-phase organics, NO_3-, SO_2-, NH_4+, Cl	Aerosol Chemical Speciation Monitor	Phil Croteau	Aerodyne
Size-resolved organic aerosol composition	MOUDI, offline AMS, UHR/MS, single particle microspectroscopy	Rachel O'Brian, Andy Ault	William & Mary, U. Michigan
Gas-phase VOCs-SVOCs (C_5-C_{25})	Offline GC-TOF/MS analysis of adsorbent tube samples	Drew Gentner	Yale
Particle-phase IVOCs-ELVOCs	Offline LC-TOF analysis of PM filter samples	Drew Gentner	Yale

Species Measured	Technique	PI-name	Institution(s)
Gas- and particle-phase organic compounds, and HNO_3, $ClNO_2$, biogenic sulfur compounds	FIGAERO HR-ToF I-CIMS	Joel Thornton, Nga Lee Ng	U Washington Georgia Tech,

Table 9: Potential instrument list of the NYC-METS 2023 Yale Coastal Site deployment.

5.6. Proposed experimental plan for FROG-NY (NYC Mineola)

The Fluxes of Reactive Organic Gases in New York (FROG-NY) project will contribute to AEROMMA by applying the eddy covariance (EC) technique to derive a better understanding of urban emissions and deposition of volatile and semi-volatile organic compounds. Specifically, the project will apply two complementary time-of-flight chemical ionization mass spectrometry (TOF-CIMS) instruments (Table 10) to directly quantify the fluxes, vertical gradients, and concentrations of an expansive suite of reactive VOCs from an existing 76-meter tower in metropolitan NY during summer 2023.

This project will address the following core questions:

- What are the bi-directional urban fluxes of reactive organic carbon? Is there a significant role for previously unidentified or unmodeled compounds?
- How do the concentrations, emissions and deposition of individual organic molecules, classes of VOCs, and the overall ensemble, vary on hourly, daily, and weekly timescales?
- What is the relative importance of VOC emissions from fossil fuels, VCPs, the biosphere, and other sources?
- How do VOC fluxes co-vary with those for greenhouse gases? What are the implications for source partitioning?
- How do the observed VOC emissions contrast with inventory estimates? What are the implications for air quality predictions? How should inventories be improved?

Urban EC raises specific challenges that require particular footprint and sampling characteristics for robust results. FROG-NY measurements will be performed at the 76 m Mineola communications tower (40°44'58.2"N 73°38'18.2"W; in Figure 31), in a predominantly residential part of the New York metropolitan area. The site is ideally suited for urban flux measurements, with relatively consistent land use (>90% developed; <10% forest) and ground elevation (±13 m) in the surrounding landscape. A major benefit of this tower site is that given the ~14 m mean building height in the area, the 76 m and 50 m measurement heights both allow us to sample above the roughness sublayer and within the constant flux layer. The site features existing CO_2 and CH_4 concentration measurements (50 and 76 m above ground level) with data hosted by the National Institute for Standards and Technology. FROG-NY measurements will feature two inlets with sonic anemometers at 50 and 76 m. A third inlet for aerosol and air sampling will be placed on the roof of the measurement shelter at ~6 m above ground level.

Species Measured	Technique	PI-name	Institution
Multi-instrument eddy covariance			
Unsaturated VOCs, oVOCs, C6-C10 aromatics, siloxanes, terpenes, etc.	PTR-QiTOF	Dylan Millet	U. Minnesota

oVOCs, chlorinated VOCs, HNCO, HCOOH, $CH_2(COOH)_2$, $C_5H_9O_4N$, O_3	Iodide ToF-CIMS	Delphine Farmer	CSU
CO, H_2O, N_2O	Cavity Enhanced Absorption	Jeff Peischl	NOAA CSL
Particulate organics, NO_3-, SO_2-, NH_4+, Cl	Aerosol Chemical Speciation Monitor	Delphine Farmer	CSU
CO_2, H_2O	NDIR	Dylan Millet	U. Minnesota

Table 10: Potential instrument list of the FROG-NY 2023 ground site deployment.

5.7. Proposed experimental plan for TOPAZ (Yale Coastal Field Station)

NOAA CSL is planning to deploy the Tunable Optical Profiler for Aerosol and oZone (TOPAZ) lidar along with a dedicated Doppler lidar during the AEROMMA and CUPIDS field studies. The TOPAZ and Doppler lidar observations will help address several key science questions that are central to these campaigns:

- Characterize the distribution and formation rate of ozone (O_3) in the urban outflow downwind of NYC.
- Assess the contributions of local production versus regional and continental transport to surface ozone levels in the NYC area.
- Document the effect of complex local flow regimes, including the land sea breeze circulation, and different properties of the atmospheric boundary layer (ABL) over land and water on the distribution and evolution of O_3 concentrations.
- Evaluate the capabilities of high-resolution air quality models to replicate observed O_3 concentrations in and downwind of the NYC area.
- Validate O_3 observations from the geostationary satellite-based TEMPO instrument. In particular, assess the accuracy of the 0-2 km above ground level (AGL) O_3 column product and how well it correlates with observed surface O_3 concentrations, and study O_3 horizontal variability within individual TEMPO ground pixels.

It is planned to deploy TOPAZ along the shore of the Long Island Sound (LIS) from July 01 to August 08, 2023. This will ensure overlap with the CUPIDS and NYC AEROMMA campaigns and also coincide with the NSF GOTHAAM experiment. TOPAZ will be co-deployed with at least three other Tropospheric Ozone Lidar Network (TOLNet) lidars. The observations from this regional O_3 lidar network will make critically important contributions to addressing the above science goals, where the last goal is one of the core TOLNet objectives.

A candidate deployment site for TOPAZ is the Yale Coastal Field Station located on a deepwater cove on Long Island Sound in Guilford Connecticut, about 125 km downwind of NYC (see Figure 31). Because of its unique scanning capability, TOPAZ is ideally suited to observe O_3 concentrations in the pollution plume over the Long Island Sound emanating from NYC. TOPAZ will implement a scan sequence that includes a zenith measurement followed by a set of slant path observations at shallow elevations angles with the laser beam pointed both in a southerly direction over the Long Island Sound and towards the north over land. With a range of 4-6 km, the TOPAZ shallow angle observation will be able to capture the O_3

gradient over the LIS and the land-sea interface. The co-located scanning Doppler lidar will facilitate the investigation of different flow and ABL turbulence regimes on O_3 levels.

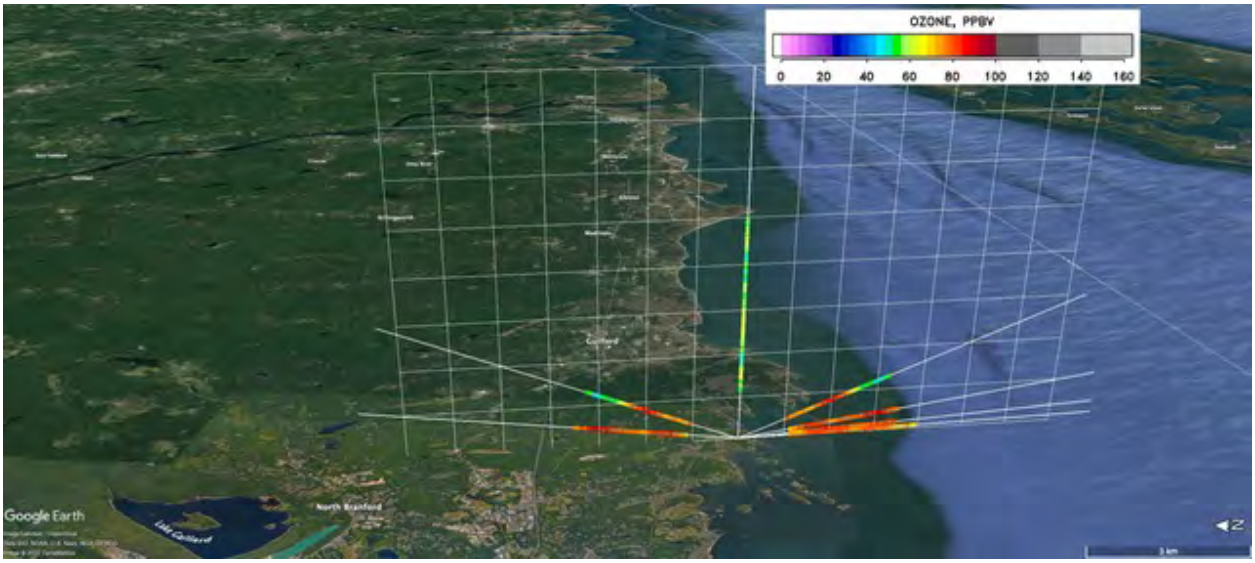

Figure 31: Illustration of TOPAZ O_3 profiling capabilities if the instrument were placed at the Yale Coastal Field site. The grid covers 8 km along the beam direction and 8 km vertically.

5.8. Proposed experimental plan for Toronto (THE CIX)

Toronto has a metropolitan population exceeding seven million and regional population approaching ten million. Although precursors to ground-level ozone have been reduced in Toronto over past decades, exceedances of the 8-hour ozone Canadian Ambient Air Quality Standard are still common. The Toronto Halogens, Emissions, Contaminants, and Inorganics eXperiment (THE CIX) will be located in an urban/suburban transition zone that is not impacted by any large local sources (i.e., >500 m from any major roads, Figure 32). At 20 km north of downtown Toronto and Lake Ontario, the site is ~2-3 hours transport time from major sources in downtown Toronto and is typically not impacted by lake breeze fronts until late in the afternoon during summer.

Measurements during THE CIX (Table 11) will target several areas of uncertainty in urban air quality, grouped into four themes (Halogens, Emissions, Contaminants, and Inorganics). Examples include: 1) improved understanding of reactive chlorine chemistry in a summertime continental environment (Halogens); 2) improved understanding of emissions of organics and greenhouse gases (Emissions); 3) understanding the sources and sinks of haloacetic and perfluorocarboxylic acids (Contaminants); and 4) a comprehensive nitrogen budget with a suite of instruments will be targeted along with source apportionment (Inorganics). There will be several unique instruments and measurements at THE CIX, including two gas-phase measurements of HCl (CRDS and TILDAS), measurement of total gaseous chlorine, an ambient ion monitor-ion chromatograph-mass spectrometer (AIM-IC-MS), measurement of total nitrogen, and a real-time measurement of perfluorocarboxylic acids using negative ion proton transfer CIMS (NI-PT-CIMS).

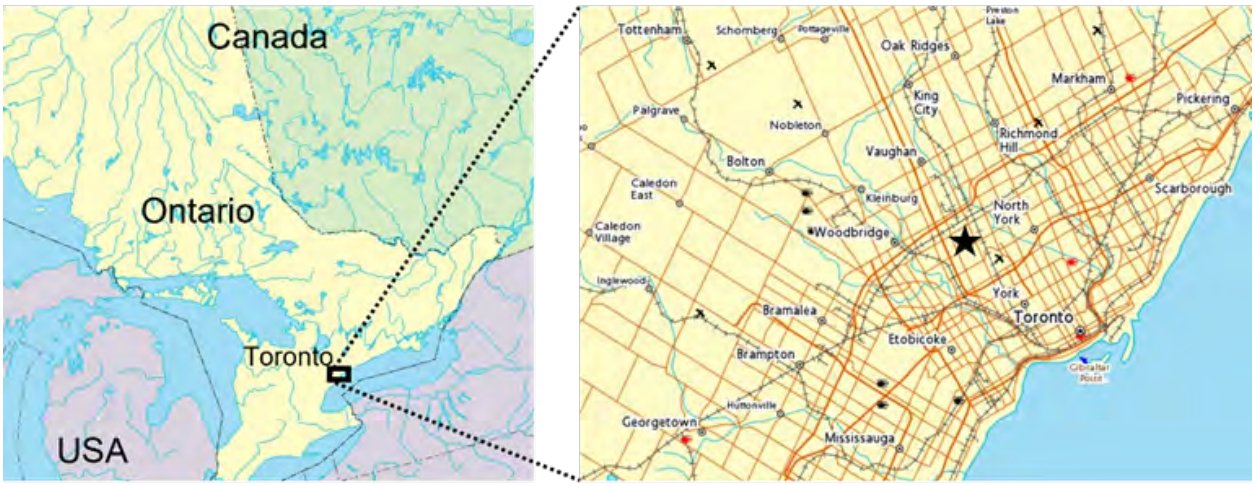

Figure 32: Location for THE CIX.

Species measured	Technique	PI and Institution
Halogens: $ClNO_2$, Cl_2, N_2O_5, HCl, pCl^-, total Cl	I-ToF-CIMS, CRDS, TILDAS, Total Cl, AIM-IC-MS	Nadine Borduas-Dedekind *(University of British Columbia)* Pete Edwards *(University of York)* Rob McLaren *(York University)* Jennifer Murphy *(University of Toronto)* Trevor VandenBoer *(York University)* Cora Young *(York University)*
Emissions: VOCs, VCPs, CO, CO_2, CH_4, N_2O, NO_x, NH_3, particle size/number distribution, organic acids	Vocus PTR, CRDS, SMPS, OPS, I-ToF-CIMS, QCL, NI-PT-CIMS	
Contaminants: Haloacetic acids, perfluorocarboxylic acids	AIM-IC-MS, NI-PT-CIMS, precipitation sampler	
Inorganics: NH_3, HCl, HNO_3, HONO, pNO_3^-, pCl^-, pNO_2^-, pSO_4^{2-}, pNH_4^+, pNa^+, pK^+, pMg^{2+}, pCa^{2+}, total N	AIM-IC-MS, QCL, NI-PT-CIMS, CRDS, TILDAS, nanoMOUDI, total N	

Table 11: Potential instrument list and PIs for THE CIX.

5.9. Proposed experimental plan for Atlanta

Atlanta is a hot-spot of both ozone and SOA, and much of the summer is typically classified as "moderate" according to the air quality index. The city is subject to high anthropogenic and biogenic emissions along with increasingly severe heat waves. Atlanta has been the location of several previous studies investigating biogenic/anthropogenic interactions, including flights during SENEX 2013 (Warneke et al., 2016) and SEAC^{4}RS. AEROMMA allows us to build on and update previous work with new chemical detail. Ground-based observations overlapping the AEROMMA flights are briefly described below.

- The South Dekalb (SDK) PAMs site is classified as an "urban background" location. It provides a long-term record of VOCs (via GC), NO_x, and other trace gases and particles.
- SDK is also an ASCENT site, and will host an ACSM (non-refractory aerosols), Xact (trace metals), Aethalometer (black carbon), and SMPS (aerosol number size distribution and concentration).
- At least 3 Pandoras will be deployed in and around during the AEROMMA time frame, including one at SDK, one located centrally downtown on Georgia Tech's campus, and one in a more rural

location outside of the city. Each Pandora is paired with an in-situ formaldehyde monitor for investigations of surface-to-column ratios.

Using these observations in conjunction with observations from overhead flights, the project will address the central questions to AEROMMA with a focus on the biosphere/urban interface.

5.10. Pandoras, TOLnet, routine AQ monitoring

Continuous tropospheric ozone profiles add a critical component needed to understand processes relevant to air quality and pollution transport with TEMPO. The NASA Tropospheric Ozone Lidar Network (TOLNet) will contribute to AEROMMA and STAQS most heavily in the New York City domain (at least 3 systems operated by NASA and CCNY) with possible additional support in the Los Angeles and Toronto areas where JPL and ECCC operate two additional systems, respectively.

Pandora spectrometers consist of a ground-based UV-VIS spectrometer capable of operating in direct-sun DOAS or multi-axis (MAX)-DOAS mode and is the primary validation instrument for the TEMPO mission. Currently, at least 20 Pandoras are operating as part of the Pandonia Global Network in the domains of interest for AEROMMA and STAQS. Products from this instrument include NO_2, HCHO, and ozone.

AEROMMA and STAQS aim to leverage existing monitoring networks operated by the EPA and state air quality agencies within the domains sampled in 2023. Relevant parameters include, but are not limited to O_3, NO_2, HCHO, and meteorology.

5.11. ASCENT: Atmospheric Science and Chemistry mEasurement NeTwork

The ASCENT project includes 12 sites distributed nationally across urban, rural, and remote sites that will be outfitted with advanced, online, long-term aerosol measurement instrumentation outlined in the Table 12, as well as an associated database for free and open access to ASCENT data. The network seeks to expand routine aerosol monitoring in the U.S. and enable detailed aerosol source apportionment that elevates the ability to discern the sources, chemistry, dynamics, chemical/physical properties, and climate and health implications of aerosols. The long-term ASCENT installations are located at established sites (e.g., NCore, PAMS, IMPROVE, NEON, SCAQMD, and HNET) and will be installed starting in 2022 and remain up throughout the AEROMMA campaign and thereafter. Urban sites (and site contacts) relevant to the AEROMMA and STAQS include: New York City, Queens (D. Gentner), Los Angeles and downwind areas (J. Seinfeld, R. Bahreini, L. Hawkins), Houston (J. Flynn, R. Griffin), and Atlanta (N. L. Ng), with additional urban sites in Pittsburgh (A. Presto, A. Robinson) and Denver (J. Jimenez), as well as rural/remote sites in Great Smoky Mountains National Park (J. Surratt), Washington (J. Thornton), Yellowstone National Park (S. Murphy), and Alaska (J. Mao). Further detail on the project, sites, and data can be found on the ASCENT website https://ascent.research.gatech.edu.

Instrument	Model and Manufacturer	Measurements	Measurement Frequency

Aerosol Chemical Speciation Monitor (ACSM), $PM_{2.5}$	ToF-ACSM, Aerodyne Research	Organics, sulfate, nitrate, ammonium, chloride with PM mass spectra	10 min
Aethalometer, $PM_{2.5}$	AE33, Magee Scientific	Wavelength-dependent absorption to measure black and brown carbon	1 min
Xact x-ray fluorescence instrument, $PM_{2.5}$	625i, Cooper Environmental	Trace metals: Sb, As, Ba, Cd, Ca Cr, Co, Cu, Fe, Pb, Hg, Mn, Ni, Se, Ag, Sn, Ti, Tl, V, Zn, more available	15-240 min
Scanning Mobility Particle Sizer (SMPS), PM_1	3938W89, TSI	Particle number size distribution, number concentration	3 min (for full scan)

Table 12: Instrumentation to be installed at each ASCENT site.

5.12. Proposed experimental plan for EPCAPE 2023-24 (La Jolla)

5.12.1. Science Objectives

The focus of the Eastern Pacific Cloud Aerosol Precipitation Experiment (EPCAPE) is to characterize the extent, radiative properties, aerosol interactions, and precipitation characteristics of stratocumulus clouds in the Eastern Pacific across all four seasons at a coastal location, the Scripps Pier and the Scripps Mt. Soledad sites in La Jolla (https://www.arm.gov/research/campaigns/amf2023epcape). The planned data record will start 15 February 2023 and continue until 14 February 2024, with two intensive operation periods (April-June; July-September). Coastal cities provide the opportunity to characterize marine clouds and the substantial effects of manmade particles on cloud properties and processes. The large dynamic range of aerosol particle concentrations combined with the multi-hour to multi-day persistence of stratocumulus cloud layers makes the site ideal for investigating the seasonal changes in cloud and aerosol properties as well as the quantitative relationships between cloud and aerosol properties. An important enhancement to this study will be the collection of simultaneous in-cloud aerosol and droplet measurements to investigate the differences in these cloud properties during regional polluted and clean marine conditions at the Mt. Soledad location. The combined observations will provide an unprecedented set of constraints for the following questions:

- Cloud and Aerosol Climatology: What are the seasonal and diurnal cycles of marine stratocumulus cloud and aerosol properties on the West coast?
- Cloud Radiative Fluxes: How do cloud properties, including the ratio of direct-to-diffuse radiation, change as coastal clouds are advected inland?

- Aerosol-Cloud Interactions: Will retrieved cloud properties reflect the regional signatures of aerosol?

Each of these questions reflects a topic of current controversy in the literature that cannot be addressed without the type of comprehensive data set that this project is expected to provide.

5.12.2. Potential Instrumentation

EPCAPE will locate most of the AMF1 instrumentation at the main site at Scripps Pier and a few additional instruments at the Scripps Mt. Soledad site (Figure 33). Below-cloud instrumentation, including cloud, precipitation, radiation, and aerosol instruments will be situated on the Scripps pier. Additional instrumentation (scanning radar) will be located at the Mt. Soledad site, located less than 2 km inland (250 m above sea level), which will allow for sampling downwind of the pier below, in, and above clouds depending on conditions. Statistics are not available on how frequently the Soledad location is below, in, and above cloud (other than the seasonally limited prior study), as that will be an important outcome of this 12-month data set.

Figure 33: Overview (top left) of Scripps sites in La Jolla, CA, with enlarged details for Mt. Soledad (top right) and pier (bottom).

The resources from ARM for this campaign are AMF1, including standard meteorological instrumentation, a broadband and spectral radiometer suite, and remote-sensing measurements including

lidars and radars, plus the AOS system for aerosol observations. AMF1 is well suited for this deployment. Specific AMF1 instrumentation included as part of this proposal are listed in Table 13.

Russell will provide filter sampling for organic functional groups (FTIR) and elements (XRF) at the Scripps pier to complement the chemical analysis available from the AMF1 ACSM. This sampling will be housed in an AMF1 AOS van at the pier. Dan Lubin will contribute a shortwave spectroradiometer for measurement of shortwave spectral irradiance between 350 and 1700 nm complements the mid-infrared AERI radiance measurements, in that cloud optical properties (optical depth and effective radius) can be retrieved under thicker clouds that emit in the longwave as blackbodies (with no spectral sensitivity to microphysics). Delphine Farmer will measure particle fluxes at Scripps pier.

Lidars	Radiometers	Aerosol and Trace Gas Systems
MPL: micropulse lidar	MWR3C: 3-channel microwave radiometer	SMPS: scanning mobility particle sizer
DL: doppler lidar	MWR: 2-channel microwave radiometer	CCN: cloud condensation nuclei counter
CEIL: ceilometer	SKYRAD: sky radiometer	UHSAS: ultra-high sensitivity aerosol spectrometer
Radars	GNDRAD: ground radiometer	APS*: aerodynamic particle sizer
KAZR: Ka-band zenith cloud radar	MWR: microwave radiometer	SP2*: single-particle soot photometer
RWP: radar wind profiler	AERI: atmospheric emitted radiance interferometer	HTDMA: humidified tandem differential mobility analyzer
KaSACR: Ka-band scanning ARM cloud radar	MFRSR: multifilter rotating shadowband radiometer	ACSM: aerosol chemical speciation mass spectrometer
Precipitation	CSPHOT: CIMEL sun photometer	NEPH (dry, wet): nephelometers at dry and ambient relative humidity
VDIS: 2D video disdrometer	MFR: multifilter radiometer	CPCF: condensation particle counter, fine
LDIS: laser disdrometer	Atmospheric and Boundary State	CPCU: condensation particle counter, ultrafine
ORG: optical rain gauge	SEBS: surface energy balance	AETH: aethelometer
PWD: present weather detector	ECOR: eddy correlation flux	PSAP: particle soot absorption photometer
TBRG: tipping bucket precipitation gauge	SONDE: balloon-borne sounding system (4/d for intensives, otherwise 2/d)	O3: ozone monitor
WB: weighing bucket precipitation gauge	TSI: total sky imager	SO2: sulfur dioxide monitor
	AOSMET: automated weather station	CO: carbon monoxide, nitrous oxide, and water monitor

Table 13: ARM instruments requested for EPCAPE.

UCSD (Russell), UCLA (Suzanne Paulson), and NCSU (Markus Petters) will deploy instruments at Mt. Soledad for in-cloud sampling of detailed aerosol chemical composition, including offline filter analysis. The Mt. Soledad measurements will include aerosol size distributions, SP2, CCN, and aqueous OH radical measurements, as well as a high-resolution, time of flight, event-enabled Aerodyne AMS to provide aerosol composition and concentration for comparison to the AOS ACSM deployed at the pier. Rachel Chang (Dalhousie) plans to deploy the fog droplet monitor at this site to characterize the droplet size distribution in cloud. Environment and Climate Change Canada (John Liggio, Jeremy Wentzell, Michael Wheeler, Alex Lee) is providing a Brechtel ground-based CVI for deployment at the Mt. Soledad site to enable in-cloud composition sampling of droplet residuals (Sanchez et al., 2016). Liggio has support to bring a chemical ionization mass spectrometer, which has previously demonstrated at Mt. Soledad that cloud water chemistry was likely responsible for enhancements in low molecular weight polar organics such as isocyanic (HNCO) and formic acids in cloud droplets, with scavenging efficiencies beyond what

can be expected from Henry's Law solubility (Zhao et al., 2014). Smith will also be measuring ultrafine particles at Mt. Soledad.

Measurement	Instrument	Inlet	PI name	Institution
Evaporates cloud droplets and provides residual particles to other instruments	Brechtel Counterflow Virtual Impactor (CVI)	N/A	Michael Wheeler	ECCC
Number distribution of particles (0.02-0.9 μm)	Brechtel Differential Mobility Analyzer (DMA)	Switched	Lynn Russell	UCSD
CCN number concentration and supersaturation spectra of particles for 0.07-0.6% supersaturation	DMT Cloud Condensation Nuclei (CCN) Counter	Switched	Markus Petters	NCSU
CCN number concentration and supersaturation spectra of particles for 0.1-1% supersaturation	Mini Handix CCN (5)	Both	Markus Petters	NCSU
Aerosol number distribution (0.15-3 μm)	Printed Optical Particle Spectrometer (POPS)	Switched	Markus Petters	NCSU
Number distribution of particles (0.5-10 μm)	TSI Aerodynamic Particle Sizer (APS)	Isokinetic	Markus Russell	NCSU
NR organic, sulfate, nitrate, chloride, ammonium mass fragment concentrations (0.07-0.8 μm) every 5 min	Aerodyne High-Resolution Aerosol Mass Spectrometer (HR-AMS) with Event Trigger (ET)	Switched	Lynn Russell	UCSD
BC mass and number distribution (0.08-1 μm)	DMT Single-Particle Soot Photometer (SP2)	Switched	Michael Wheeler	ECCC
Gas-phase compounds ionized by Iodide	Aerodyne Chemical Ionization Mass Spectrometer (CIMS)	Switched	John Liggio	ECCC
Number size distribution of fog (cloud) droplets	Fog Droplet Monitor	N/A	Rachel Chang	Dalhousie
BC and aerosol light scattering/absorption coefficients	DMT Photoacoustic Extinctiometer (PAX)	Switched	Alex Lee	ECCC
Hydroxyl radical formation by particles using direct-to-liquid sampling and fluorescence	Direct-to-Liquid Cloud Droplet OH Burst (DtL-OH)	Switched	Suzanne Paulson	UCLA
Soluble metals by ICPMS and OH burst	Filters for transition metals and OH burst	Switched	Suzanne Paulson	UCLA
Chemical composition, hygroscopicity, and volatility of ultrafine particles	TDCIMS, UHPLC-HRMS, and H/VTDMA	Isokinetic	James Smith	UCI
Organic functional group and element concentrations	Filters for FTIR and XRF	Both	Lynn Russell	UCSD
Aerosol source for sized calibration particles	TSI Atomizer with DMA for size selection	N/A	Lynn Russell	UCSD

CO, NO, and NOx concentration	Teledyne CO, NO, NOx	Isokinetic	Lynn Russell	UCSD
Temperature, relative humidity, winds, pressure	Weather Station	N/A	Lynn Russell	UCSD

Table 14. Potential instrumentation for Mt. Soledad between February 2023 and February 2024. Inlet column indicates isokinetic (aerosol), CVI, switched between inlets, or duplicated on both inlets.

The Naval Postgraduate School (NPS, formerly CIRPAS) Twin Otter aircraft, led by Witte, will deploy to San Diego for the Southern California Interactions of Low cloud and Land Aerosol (SCILLA) experiment. Flights will span a 4-week intensive observational period during June 2023, the month of climatological maximum low cloud cover, and are designed to sample aerosol, microphysics, and meteorological state upwind of the Scripps Pier during the mesoscale eddy events that typically accompany "June gloom" low cloud occurrence at the coast. SCILLA science objectives are to 1) investigate dynamical controls on aerosol transport into, and distribution within, the Southern California Bight; 2) quantify the impact of aerosol-cloud interactions on PBL structure and evolution; and 3) characterize gradients in atmospheric properties across the PBL-capping inversion to constrain vertical mixing/turbulent transport hypotheses. A summary of Twin Otter instrumentation for SCILLA is given in Table 15. In-cloud sampling of cloud droplet residuals will be performed with a counterflow virtual impactor inlet (Brechtel model 1204 CVI). Finally, the Twin Otter will be equipped to measure surface fluxes over the ocean that can be used to constrain Lagrangian modeling studies of air masses arriving at the ground-based measurement sites.

Measurement	Instrument	PI name	Institution
Meteorology (T, RH, P, 3-D wind)	Thermistor, chilled mirror hygrometer, P transducers, radome/flow angle probe	Mikael Witte	NPS
Dry particle size distribution ($0.02<D_p<0.5\ \mu m$)	Brechtel SEMS 2100	Andrew Metcalf	Clemson
Dry particle size distribution ($0.1<D_p<3.0\ \mu m$)	PMS PCASP SPP200	Andrew Metcalf	Clemson
Dry particle concentration ($D_p>0.003\ \mu m$)	Aerosol Devices MAGIC CPC, TSI UFCPC 3025	Don Collins	UC Riverside
CCN concentration	DMT CCN-100 (x2)	Don Collins	UC Riverside
Non-refractory aerosol composition	Aerodyne C-ToF-mAMS	Roya Bahreini	UC Riverside
Refractory black carbon	DMT SP2	Andrew Metcalf	Clemson
Fast gas analyzer (CO_2, H_2O)	LI-COR 7500DS	Mikael Witte	NPS
Trace gases (NO_x, O_3, CO)	Teledyne-APi T200U, T400; Ecotech EC9830T	Don Collins/ Andrew Metcalf	UC Riverside/ Clemson
Water vapor isotopic analyzer	LGR WVIA-911	Lisa Welp	Purdue
Secondary aerosol formation	Oxidation flow reactor with dedicated SMPS	Don Collins	UC Riverside
Bulk liquid water content	Gerber PVM-100A	Mikael Witte	NPS

Cloud and drizzle drop size distribution ($2<D_p<1000\ \mu m$)	Artium dual range PDI	Patrick Chuang	UC Santa Cruz
Cloud and drizzle drop size distribution ($3<D_p<1550\ \mu m$)	DMT CAPS (CDP+CIP)	Mikael Witte	NPS
Sea surface temperature	Heitronics KT 19.85 pyrometer	Mikael Witte	NPS
Down-/upwelling solar irradiance	Kipp & Zonen modified CM22 pyranometer	Mikael Witte	NPS
Down-/upwelling infrared irradiance	Kipp & Zonen modified CG4 pyrgeometer	Mikael Witte	NPS

Table 15. Potential NPS Twin Otter instrument payload for SCILLA**.**

6. AEROMMA 2023 participants

6.1. List of participating federal institutes

- NOAA Chemical Sciences Laboratory
- NOAA National Environmental Satellite Data and Information Service
- NOAA Atmospheric Chemistry, Carbon Cycle & Climate Program
- NOAA Global Monitoring Laboratory
- NOAA Global Systems Laboratory
- NOAA Air Resources Laboratory
-
- NOAA Physical Sciences Laboratory
- NIST Greenhouse Gas Measurements Program
- EPA Office of Research and Development
- EPA Office of Air Quality Planning and Standards
- NASA Tropospheric Composition Program
- NASA Goddard Space Flight Center
- NASA Langley Research Center

6.2. List of participating institutes

- Colorado State University
- Forschungszentrum Jülich
- Environment and Climate Change Canada
- Stony Brook University
- Georgia Institute of Technology
- York University
- University of Toronto
- University of Wisconsin
- University of Colorado Boulder
- Aerodyne Research Inc.

- Yale University
- University of Texas Austin
- University of California Irvine
- College of William & Mary
- University of Michigan
- University of Washington
- University of Minnesota
- Columbia University
- City College of New York
- Scripps Institution of Oceanography
- Drexel University

6.3. Stakeholders in state and regional organizations

- California: ARB, SCAQMD
- Midwest: LADCO
- Northeast US: NESCAUM, NYSERDA
- Texas: TCEQ
- Nevada: Clark County Air Quality Management
- Canada: ECCC

7. Previous experiments in the study region with CSL involvement

The previous campaigns that NOAA CSL initiated or participated in that relate to AEROMMA science are listed in Table 16.

Platform	Experiment name	PIs	Affiliation	Sponsor	Web resource
		Aircraft			
NCAR Electra	TEXAS 2000 (Texas Air Quality Study)	Fred Fehsenfeld	NOAA CSL	NOAA	https://csl.noaa.gov/projects/texaqs2k/
NOAA WP-3, NASA DC-8	ICARTT2004 (International Consortium for Atmospheric Research on Transport and Transformation)	Fred Fehsenfeld, James Gleason, Peter Daum, Richard Leaitch, Stuart Penkett, John Seinfeld	NOAA, NASA, DOE, MSC, UAE, CalTech	NOAA, NASA, DOE	https://csl.noaa.gov/projects/icartt/
NOAA WP-3	CalNex2010 (California Nexus Research at the Nexus of Air Quality and Climate Change)	Thomas Ryerson, David Parrish	NOAA CSL	NOAA	https://csl.noaa.gov/projects/calnex/
NOAA WP-3	SENEX2013 (SouthEast Nexus)	Joost deGouw, Carsten Warneke		NOAA	https://csl.noaa.gov/projects/senex/
NCAR C130	WINTER2015 (Wintertime INvestigation	Joel Thornton Steven Brown	Uni. of Washington	NSF	https://www.eol.ucar.edu/field_projects/wi

	of Transport, Emissions, and Reactivity)				nter
NASA DC-8	FIREX-AQ 2019 transits (Fire *I*nfluence on Regional to Global Environments and Air Quality)	Carsten Warneke, Joshua Schwarz, James Crawford, Jack Dibb	NOAA CSL, NASA Langley, UNH	NOAA, NASA	https://csl.noaa.gov/projects/firex-aq/
Ship					
NOAA R/V Brown	NEAQS2002 (New England Air Quality Study)		NOAA CSL, NOAA PMEL	NOAA, NOAA ERB	https://csl.noaa.gov/projects/neaqs/
Ground sites and mobile laboratory					
New York NOAA CSL mobile lab	NYC-ICE/LISTOS2018 (New York Investigations of Consumer Emissions)	Carsten Warneke	NOAA CSL	NOAA AC4	https://csl.noaa.gov/groups/csl7/measurements/2018nyice/
Las Vegas and Los Angeles NOAA CSL mobile lab	SUNVEx2021 (Southwest Urban NOx and VOC Experiment)	Jessica Gilman, Carsten Warneke, Paul Wennberg	NOAA CSL, CalTech	Clark County, CARB	https://csl.noaa.gov/projects/sunvex/

Table 16: Previous NOAA CSL experiments relevant to AEROMMA.

Contributions

- Contributed to conception and design: CW, RS, PV, AR, SB, WAB, BMcD
- Contributed to programmatic design: SB, GF, DF
- Data management: KA
- STAQS: LJ, BL, JS
- Satellite Science: RBP, SK
- Ground Sites NYC: CS
- NYC downtown + Downwind CT sites: DG, JK, AL
- Minneola site NYC: DBM, DF
- Atlanta: NLN, JK
- Ground Sites Toronto: CY
- GOTHAAM: JM, GW
- TolNet/Aeronet/Pandora Liason: JS
- ASCENT: NLN
- NIST GHGs: KM, AK
- EPA: LV
- EPCAPE: LR, MW
- NEC-AQ-GHG: XR, RD, PD
- Drafted and revised the article: all authors
- Approved the submitted version for publication: all authors

Acknowledgements

CSL gratefully acknowledges the generous support of the NOAA NESDIS GEO-XO Program, which is enabling the use of the NASA DC-8 aircraft and associated costs for NASA flight crew, engineering, integration, and logistics for the AEROMMA mission.

CSL gratefully acknowledges the support from the NOAA Office of Marine and Aviation Operations, which is enabling the use of NOAA Twin Otter aircraft for the CUPiDS mission.

We acknowledge the use of imagery from the NASA Worldview application (https://worldview.earthdata.nasa.gov/), part of the NASA Earth Observing System Data and Information System (EOSDIS).

CSL and collaborators gratefully acknowledge the support from the NOAA AC4 program, which is enabling the New York City ground site deployments and the AGES workshop in Boulder, CO.

We acknowledge NYSERDA (New York State Energy Research and Development Authority) for their support of research activities in the greater New York area during the AEROMMA (and GOTHAMM) field campaigns.

We also acknowledge the greater AGES+ science team and collaborations.

Competing interests

The authors have declared that no competing interests exist.

Data accessibility statement

Future AEROMMA data will be archived and publicly available one year after the end of the experiment in ICARTT file format at: https://csl.noaa.gov/projects/aeromma/data.html

Figures

Figure 1: (Past Trend) Trends in Los Angeles anthropogenic VOC emissions show sharp decreases in fossil-VOCs observed from 1960 to 2010 (Warneke et al., 2012). (Current Inventory) Future decreases in fossil-derived VOCs expected to be slower due to growing influence of VCP emissions (McDonald et al., 2018a).

Figure 2: (NYC Monoterpenes in Winter) The drive track of the NOAA mobile laboratory color-coded with the sum of the monoterpenes measured with PTR-ToF-MS on top of the population density map of the New York City metropolitan area. The pie charts indicate the monoterpene composition determined by GC-MS. (Population Density Dependence of VCPs) The enhancements of D5-siloxane and monoterpenes relative to the traffic marker benzene for U.S. cities with different population densities. (Reproduced from Coggon et al., (2021))

Figure 3: WRF-Chem simulations of MDA8 ozone (parts per billion) and midday (2:00 PM local time) column integrated PAN (molecules cm^{-2}) during the July 2, 2018, pollution episode. Shown are the simulations for global background ozone + NO_x and BVOCs (A and E), results from A and E with fossil fuel VOCs added (B and F), and results from B and F with VOCs from VCPs added (C and G). A–C and E–G show ozone and PAN produced without oVCP chemistry. D and H shows the simulation using full emissions but under the assumption of oVCP chemistry. Circles show the ozone mixing ratios measured at monitoring stations in the NYC area; those bolded in white exceeded US NAAQS. The numbers above each panel show the surface ozone or column PAN simulated in NYC and at the location of the MDA8 ozone maximum downwind of NYC (max). The pie charts show the ozone attribution by source, source category, and chemical class. (Reproduced from Coggon et al., (2021))

Figure 4: Measured and predicted SOA in urban and industrial environments at 2 equivalent days of OH exposure. SOA measured in the OFR is shown by the green bar and predicted SOA based on speciated VOC data by the pink tints. The predicted SOA only accounts for traditional gasoline, diesel and biogenic sources of precursors and under-predicts the observed values by a factor of ~2 in the morning time street canyon and suggests the influence of VCPs on SOA (Shah et al., 2020).

Figure 5: Trends in US NO_x emissions derived from OMI satellite products using an inverse modeling framework (Jiang et al., 2018). NO_x emissions decreased from 2005-2009 (Past Trend) but the rate of decrease slowed during 2011-2015 (Current Trend). (Soil NO_x) NO_x emissions from California soils (natural and cropland) generated using stable isotopic modeling and the IMAGE model (Almaraz et al., 2018)

Figure 6: (top) Trends in the 4th highest annual maximum of the MDA8 ozone in the AEROMMA target cities and their downwind areas since 1980. (bottom) Trends in the FIVE-VCP NO_x and VOC total and sectoral emissions (ton day^{-1}, t/d) in the Los Angeles Basin from 1987 to 2014. Trends in the FIVE-VCP emissions normalized to the values in 1987 for NO_x, VOC, CO and VOC/NO_x. The top-down model adjusted VOC/NO_x emissions trend is shown by the dashed black line and open markers denote model years simulated in WRF-Chem (Kim et al., 2022).

Figure 7: Trends in organic aerosol concentrations in the Los Angeles basin (McDonald et al., 2015) and in the U.S. from GEOS-Chem and IMPROVE sites (Ridley et al., 2018). Decreases are attributed to reductions in motor vehicle emissions and other sources of SOA.

Figure 8. Transport of ozone (in ppb) as modeled in WRF-Chem along the US East Coast, from the Mid-Atlantic through the Gulf of Maine, during the ICARTT 2004 field campaign (Lee et al., 2011).

Figure 9: Example of ozone lidar measurements by NASA Langley during LISTOS 2018 at Westport, CT.

Figure 10: A simplified overview of the linkages between oceanic emissions and processes that contribute to the formation and growth of clouds. The AEROMMA marine flights will be designed to provide addition insight into these gas and aerosol processes.

Figure 11: Linkages between air-sea exchange and the production of CCN in the remote marine atmosphere [*Quinn and Bates*, 2011]**.**

Figure 12: Tropospheric NO_2 from TropOMI on the TEMPO field of regard which includes most of the AEROMMA 2023 study region**.**

Figure 13: The GeoXO constellation planned for 2030 and beyond**.**

Figure 14. Sites that are currently active from AERONET (purple) and Pandora (green) located in the AEROMMA target city regions.

Figure 15. GOES-16 ABI AOD without and with empirical bias correction (Zhang et al., 2020a).

Figure 16: (top from Brock et al. (2021)) Aerosol extinction profiles derived from in-situ airborne instrumentation on-board the NASA DC-8 during the ATom field campaign. (bottom) Evaluation of AOD derived from airborne data with Suomi-NPP/VIIRS AOD products.

Figure 17: The U.S. weather mortality rates (figure from GeoXO Value Assessment, 2020)**.**

Figure 18: The deployment areas for AEROMMA and related activities in 2023.

Figure 19: Suggested payload for the NASA DC-8 aircraft for AEROMMA. Diagram is current as of December 2022.

Figure 20: Examples of potential flight plans for the NASA DC-8 aircraft for urban focused flights over Los Angeles, New York City, Toronto, Chicago, Houston, Dallas, and Atlanta.

Figure 21: Examples of potential plans for the NASA DC-8 aircraft for marine focused research flights over the Pacific Ocean. Altitude profiles shown on the right are examples of the types of flight modules that will be used to perform vertical profile and airborne flux observations throughout the marine boundary layer.

Figure 22: The study region for the NOAA Twin Otter for CUPiDS 2023.

Figure 23: The proposed payload of the NOAA Twin Otter for CUPiDS 2023.

Figure 24: Example of airborne Doppler lidar vertical velocity data. (Left) and sensing volumes of remote measurements made from the NOAA Twin Otter during CUPiDS 2023 (Right).

Figure 25: Map of the annual average TROPOMI NO_2 column density measurements for April 2018-March 2019 showing the currently planned primary (solid circles) sampling domains during STAQS within the TEMPO field of regard (black outline).

Tables

Table 10: Potential instrument list of the FROG-NY 2023 ground site deployment.

Table 11: Potential instrument list and PIs for THE CIX.

Table 12: Instrumentation to be installed at each ASCENT site.

Table 13: ARM instruments requested for EPCAPE.

Table 14. Potential instrumentation for Mt. Soledad between February 2023 and February 2024. Inlet column indicates isokinetic (aerosol), CVI, switched between inlets, or duplicated on both inlets.

Table 15. Potential NPS Twin Otter instrument payload for SCILLA.

Table 16: Previous NOAA CSL experiments relevant to AEROMMA.

References

Ahmadov R, McKeen S, Trainer M, Banta R, Brewer A, et al. 2015. Understanding high wintertime ozone pollution events in an oil- and natural gas-producing region of the western US. *Atmos Chem Phys* **15**(1): 411-429. doi:10.5194/acp-15-411-2015.

Almaraz M, Bai E, Wang C, Trousdell J, Conley S, et al. 2018. Agriculture is a major source of NOx pollution in California. *Science Advances* **4**(1). doi:10.1126/sciadv.aao3477.

Alvarez RA, Zavala-Araiza D, Lyon DR, Allen DT, Barkley ZR, et al. 2018. Assessment of methane emissions from the US oil and gas supply chain. *Science* **361**(6398): 186-188. doi:10.1126/science.aar7204.

Andreae MO. 1990. Ocean-Atmosphere Interactions in the Global Biogeochemical Sulfur Cycle. *Mar Chem* **30**(1-3): 1-29. doi:10.1016/0304-4203(90)90059-l.

Andreae MO, Andreae TW, Ditas F, Pohlker C. 2022. Frequent new particle formation at remote sites in the subboreal forest of North America. *Atmos Chem Phys* **22**(4): 2487-2505. doi:10.5194/acp-22-2487-2022.

Andreae MO, Ferek RJ, Bermond F, Byrd KP, Engstrom RT, et al. 1985. Dimethyl sulfide in the marine atmosphere. *J Geophys Res-Atmos* **90**(D7): 2891-2900. doi:10.1029/JD090iD07p12891.

Andreae MO, Rosenfeld D. 2008. Aerosol–cloud–precipitation interactions. Part 1. The nature and sources of cloud-active aerosols. *Earth-Science Reviews* **89**(1): 13-41. doi:https://doi.org/10.1016/j.earscirev.2008.03.001.

Angevine WM, Brioude J, McKeen S, Holloway JS, Lerner BM, et al. 2013. Pollutant transport among California regions. *J Geophys Res-Atmos* **118**(12): 6750-6763. doi:10.1002/jgrd.50490.

Angevine WM, Buhr MP, Holloway JS, Trainer M, Parrish DD, et al. 1996. Local meteorological features affecting chemical measurements at a North Atlantic coastal site. *J Geophys Res* **101**: 28935-28946.

Angevine WM, Eddington L, Durkee K, Fairall C, Bianco L, et al. 2012. Meteorological Model Evaluation for CalNex 2010. *Monthly Weather Review* **140**(12): 3885-3906. doi:10.1175/mwr-d-12-00042.1.

Bahreini R, Middlebrook AM, de Gouw JA, Warneke C, Trainer M, et al. 2012. Gasoline emissions dominate over diesel in formation of secondary organic aerosol mass. *Geophys Res Lett* **39**. doi:L06805 10.1029/2011gl050718.

Banta RM, Pichugina YL, Brewer WA, James EP, Olson JB, et al. 2018. EVALUATING AND IMPROVING NWP FORECAST MODELS FOR THE FUTURE How the Needs of Offshore Wind Energy Can Point the Way. *Bulletin of the American Meteorological Society* **99**(6): 1155-1176. doi:10.1175/bams-d-16-0310.1.

Banta RM, Senff CJ, Alvarez RJ, Langford AO, Parrish DD, et al. 2011. Dependence of daily peak O-3 concentrations near Houston, Texas on environmental factors: Wind speed, temperature, and boundary-layer depth. *Atmos Environ* **45**(1): 162-173. doi:10.1016/j.atmosenv.2010.09.030.

Banta RM, Senff CJ, Nielsen-Gammon J, Darby LS, Ryerson TB, et al. 2005. A bad air day in Houston. *Bulletin of the American Meteorological Society* **86**(5): 657-+. doi:10.1175/bams-86-5-657.

Bates TS, Lamb BK, Guenther A, Dignon J, Stoiber RE. 1992. Sulfur emissions to the atmosphere from natural sources. *Journal of Atmospheric Chemistry* **14**(1-4): 315-337. doi:10.1007/bf00115242.

Beirle S, Borger C, Doerner S, Li A, Hu Z, et al. 2019. Pinpointing nitrogen oxide emissions from space. *Science Advances* **5**(11). doi:10.1126/sciadv.aax9800.

Bianchi F, Kurten T, Riva M, Mohr C, Rissanen MP, et al. 2019. Highly Oxygenated Organic Molecules (HOM) from Gas-Phase Autoxidation Involving Peroxy Radicals: A Key Contributor to Atmospheric Aerosol. *Chemical Reviews* **119**(6): 3472-3509. doi:10.1021/acs.chemrev.8b00395.

Blanchard CL, Hidy GM, Tanenbaum S. 2014. Ozone in the southeastern United States: An observation-based model using measurements from the SEARCH network. *Atmos Environ* **88**: 192-200. doi:10.1016/j.atmosenv.2014.02.006.

Boniface J, Shi Q, Li YQ, Cheung JL, Rattigan OV, et al. 2000. Uptake of gas-phase SO2, H2S, and CO2 by aqueous solutions. *Journal of Physical Chemistry A* **104**(32): 7502-7510. doi:10.1021/jp000479h.

Brock CA, Froyd KD, Dollner M, Williamson CJ, Schill G, et al. 2021. Ambient aerosol properties in the remote atmosphere from global-scale in situ measurements. *Atmos Chem Phys* **21**(19): 15023-15063. doi:10.5194/acp-21-15023-2021.

Bruhl C, Lelieveld J, Crutzen PJ, Tost H. 2012. The role of carbonyl sulphide as a source of stratospheric sulphate aerosol and its impact on climate. *Atmos Chem Phys* **12**(3): 1239-1253. doi:10.5194/acp-12-1239-2012.

Campbell PC, Tong D, Tang YH, Baker B, Lee P, et al. 2021. Impacts of the COVID-19 economic slowdown on ozone pollution in the U. S. *Atmos Environ* **264**. doi:10.1016/j.atmosenv.2021.118713.

Cao HS, Henze DK, Shephard MW, Dammers E, Cady-Pereira K, et al. 2020. Inverse modeling of NH3 sources using CrIS remote sensing measurements. *Environmental Research Letters* **15**(10). doi:10.1088/1748-9326/abb5cc.

Carpenter LJ, Nightingale PD. 2015. Chemistry and Release of Gases from the Surface Ocean. *Chemical Reviews* **115**(10): 4015-4034. doi:10.1021/cr5007123.

Carslaw KS, Lee LA, Reddington CL, Pringle KJ, Rap A, et al. 2013. Large contribution of natural aerosols to uncertainty in indirect forcing. *Nature* **503**(7474): 67-71. doi:10.1038/nature12674.

Chance K, Liu X, Suleiman RM, Flittner DE, Al-Saadi J, et al. 2013. Tropospheric emissions: Monitoring of pollution (TEMPO), in Butler JJ, Xiong X, Gu X eds., *Earth Observing Systems Xviii*.

Charlson RJ, Lovelockt JE, Warren SG. 1987. Oceanic phytoplankton, atmospheric sulphur, cloud albedo and climate.

Chen QJ, Sherwen T, Evans M, Alexander B. 2018. DMS oxidation and sulfur aerosol formation in the marine troposphere: a focus on reactive halogen and multiphase chemistry. *Atmos Chem Phys* **18**(18): 13617-13637. doi:10.5194/acp-18-13617-2018.

Chin M, Jacob DJ, Gardner GM, ForemanFowler MS, Spiro PA, et al. 1996. A global three-dimensional model of tropospheric sulfate. *J Geophys Res-Atmos* **101**(D13): 18667-18690. doi:10.1029/96jd01221.

Coggon MM, Gkatzelis GI, McDonald BC, Gilman JB, Schwantes RH, et al. 2021. Volatile chemical product emissions enhance ozone and modulate urban chemistry. *Proceedings of the National Academy of Sciences of the United States of America* **118**(32). doi:10.1073/pnas.2026653118.

Cohen AJ, Brauer M, Burnett R, Anderson HR, Frostad J, et al. 2017. Estimates and 25-year trends of the global burden of disease attributable to ambient air pollution: an analysis of data from the Global Burden of Diseases Study 2015. *Lancet* **389**(10082): 1907-1918. doi:10.1016/s0140-6736(17)30505-6.

Cooper OR, Langford AO, Parrish DD, Fahey DW. 2015. Challenges of a lowered US ozone standard. *Science* **348**(6239): 1096-1097. doi:10.1126/science.aaa5748.

Cooper OR, Parrish DD, Stohl A, Trainer M, Nedelec P, et al. 2010. Increasing springtime ozone mixing ratios in the free troposphere over western North America. *Nature* **463**(7279): 344-348. doi:10.1038/nature08708.

Crilley LR, Kramer LJ, Pope FD, Reed C, Lee JD, et al. 2021. Is the ocean surface a source of nitrous acid (HONO) in the marine boundary layer? *Atmos Chem Phys* **21**(24): 18213-18225. doi:10.5194/acp-21-18213-2021.

Darby LS, McKeen SA, Senff CJ, White AB, Banta RM, et al. 2007. Ozone differences between near-coastal and offshore sites in New England: Role of meteorology. *J Geophys Res-Atmos* **112**(D16). doi:10.1029/2007jd008446.

Demetillo MAG, Harkins C, McDonald BC, Chodrow PS, Sun K, et al. 2021. Space-Based Observational Constraints on NO2 Air Pollution Inequality From Diesel Traffic in Major US Cities. *Geophys Res Lett* **48**(17). doi:10.1029/2021gl094333.

Demetillo MAG, Navarro A, Knowles KK, Fields KP, Geddes JA, et al. 2020. Observing Nitrogen Dioxide Air Pollution Inequality Using High-Spatial-Resolution Remote Sensing Measurements in Houston, Texas. *Environ Sci Technol* **54**(16): 9882-9895. doi:10.1021/acs.est.0c01864.

Dixit P, Miller JW, Cocker DR, Oshinuga A, Jiang Y, et al. 2017. Differences between emissions measured in urban driving and certification testing of heavy-duty diesel engines. *Atmos Environ* **166**: 276-285. doi:10.1016/j.atmosenv.2017.06.037.

Doherty RM, Heal MR, O'Connor FM. 2017. Climate change impacts on human health over Europe through its effect on air quality. *Environmental Health* **16**: 33-44. doi:10.1186/s12940-017-0325-2.

Dunne EM, Gordon H, Kurten A, Almeida J, Duplissy J, et al. 2016. Global atmospheric particle formation from CERN CLOUD measurements. *Science* **354**(6316): 1119-1124. doi:10.1126/science.aaf2649.

Duren RM, Miller CE. 2012. COMMENTARY: Measuring the carbon emissions of megacities. *Nature Climate Change* **2**(8): 560-562. doi:10.1038/nclimate1629.

Eckl M, Roiger A, Kostinek J, Fiehn A, Huntrieser H, et al. 2021. Quantifying Nitrous Oxide Emissions in the US Midwest: A Top-Down Study Using High Resolution Airborne In-Situ Observations. *Geophys Res Lett* **48**(5). doi:10.1029/2020gl091266.

Fann N, Lamson AD, Anenberg SC, Wesson K, Risley D, et al. 2012. Estimating the National Public Health Burden Associated with Exposure to Ambient PM2.5 and Ozone. *Risk Analysis* **32**(1): 81-95. doi:10.1111/j.1539-6924.2011.01630.x.

Francoeur CB, McDonald BC, Gilman JB, Zarzana KJ, Dix B, et al. 2021. Quantifying Methane and Ozone Precursor Emissions from Oil and Gas Production Regions across the Contiguous US. *Environ Sci Technol* **55**(13): 9129-9139. doi:10.1021/acs.est.0c07352.

Frost GJ, Kopacz M, Kondragunta S, Ahmadov R, Al-Saadi J, et al. 2020. A Value Assessment of an Atmospheric Composition Capability on the NOAA Next-Generation Geostationary and Extended Orbits (GEO-XO) Missions. doi:https://doi.org/10.25923/1s4s-t405.

Fung KM, Heald CL, Kroll JH, Wang SY, Jo DS, et al. 2022. Exploring dimethyl sulfide (DMS) oxidation and implications for global aerosol radiative forcing. *Atmos Chem Phys* **22**(2): 1549-1573. doi:10.5194/acp-22-1549-2022.

Gakidou E, Afshin A, Abajobir AA, Abate KH, Abbafati C, et al. 2017. Global, regional, and national comparative risk assessment of 84 behavioural, environmental and occupational, and metabolic risks or clusters of risks, 1990-2016: a systematic analysis for the Global Burden of Disease Study 2016. *Lancet* **390**(10100): 1345-1422. doi:10.1016/s0140-6736(17)32366-8.

Galí M, Devred E, Babin M, Levasseur M. 2019. Decadal increase in Arctic dimethylsulfide emission. *Proceedings of the National Academy of Sciences* **116**(39): 19311. doi:10.1073/pnas.1904378116.

Gately CK, Hutyra LR. 2017. Large Uncertainties in Urban-Scale Carbon Emissions. *J Geophys Res-Atmos* **122**(20): 11242-11260. doi:10.1002/2017jd027359.

Gately CK, Hutyra LR, Wing IS. 2015. Cities, traffic, and CO2: A multidecadal assessment of trends, drivers, and scaling relationships. *Proceedings of the National Academy of Sciences of the United States of America* **112**(16): 4999-5004. doi:10.1073/pnas.1421723112.

Gaudel A, Cooper OR, Ancellet G, Barret B, Boynard A, et al. 2018. Tropospheric Ozone Assessment Report: Present-day distribution and trends of tropospheric ozone relevant to climate and global atmospheric chemistry model evaluation. *Elementa-Science of the Anthropocene* **6**. doi:10.1525/elementa.291.

Gkatzelis GI, Coggon MM, McDonald BC, Peischl J, Aikin KC, et al. 2021a. Identifying Volatile Chemical Product Tracer Compounds in US Cities. *Environ Sci Technol* **55**(1): 188-199. doi:10.1021/acs.est.0c05467.

Gkatzelis GI, Coggon MM, McDonald BC, Peischl J, Gilman JB, et al. 2021b. Observations Confirm that Volatile Chemical Products Are a Major Source of Petrochemical Emissions in US Cities. *Environ Sci Technol* **55**(8): 4332-4343. doi:10.1021/acs.est.0c05471.

Gkatzelis GI, Gilman JB, Brown SS, Eskes H, Gomes AR, et al. 2021c. The global impacts of COVID-19 lockdowns on urban air pollution: A critical review and recommendations. *Elementa-Science of the Anthropocene* **9**(1). doi:10.1525/elementa.2021.00176.

Goldberg DL, Lu Z, Streets DG, de Foy B, Griffin D, et al. 2019. Enhanced Capabilities of TROPOMI NO2: Estimating NOx from North American Cities and Power Plants. *Environ Sci Technol* **53**(21): 12594-12601. doi:10.1021/acs.est.9b04488.

Gondwe M, Krol M, Gieskes W, Klaassen W, de Baar H. 2003. The contribution of ocean-leaving DMS to the global atmospheric burdens of DMS, MSA, SO2, and NSS SO4=. *Global Biogeochemical Cycles* **17**(2). doi:10.1029/2002gb001937.

Gordon H, Sengupta K, Rap A, Duplissy J, Frege C, et al. 2016. Reduced anthropogenic aerosol radiative forcing caused by biogenic new particle formation. *Proceedings of the National Academy of Sciences of the United States of America* **113**(43): 12053-12058. doi:10.1073/pnas.1602360113.

Grandey BS, Wang C. 2015. Enhanced marine sulphur emissions offset global warming and impact rainfall. *Scientific Reports* **5**: 7. doi:10.1038/srep13055.

Gronoff G, Robinson J, Berkoff T, Swap R, Farris B, et al. 2019. A method for quantifying near range point source induced O3 titration events using Co-located Lidar and Pandora measurements. *Atmos Environ* **204**: 43-52. doi:https://doi.org/10.1016/j.atmosenv.2019.01.052.

Habeeb D, Vargo J, Stone B, Jr. 2015. Rising heat wave trends in large US cities. *Natural Hazards* **76**(3): 1651-1665. doi:10.1007/s11069-014-1563-z.

Hannun RA, Swanson AK, Bailey SA, Hanisco TF, Bui TP, et al. 2020. A cavity-enhanced ultraviolet absorption instrument for high-precision, fast-time-response ozone measurements. *Atmos Meas Tech* **13**(12): 6877-6887. doi:10.5194/amt-13-6877-2020.

Helmig D, Lang EK, Bariteau L, Boylan P, Fairall CW, et al. 2012. Atmosphere-ocean ozone fluxes during the TexAQS 2006, STRATUS 2006, GOMECC 2007, GasEx 2008, and AMMA 2008 cruises. *Journal of Geophysical Research: Atmospheres* **117**(D4). doi:https://doi.org/10.1029/2011JD015955.

Hodshire AL, Campuzano-Jost P, Kodros JK, Croft B, Nault BA, et al. 2019. The potential role of methanesulfonic acid (MSA) in aerosol formation and growth and the associated radiative forcings. *Atmos Chem Phys* **19**(5): 3137-3160. doi:10.5194/acp-19-3137-2019.

Hoffmann EH, Tilgner A, Schrodner R, Brauera P, Wolke R, et al. 2016. An advanced modeling study on the impacts and atmospheric implications of multiphase dimethyl sulfide chemistry. *Proceedings of the National Academy of Sciences of the United States of America* **113**(42): 11776-11781. doi:10.1073/pnas.1606320113.

Hossaini R, Chipperfield MP, Saiz-Lopez A, Fernandez R, Monks S, et al. 2016. A global model of tropospheric chlorine chemistry: Organic versus inorganic sources and impact on methane oxidation. *Journal of Geophysical Research: Atmospheres* **121**(23): 14,271-14,297. doi:10.1002/2016JD025756.

IPCC. 2018. Summary for Policymakers of IPCC Special Report on Global Warming of 1.5°C approved by governments.

Jensen MP, Flynn JH, Judd LM, Kollias P, Kuang C, et al. 2022. A Succession of Cloud, Precipitation, Aerosol, and Air Quality Field Experiments in the Coastal Urban Environment. *Bulletin of the American Meteorological Society* **103**(2): 103-105. doi:10.1175/bams-d-21-0104.1.

Jernigan CM, Fite CH, Vereecken L, Berkelhammer MB, Rollins AW, et al. 2022. Efficient Production of Carbonyl Sulfide in the Low-NOx Oxidation of Dimethyl Sulfide. *Geophys Res Lett* **49**(3). doi:10.1029/2021gl096838.

Jiang Z, McDonald BC, Worden H, Worden JR, Miyazaki K, et al. 2018. Unexpected slowdown of US pollutant emission reduction in the past decade. *Proceedings of the National Academy of Sciences of the United States of America* **115**(20): 5099-5104. doi:10.1073/pnas.1801191115.

Johansson JKE, Mellqvist J, Samuelsson J, Offerle B, Lefer B, et al. 2014. Emission measurements of alkenes, alkanes, SO2, and NO2 from stationary sources in Southeast Texas over a 5 year period using SOF and mobile DOAS. *J Geophys Res-Atmos* **119**(4): 1973-1991. doi:10.1002/2013jd020485.

Kim SW, McDonald BC, Baidar S, Brown SS, Dube B, et al. 2016. Modeling the weekly cycle of NOx and CO emissions and their impacts on O-3 in the Los Angeles-South Coast Air Basin during the CalNex 2010 field campaign. *J Geophys Res-Atmos* **121**(3): 1340-1360. doi:10.1002/2015jd024292.

Kim SW, McDonald BC, Seo S, Kim K-M, Trainer M. 2022. Understanding the Paths of Surface Ozone Abatement in the Los Angeles Basin. *Journal of Geophysical Research: Atmospheres* **127**(4): e2021JD035606. doi:https://doi.org/10.1029/2021JD035606.

Kim SW, Natraj V, Lee S, Kwon H-A, Park R, et al. 2018. Impact of high-resolution a priori profiles on satellite-based formaldehyde retrievals. *Atmos Chem Phys* **18**(10): 7639-7655. doi:10.5194/acp-18-7639-2018.

Klein F, Platt SM, Farren NJ, Detournay A, Bruns EA, et al. 2016. Characterization of Gas-Phase Organics Using Proton Transfer Reaction Time-of-Flight Mass Spectrometry: Cooking Emissions. *Environ Sci Technol* **50**(3): 1243-1250. doi:10.1021/acs.est.5b04618.

Klimont Z, Smith SJ, Cofala J. 2013. The last decade of global anthropogenic sulfur dioxide: 2000-2011 emissions. *Environmental Research Letters* **8**(1): 6. doi:10.1088/1748-9326/8/1/014003.

Kondragunta S, Wei Z, McDonald BC, Goldberg DL, Tong DQ. 2021. COVID-19 Induced Fingerprints of a New Normal Urban Air Quality in the United States. *J Geophys Res-Atmos* **126**(17). doi:10.1029/2021jd034797.

Krotkov NA, McLinden CA, Li C, Lamsal LN, Celarier EA, et al. 2016. Aura OMI observations of regional SO2 and NO2 pollution changes from 2005 to 2015. *Atmos Chem Phys* **16**(7): 4605-4629. doi:10.5194/acp-16-4605-2016.

Kulmala M. 2003. How particles nucleate and grow. *Science* **302**(5647): 1000-1001. doi:10.1126/science.1090848.

Kuwayama T, Charrier-Klobas JG, Chen Y, Vizenor NM, Blake DR, et al. 2019. Source Apportionment of Ambient Methane Enhancements in Los Angeles, California, To Evaluate Emission Inventory Estimates. *Environ Sci Technol* **53**(6): 2961-2970. doi:10.1021/acs.est.8b02307.

Langford AO, Alvarez RJ, II, Brioude J, Fine R, Gustin MS, et al. 2017. Entrainment of stratospheric air and Asian pollution by the convective boundary layer in the southwestern US. *J Geophys Res-Atmos* **122**(2): 1312-1337. doi:10.1002/2016jd025987.

Langford AO, Senff CJ, Alvarez RJ, II, Banta RM, Hardesty RM. 2010. Long-range transport of ozone from the Los Angeles Basin: A case study. *Geophys Res Lett* **37**. doi:10.1029/2010gl042507.

Langford AO, Senff CJ, Alvarez RJ, II, Brioude J, Cooper OR, et al. 2015. An overview of the 2013 Las Vegas Ozone Study (LVOS): Impact of stratospheric intrusions and long-range transport on surface air quality. *Atmos Environ* **109**: 305-322. doi:10.1016/j.atmosenv.2014.08.040.

Laughner JL, Cohen RC. 2019. Direct observation of changing NOx lifetime in North American cities. *Science* **366**(6466): 723-+. doi:10.1126/science.aax6832.

Lawson SJ, Law CS, Harvey MJ, Bell TG, Walker CF, et al. 2020. Methanethiol, dimethyl sulfide and acetone over biologically productive waters in the southwest Pacific Ocean. *Atmos Chem Phys* **20**(5): 3061-3078. doi:10.5194/acp-20-3061-2020.

Lee SH, Kim SW, Trainer M, Frost GJ, McKeen SA, et al. 2011. Modeling ozone plumes observed downwind of New York City over the North Atlantic Ocean during the ICARTT field campaign. *Atmos Chem Phys* **11**(14): 7375-7397. doi:10.5194/acp-11-7375-2011.

Li M, McDonald BC, McKeen SA, Eskes H, Levelt P, et al. 2021. Assessment of Updated Fuel-Based Emissions Inventories Over the Contiguous United States Using TROPOMI NO2 Retrievals. *Journal of Geophysical Research-Atmospheres* **126**(24). doi:10.1029/2021jd035484.

Ma SQ, Tong D, Lamsal L, Wang J, Zhang XL, et al. 2021. Improving predictability of high-ozone episodes through dynamic boundary conditions, emission refresh and chemical data assimilation during the Long Island Sound Tropospheric Ozone Study (LISTOS) field campaign. *Atmos Chem Phys* **21**(21): 16531-16553. doi:10.5194/acp-21-16531-2021.

Manoli G, Fatichi S, Schlapfer M, Yu K, Crowther TW, et al. 2019. Magnitude of urban heat islands largely explained by climate and population. *Nature* **573**(7772): 55-+. doi:10.1038/s41586-019-1512-9.

McDonald BC, de Gouw JA, Gilman JB, Jathar SH, Akherati A, et al. 2018a. Volatile chemical products emerging as largest petrochemical source of urban organic emissions. *Science* **359**(6377): 760-764. doi:10.1126/science.aaq0524.

McDonald BC, Goldstein AH, Harley RA. 2015. Long-Term Trends in California Mobile Source Emissions and Ambient Concentrations of Black Carbon and Organic Aerosol. *Environ Sci Technol* **49**(8): 5178-5188. doi:10.1021/es505912b.

McDonald BC, McBride ZC, Martin EW, Harley RA. 2014. High-resolution mapping of motor vehicle carbon dioxide emissions. *J Geophys Res-Atmos* **119**(9): 5283-5298. doi:10.1002/2013jd021219.

McDonald BC, McKeen SA, Cui YY, Ahmadov R, Kim SW, et al. 2018b. Modeling Ozone in the Eastern US using a Fuel-Based Mobile Source Emissions Inventory. *Environ Sci Technol* **52**(13): 7360-7370. doi:10.1021/acs.est.8b00778.

McFiggans G, Bale CSE, Ball SM, Beames JM, Bloss WJ, et al. 2010. Iodine-mediated coastal particle formation: an overview of the Reactive Halogens in the Marine Boundary Layer (RHaMBLe) Roscoff coastal study. *Atmos Chem Phys* **10**(6): 2975-2999. doi:10.5194/acp-10-2975-2010.

Meehl GA, Tebaldi C, Tilmes S, Lamarque J-F, Bates S, et al. 2018. Future heat waves and surface ozone. *Environmental Research Letters* **13**(6). doi:10.1088/1748-9326/aabcdc.

Merikanto J, Spracklen DV, Mann GW, Pickering SJ, Carslaw KS. 2009. Impact of nucleation on global CCN. *Atmos Chem Phys* **9**(21): 8601-8616. doi:10.5194/acp-9-8601-2009.

Meskhidze N, Nenes A. 2006. Phytoplankton and Cloudiness in the Southern Ocean. *Science* **314**(5804): 1419. doi:10.1126/science.1131779.

Montzka SA, Krol M, Dlugokencky E, Hall B, Jockel P, et al. 2011. Small Interannual Variability of Global Atmospheric Hydroxyl. *Science* **331**(6013): 67-69. doi:10.1126/science.1197640.

Moore RH, Karydis VA, Capps SL, Lathem TL, Nenes A. 2013. Droplet number uncertainties associated with CCN: an assessment using observations and a global model adjoint. *Atmos Chem Phys* **13**(8): 4235-4251. doi:10.5194/acp-13-4235-2013.

Mora C, Dousset B, Caldwell IR, Powell FE, Geronimo RC, et al. 2017. Global risk of deadly heat. *Nature Climate Change* **7**(7): 501-+. doi:10.1038/nclimate3322.

Muñiz-Unamunzaga M, Borge R, Sarwar G, Gantt B, de la Paz D, et al. 2018. The influence of ocean halogen and sulfur emissions in the air quality of a coastal megacity: The case of Los Angeles. *Science of The Total Environment* **610-611**: 1536-1545. doi:https://doi.org/10.1016/j.scitotenv.2017.06.098.

Murray CJL, Aravkin AY, Zheng P, Abbafati C, Abbas KM, et al. 2020. Global burden of 87 risk factors in 204 countries and territories, 1990-2019: a systematic analysis for the Global Burden of Disease Study 2019. *Lancet* **396**(10258): 1223-1249. doi:10.1016/s0140-6736(20)30752-2.

Narenpitak P, Kazil J, Yamaguchi T, Quinn P, Feingold G. 2021. From Sugar to Flowers: A Transition of Shallow Cumulus Organization During ATOMIC. *Journal of Advances in Modeling Earth Systems* **13**. doi:10.1029/2021MS002619.

Negron AMG, McDonald BC, McKeen SA, Peischl J, Ahmadov R, et al. 2018. Development of a Fuel-Based Oil and Gas Inventory of Nitrogen Oxides Emissions. *Environ Sci Technol* **52**(17): 10175-10185. doi:10.1021/acs.est.8b02245.

Novak GA, Fite CH, Holmes CD, Veres PR, Neuman JA, et al. 2021. Rapid cloud removal of dimethyl sulfide oxidation products limits SO2 and cloud condensation nuclei production in the marine atmosphere. *Proceedings of the National Academy of Sciences of the United States of America* **118**(42). doi:10.1073/pnas.2110472118.

Novak GA, Kilgour DB, Jernigan CM, Vermeuel MP, Bertram TH. 2022. Oceanic emissions of dimethyl sulfide and methanethiol and their contribution to sulfur dioxide production in the marine atmosphere. *Atmos Chem Phys* **22**(9): 6309-6325. doi:10.5194/acp-22-6309-2022.

Novak GA, Vermeuel MP, Bertram TH. 2020. Simultaneous detection of ozone and nitrogen dioxide by oxygen anion chemical ionization mass spectrometry: a fast-time-response sensor suitable for eddy covariance measurements. *Atmospheric Measurement Techniques* **13**(4): 1887-1907. doi:10.5194/amt-13-1887-2020.

O'Dowd CD, De Leeuw G. 2007. Marine aerosol production: a review of the current knowledge. *Philos Trans R Soc A-Math Phys Eng Sci* **365**(1856): 1753-1774. doi:10.1098/rsta.2007.2043.

Osthoff HD, Roberts JM, Ravishankara AR, Williams EJ, Lerner BM, et al. 2008. High levels of nitryl chloride in the polluted subtropical marine boundary layer. *Nature Geoscience* **1**(5): 324-328. doi:10.1038/ngeo177.

Parrish DD, Kuster WC, Shao M, Yokouchi Y, Kondo Y, et al. 2009. Comparison of air pollutant emissions among mega-cities. *Atmos Environ* **43**(40): 6435-6441. doi:10.1016/j.atmosenv.2009.06.024.

Peischl J, Ryerson TB, Brioude J, Aikin KC, Andrews AE, et al. 2013. Quantifying sources of methane using light alkanes in the Los Angeles basin, California. *J Geophys Res-Atmos* **118**(10): 4974-4990. doi:10.1002/jgrd.50413.

Pennington EA, Seltzer KM, Murphy BN, Qin MM, Seinfeld JH, et al. 2021. Modeling secondary organic aerosol formation from volatile chemical products. *Atmos Chem Phys* **21**(24): 18247-18261. doi:10.5194/acp-21-18247-2021.

Pichugina YL, Banta RM, Olson JB, Carley JR, Marquis MC, et al. 2017. Assessment of NWP Forecast Models in Simulating Offshore Winds through the Lower Boundary Layer by Measurements from a Ship-Based Scanning Doppler Lidar. *Monthly Weather Review* **145**(10): 4277-4301. doi:10.1175/mwr-d-16-0442.1.

Pitiranggon M, Johnson S, Haney J, Eisl H, Ito K. 2021. Long-term trends in local and transported PM2.5 pollution in New York City. *Atmos Environ* **248**: 118238. doi:https://doi.org/10.1016/j.atmosenv.2021.118238.

Plant G, Kort EA, Floerchinger C, Gvakharia A, Vimont I, et al. 2019. Large Fugitive Methane Emissions From Urban Centers Along the US East Coast. *Geophys Res Lett* **46**(14): 8500-8507. doi:10.1029/2019gl082635.

Platt U, Honninger G. 2003. The role of halogen species in the troposphere. *Chemosphere* **52**(2): 325-338. doi:10.1016/s0045-6535(03)00216-9.

Pollack IB, Ryerson TB, Trainer M, Neuman JA, Roberts JM, et al. 2013. Trends in ozone, its precursors, and related secondary oxidation products in Los Angeles, California: A synthesis of measurements from 1960 to 2010. *J Geophys Res-Atmos* **118**(11): 5893-5911. doi:10.1002/jgrd.50472.

Prather KA, Bertram TH, Grassian VH, Deane GB, Stokes MD, et al. 2013. Bringing the ocean into the laboratory to probe the chemical complexity of sea spray aerosol. *Proceedings of the National Academy of Sciences of the United States of America* **110**(19): 7550-7555. doi:10.1073/pnas.1300262110.

Pye HOT, Place BK, Murphy BN, Seltzer KM, D'Ambro EL, et al. 2022. Linking gas, particulate, and toxic endpoints to air emissions in the Community Regional Atmospheric Chemistry Multiphase Mechanism (CRACMM) version 1.0. *Atmos Chem Phys Discuss* **2022**: 1-88. doi:10.5194/acp-2022-695.

Qin MM, Murphy BN, Isaacs KK, McDonald BC, Lu QY, et al. 2021. Criteria pollutant impacts of volatile chemical products informed by near-field modelling. *Nature Sustainability* **4**(2): 129-+. doi:10.1038/s41893-020-00614-1.

Quinn PK, Bates TS. 2011. The case against climate regulation via oceanic phytoplankton sulphur emissions. *Nature* **480**(7375): 51-56. doi:10.1038/nature10580.

Raff JD, Njegic B, Chang WL, Gordon MS, Dabdub D, et al. 2009. Chlorine activation indoors and outdoors via surface-mediated reactions of nitrogen oxides with hydrogen chloride. *Proceedings of the National Academy of Sciences*: pnas.0904195106. doi:10.1073/pnas.0904195106.

Reed C, Evans MJ, Crilley LR, Bloss WJ, Sherwen T, et al. 2017. Evidence for renoxification in the tropical marine boundary layer. *Atmos Chem Phys* **17**(6): 4081-4092. doi:10.5194/acp-17-4081-2017.

Ridley DA, Heald CL, Ridley KJ, Kroll JH. 2018. Causes and consequences of decreasing atmospheric organic aerosol in the United States. *Proceedings of the National Academy of Sciences of the United States of America* **115**(2): 290-295. doi:10.1073/pnas.1700387115.

Rollins AW, Rickly PS, Gao RS, Ryerson TB, Brown SS, et al. 2020. Single-photon laser-induced fluorescence detection of nitric oxide at sub-parts-per-trillion mixing ratios. *Atmos Meas Tech* **13**(5): 2425-2439. doi:10.5194/amt-13-2425-2020.

Saiz-Lopez A, von Glasow R. 2012. Reactive halogen chemistry in the troposphere. *Chemical Society Reviews* **41**(19): 6448-6472. doi:10.1039/C2CS35208G.

Saltzman ES, Savoie DL, Zika RG, Prospero JM. 1983. Methane sulfonic-acid in the marine atmosphere. *Journal of Geophysical Research-Oceans* **88**(NC15): 897-902. doi:10.1029/JC088iC15p10897.

Sanchez KJ, Russell LM, Modini RL, Frossard AA, Ahlm L, et al. 2016. Meteorological and aerosol effects on marine cloud microphysical properties. *J Geophys Res-Atmos* **121**(8): 4142-4161. doi:10.1002/2015jd024595.

Shah RU, Coggon MM, Gkatzelis GI, McDonald BC, Tasoglou A, et al. 2020. Urban Oxidation Flow Reactor Measurements Reveal Significant Secondary Organic Aerosol Contributions from Volatile Emissions of Emerging Importance. *Environ Sci Technol* **54**(2): 714-725. doi:10.1021/acs.est.9b06531.

Sherwen T, Schmidt JA, Evans MJ, Carpenter LJ, Großmann K, et al. 2016. Global impacts of tropospheric halogens (Cl, Br, I) on oxidants and composition in GEOS-Chem. *Atmos Chem Phys* **16**(18): 12239-12271. doi:10.5194/acp-16-12239-2016.

Silvern RF, Jacob DJ, Mickley LJ, Sulprizio MP, Travis KR, et al. 2019. Using satellite observations of tropospheric NO2 columns to infer long-term trends in US NOx emissions: the importance of accounting for the free tropospheric NO2 background. *Atmos Chem Phys* **19**(13): 8863-8878. doi:10.5194/acp-19-8863-2019.

Simpson WR, Brown SS, Saiz-Lopez A, Thornton JA, von Glasow R. 2015. Tropospheric Halogen Chemistry: Sources, Cycling, and Impacts. *Chemical Reviews* **115**(10): 4035-4062. doi:10.1021/cr5006638.

Singer BC, Delp WW, Black DR, Destaillats H, Walker IS. 2016. Reducing In-Home Exposure to Air Pollution. Final Report to California Air Resources Board for Contract 11-311. *Sacramento, CA*.

Sipila M, Sarnela N, Jokinen T, Henschel H, Junninen H, et al. 2016. Molecular-scale evidence of aerosol particle formation via sequential addition of HIO3. *Nature* **537**(7621): 532-534. doi:10.1038/nature19314.

Sullivan JT, McGee TJ, Thompson AM, Pierce RB, Sumnicht GK, et al. 2015. Characterizing the lifetime and occurrence of stratospheric-tropospheric exchange events in the rocky mountain region using high-resolution ozone measurements. *Journal of Geophysical Research: Atmospheres* **120**(24): 12410-12424. doi:https://doi.org/10.1002/2015JD023877.

Sullivan JT, Rabenhorst SD, Dreessen J, McGee TJ, Delgado R, et al. 2017. Lidar observations revealing transport of O3 in the presence of a nocturnal low-level jet: Regional implications for "next-day" pollution. *Atmos Environ* **158**: 160-171. doi:https://doi.org/10.1016/j.atmosenv.2017.03.039.

Thiruvengadam A, Besch MC, Thiruvengadam P, Pradhan S, Carder D, et al. 2015. Emission Rates of Regulated Pollutants from Current Technology Heavy-Duty Diesel and Natural Gas Goods Movement Vehicles. *Environ Sci Technol* **49**(8): 5236-5244. doi:10.1021/acs.est.5b00943.

Tilmes S, Hodzic A, Emmons LK, Mills MJ, Gettelman A, et al. 2019. Climate Forcing and Trends of Organic Aerosols in the Community Earth System Model (CESM2). *Journal of Advances in Modeling Earth Systems* **11**(12): 4323-4351. doi:10.1029/2019ms001827.

Tong DQ, Lamsal L, Pan L, Ding C, Kim H, et al. 2015. Long-term NOx trends over large cities in the United States during the great recession: Comparison of satellite retrievals, ground observations, and emission inventories. *Atmos Environ* **107**: 70-84. doi:10.1016/j.atmosenv.2015.01.035.

Tong DQ, Lee P, Saylor RD. 2012. New Directions: The need to develop process-based emission forecasting models. *Atmos Environ* **47**: 560-561. doi:10.1016/j.atmosenv.2011.10.070.

Torres-Vazquez A, Pleim J, Gilliam R, Pouliot G. 2022. Performance Evaluation of the Meteorology and Air Quality Conditions From Multiscale WRF-CMAQ Simulations for the Long Island Sound Tropospheric Ozone Study (LISTOS). *Journal of Geophysical Research: Atmospheres* **127**(5): e2021JD035890. doi:https://doi.org/10.1029/2021JD035890.

Travis KR, Heald CL, Allen HM, Apel EC, Arnold SR, et al. 2020. Constraining remote oxidation capacity with ATom observations. *Atmos Chem Phys* **20**(13): 7753-7781. doi:10.5194/acp-20-7753-2020.

Travis KR, Jacob DJ, Fisher JA, Kim PS, Marais EA, et al. 2016. NOx emissions, isoprene oxidation pathways, vertical mixing, and implications for surface ozone in the Southeast United States. *Atmos Chem Phys Discuss* **2016**: 1-32. doi:10.5194/acp-2016-110.

Tunved P, Hansson HC, Kerminen VM, Strom J, Dal Maso M, et al. 2006. High natural aerosol loading over boreal forests. *Science* **312**(5771): 261-263.

UN. 2018. https://www.un.org/development/desa/en/news/population/2018-revision-of-world-urbanization-prospects.html.

Vahmani P, Ban-Weiss GA. 2016. Impact of remotely sensed albedo and vegetation fraction on simulation of urban climate in WRF-urban canopy model: A case study of the urban heat island in Los Angeles. *J Geophys Res-Atmos* **121**(4): 1511-1531. doi:10.1002/2015jd023718.

Veefkind JP, Aben I, McMullan K, Forster H, de Vries J, et al. 2012. TROPOMI on the ESA Sentinel-5 Precursor: A GMES mission for global observations of the atmospheric composition for climate, air quality and ozone layer applications. *Remote Sensing of Environment* **120**: 70-83. doi:10.1016/j.rse.2011.09.027.

Veres PR, Neuman JA, Bertram TH, Assaf E, Wolfe GM, et al. 2020. Global airborne sampling reveals a previously unobserved dimethyl sulfide oxidation mechanism in the marine atmosphere. *Proceedings of the National Academy of Sciences of the United States of America* **117**(9): 4505-4510. doi:10.1073/pnas.1919344117.

Vermeuel MP, Novak GA, Alwe HD, Hughes DD, Kaleel R, et al. 2019. Sensitivity of Ozone Production to NOx and VOC Along the Lake Michigan Coastline. *J Geophys Res-Atmos* **124**(20): 10989-11006. doi:10.1029/2019jd030842.

Wang SY, Hornbrook RS, Hills A, Emmons LK, Tilmes S, et al. 2019. Atmospheric Acetaldehyde: Importance of Air-Sea Exchange and a Missing Source in the Remote Troposphere. *Geophys Res Lett* **46**(10): 5601-5613. doi:10.1029/2019gl082034.

Wang X, Jacob DJ, Downs W, Zhai S, Zhu L, et al. 2021. Global tropospheric halogen (Cl, Br, I) chemistry and its impact on oxidants. *Atmos Chem Phys* **21**(18): 13973-13996. doi:10.5194/acp-21-13973-2021.

Warneke C, de Gouw JA, Holloway JS, Peischl J, Ryerson TB, et al. 2012. Multiyear trends in volatile organic compounds in Los Angeles, California: Five decades of decreasing emissions. *J Geophys Res-Atmos* **117**. doi:D00v17 10.1029/2012jd017899.

Warneke C, Trainer M, de Gouw JA, Parrish DD, Fahey DW, et al. 2016. Instrumentation and Measurement Strategy for the NOAA SENEX Aircraft Campaign as Part of the Southeast Atmosphere Study 2013. *Atmos Meas Tech Discuss* **2016**: 1-39. doi:10.5194/amt-2015-388.

Wells KC, Millet DB, Payne VH, Deventer MJ, Bates KH, et al. 2020. Satellite isoprene retrievals constrain emissions and atmospheric oxidation. *Nature* **585**(7824): 225-+. doi:10.1038/s41586-020-2664-3.

Wells KC, Millet DB, Payne VH, Vigouroux C, Aquino CAB, et al. 2022. Next-Generation Isoprene Measurements From Space: Detecting Daily Variability at High Resolution. *J Geophys Res-Atmos* **127**(5). doi:10.1029/2021jd036181.

Weschler CJ. 2009. Changes in indoor pollutants since the 1950s. *Atmos Environ* **43**(1): 153-169. doi:10.1016/j.atmosenv.2008.09.044.

White AB, Darby LS, Senff CJ, King CW, Banta RM, et al. 2007. Comparing the impact of meteorological variability on surface ozone during the NEAQS (2002) and ICARTT (2004) field campaigns. *J Geophys Res-Atmos* **112**(D10). doi:10.1029/2006jd007590.

Williamson CJ, Kupc A, Axisa D, Bilsback KR, Bui T, et al. 2019. A large source of cloud condensation nuclei from new particle formation in the tropics. *Nature* **574**(7778): 399-403. doi:10.1038/s41586-019-1638-9.

Wu Y, Arapi A, Huang J, Gross B, Moshary F. 2018. Intra-continental wildfire smoke transport and impact on local air quality observed by ground-based and satellite remote sensing in New York City. *Atmos Environ* **187**: 266-281. doi:10.1016/j.atmosenv.2018.06.006.

Wu Y, Nehrir AR, Ren X, Dickerson RR, Huang J, et al. 2021. Synergistic aircraft and ground observations of transported wildfire smoke and its impact on air quality in New York City during the summer 2018 LISTOS campaign. *Science of The Total Environment* **773**: 145030. doi:https://doi.org/10.1016/j.scitotenv.2021.145030.

Yang Y, Wang HL, Smith SJ, Easter R, Ma PL, et al. 2017. Global source attribution of sulfate concentration and direct and indirect radiative forcing. *Atmos Chem Phys* **17**(14): 8903-8922. doi:10.5194/acp-17-8903-2017.

Zhang H, Kondragunta S, Laszlo I, Zhou M. 2020a. Improving GOES Advanced Baseline Imager (ABI) aerosol optical depth (AOD) retrievals using an empirical bias correction algorithm. *Atmospheric Measurement Techniques* **13**(11): 5955-5975. doi:10.5194/amt-13-5955-2020.

Zhang J, Ninneman M, Joseph E, Schwab MJ, Shrestha B, et al. 2020b. Mobile Laboratory Measurements of High Surface Ozone Levels and Spatial Heterogeneity During LISTOS 2018: Evidence for Sea Breeze Influence. *Journal of Geophysical Research: Atmospheres* **125**(11): e2019JD031961. doi:https://doi.org/10.1029/2019JD031961.

Zhang L, Jacob DJ, Downey NV, Wood DA, Blewitt D, et al. 2011. Improved estimate of the policy-relevant background ozone in the United States using the GEOS-Chem global model with 1/2 degrees x 2/3 degrees horizontal resolution over North America. *Atmos Environ* **45**(37): 6769-6776. doi:10.1016/j.atmosenv.2011.07.054.

Zhao R, Lee AKY, Wentzell JJB, McDonald AM, Toom-Sauntry D, et al. 2014. Cloud partitioning of isocyanic acid (HNCO) and evidence of secondary source of HNCO in ambient air. *Geophys Res Lett* **41**(19): 6962-6969. doi:10.1002/2014gl061112.

Zoogman P, Liu X, Suleiman RM, Pennington WF, Flittner DE, et al. 2017. Tropospheric emissions: Monitoring of pollution (TEMPO). *Journal of Quantitative Spectroscopy & Radiative Transfer* **186**: 17-39. doi:10.1016/j.jqsrt.2016.05.008.